

STRUCTURAL PETROLOGY OF AN AREA NEAR SANTIAGO DE COMPOSTELA (NW SPAIN)

BY

A. VAN ZUUREN

ABSTRACT

The area around Santiago de Compostela has been subjected to petrological and structural investigations. The rocks present in the mapped area have been divided into two complexes (the Ordenes Complex and the Complex of Santiago de Compostela) on the basis of their petrography, structure and grade of metamorphism. An additional group consists of the intrusive rocks still recognizable as such.

The intermediate-grade rocks of the Ordenes Complex mainly comprise retrograded mafic granulite-facies rocks, garnet-amphibolites, amphibolites, metagabbros, peridotite and kyanite-staurolite-garnet-gneisses or schists. Part of these rocks underwent amphibolite-facies metamorphism during a probably pre-Hercynian orogeny and in places granulite-facies conditions were attained. Isoclinal to tight folding (F_1) accompanied the first metamorphic phase; the axial planes are subhorizontally to gently inclined and the fold axes plunge N or NNW. A period of thrusting, accompanied by mylonitization and resulting in an imbricate structure, was followed by recrystallization under amphibolite-facies conditions, forming blastomylonites in certain zones. The emplacement of the metagabbros probably preceded this recrystallization. The related F_2 -structures were found in thrust zones, having approximate E-W axes and in general gently inclined axial planes. F_3 was tentatively placed after F_2 and is a postcrystalline deformation, characterized by the formation of a steeply inclined E-W striking crenulation cleavage and subhorizontally plunging axes.

All these events presumably occurred during a pre-Hercynian orogeny, but this will not be certain until conglomerates marking an angular unconformity are found or until radiometric data become available.

The pre-Hercynian orogeny was followed by a period in which intrusions of dioritic and granitic rocks took place. The latter are tentatively correlated with similar rocks in S Galicia which were radiometrically dated as Cambro-Ordovician.

The Complex of Santiago de Compostela contains low-grade schists, for example albiteporphyroblast-bearing schists and migmatized metasediments. During the first Hercynian phase, these rocks underwent predominantly greenschist-facies conditions. The rocks of the Ordenes Complex have been locally retrograded to epidote-bearing amphibolites during this phase. Metamorphism continued giving rise to the growth of albite-porphyroblasts and culminating in partial fusion of the metasediments. This period terminated with intrusions of two-mica granites, which resulted in contact metamorphic aureoles. Subsequently the rocks were retrograded during the greenschist-facies metamorphism (the basic rocks in places into greenstones). The structural main phase (F_4) of the Hercynian orogeny resulted in the formation of folds with steeply inclined axial planes and axes plunging gently to the N. F_5 coincided with the growth of the albite-blasts. This folding produced the same N-S striking axial planes but the B-axis plunges steeply to the E. A well-developed crenulation cleavage (F_6) occurs throughout the area. The associated lineation ("Runzelungen") on the schistosity planes plunges gently to the N. It is argued that during F_6 the basic rocks were upthrust to about their present position. Late-Hercynian phyllonitization and fault-movements were accompanied by the previously mentioned greenschist-facies retrogradation which presumably started at the time that F_6 was active. The emplacement of pegmatites and dolerites also took place at the end of the orogeny.

Microscopical fabric analyses of metabasites and albiteporphyroblast-bearing schists corroborate the field observations. The amphibole fabrics show that at least three generations of hornblende, each of them formed under different metamorphic and structural conditions, may be postulated.

The mathematical distribution model, proposed by Bingham, is shown to fit the observed distributions (an elongated or circular maximum which may lie in a great-circle girdle) quite well.

SUMARIO

La región alrededor de Santiago de Compostela ha sido objeto de investigaciones petrológicas y estructurales. Las rocas presentes en el área trazada han sido divididas en dos complejos (el Complejo de Ordenes y el Complejo de Santiago de Compostela) tomando como base su petrografía, estructuras y el grado de metamorfismo. Existe además un grupo adicional consistente en rocas intrusivas, que aún se pueden reconocer como tales.

Las rocas de grado intermedio del Complejo de Ordenes comprenden principalmente rocas máficas retrógradas de facies granulítica, anfíbolitas granatíferas, anfíbolitas, metagabros, peridotitas y gneis o esquistos cianíticos, estaurolíticos y granatíferos. Parte de estas rocas sufrieron un metamorfismo de facies anfíbolítica durante una orogénesis probablemente prehercínica, alcanzándose en algunos sitios condiciones de facies granulítica. La primera fase metamórfica estaba acompañada desde plegamientos isoclinales hasta estrechos (F_1) y sus planos axiales son desde subhorizontales hasta levemente inclinados, dirigiéndose la inclinación de sus ejes de plegamiento hacia el N o NNW. A un período de corrimiento, acompañado de milonitización cuyo resultado fue una estructura imbricada, siguió una recrystalización bajo condiciones de facies anfíbolítica, formando blastomylonitas en ciertas zonas. El emplazamiento de los metagabros probablemente precedió a esta recrystalización. Las estructuras F_2 relacionadas al período anterior fueron encontradas en zonas de corrimiento, teniendo ejes aproximadamente en dirección E-W y sus planos axiales en general levemente inclinados. F_3 fue colocada después de F_2 , siendo una deformación post-cristalina, que muestra la formación de un clivaje *crenulation* fuertemente inclinado con rumbo E-W y cuyos ejes se inclinan subhorizontalmente.

Todos estos sucesos se presume ocurrieron durante una orogénesis prehercínica; sin embargo no existirá una certidumbre hasta que no se hayan encontrado conglomerados marcando una discordancia angular o hasta que se dispongan de datos radiométricos.

La orogénesis prehercínica fue seguida de un período en el que tuvo lugar intrusiones de rocas dioríticas y graníticas. Las últimas han sido correlacionadas con rocas similares en el sur de Galicia, que fueron radiométricamente determinadas como Cambro-Ordoviciense.

El Complejo de Santiago de Compostela abarca esquistos de grado bajo, más esquistos portadores de porfiroblastos de albita, más meta-sedimentos migmatizados. Durante la primera fase hercínica estas rocas sufrieron condiciones predominantes de facies de esquistos verde. Durante esta fase las rocas del Complejo de Ordenes han sido localmente retrógradas a anfíbolitas portadoras de epidota. El metamorfismo continuó dando lugar al crecimiento de porfiroblastos de albita, culminando en una fusión parcial de los metasedimentos. Este período terminó con intrusiones de granitos de dos micas que originaron aureolas de metamorfismo de contacto. Posteriormente las rocas fueron retrógradas durante un metamorfismo de facies de esquisto verde; así como las rocas básicas en ciertos sitios en *greenstones*. La fase estructural principal (F_4) de la orogénesis hercínica dió lugar a la formación de pliegues con planos axiales profundamente inclinados y ejes submergidados suavemente hacia el N. F_5 coincidió con el crecimiento de blastos de albita. Este plegamiento tiene los mismos planos axiales con rumbo N-S, pero los ejes B se submergen en declive hacia el E. Existe una distribución extensa de un bien desarrollado clivaje *crenulation*. La alineación asociada (*Runzelungen*) sobre los planos de esquistosidad se inclina suavemente hacia el N. Se argumenta que durante F_6 las rocas básicas fueron corridas aproximadamente a su situación actual. A filonitización y movimientos de falla hercínica tardíos acompañó la retrogradación de facies de esquisto verde ya mencionado, que probablemente empezó en el tiempo en que F_6 fue activo. El emplazamiento de pegmatitas y doleritas también tuvo lugar al final de la orogénesis.

Los análisis microscópicos de texturas de metabasitas y esquistos portadores de porfiroblastos de albita confirman las observaciones hechas en el campo. La textura de los anfíboles enseña que pueden ser postulados al menos tres generaciones de hornblenda, cada una de ellas formadas bajo diferentes condiciones metamórficas y estructurales.

El modelo de distribución matemático, propuesto por Bingham, se adapta bastante bien a aquellas distribuciones observadas con un máximo alargado (o de forma circular), que puede yacer en un gran círculo.

CONTENTS

I. Introduction	3	Nomenclature	27
Geography	3	Applied methods	27
Geological setting	3	Pre-Hercynian structures (?)	27
Petrological investigation by the University of Leiden	4	F_1 -folding	28
Previous work	4	F_2 -folding	31
Explanation of symbols and terms used	4	F_3 -folding	33
Sample numbers	4	Conclusions	34
Terms and abbreviations	6	Hercynian structures	35
Acknowledgements	6	F_4 -folding	35
II. Petrography	6	F_5 -folding	38
Introduction	6	F_6 -folding	41
A. The Ordenes Complex	7	Phyllonitization, mylonitization, wrench faults and kink banding	42
Position of the non-migmatized rocks	8	Concluding remarks	43
Petrography of the non-migmatized rocks	8	IV. Petrofabric analyses	44
General description of the migmatized metasediments	11	Introduction	44
Petrography of the migmatized metasediments	11	Applied methods	44
Metabasic rocks	12	Measurements of amphibole and clinopyroxene orientations with the aid of a four-axis universal stage	44
Ultramafic rocks	15	Measurements of the indicatrix axes of albite with the aid of a four-axis universal stage	45
Comparable occurrences of intermediate- to high-pressure metamorphic rocks in western Europe	16	Statistics	45
B. The Complex of Santiago de Compostela	16	Method of sampling	45
Introduction	16	Comparison between the uniform distribution and observed distributions	46
Petrography	17	A distribution on the sphere with antipodal symmetry	47
C. Intrusive rocks	19	Amphibole, clinopyroxene, (scapolite) fabrics in rocks of the basic massif	49
Metagabbroic rocks	19	Hand-specimen 95-A4-217 C: hornblende-plagiopyrigarnite	49
Orthogneisses in the Complex of Santiago de Compostela	20	Hand-specimen 95-A4-217 B: hornblende-plagiopyrigarnite	49
Orthogneisses in the Ordenes Complex	21	Hand-specimen 95-A4-221: garnet-amphibolite	50
Metadiorites	21	Hand-specimen 95-A4-218: hornblende-plagiopyrigarnite	52
Megacrystal-bearing two-mica granites	21	Hand-specimen 95-B4-221 A: pyroxene-amphibolite	52
Dolerites, pegmatites and quartz veins	22		
Concluding remarks	23		
Mineralogy	23		
Hornblende	23		
Garnets	24		
III. Tectonics	26		
Introduction	26		
General remarks	26		

	<i>Introduction</i>	3
Hand-specimen 95-A3-186: pyroxene-amphibolite	53	Literature 62
Hand-specimen 95-A3-189: garnet-amphibolite	53	Remarks about the cause of the observed preferred orientations 63
Hand-specimen 95-A3-190: garnet-amphibolite	53	Albite and tourmaline fabrics of low-grade schists . . 63
Hand-specimen 95-B3-212: amphibolite	55	Hand-specimen 121-A1-206: porphyroblastic albite-schist 63
Hand-specimen 95-A3-184: metagabbro	55	Hand-specimen 94-E4-149: porphyroblastic albite-schist 64
Hand-specimen 95-A4-235: amphibolite	56	Hand-specimen 94-E4-150: porphyroblastic albite-schist 64
Hand-specimen 95-A4-234: amphibolite	56	Hand-specimen 94-E4-140 A: porphyroblastic albite-schist 64
Hand-specimen 95-A4-252: pyroxene-amphibolite	58	Hand-specimen 94-E2-152 C: porphyroblastic albite-schist 64
Hand-specimen 95-B3-86: retrograded hornblende-plagiopyrigarnite	58	Hand-specimen 94-E2-152 B: porphyroblastic albite-schist 67
Hand-specimen 121-B1-305: hornblende-plagiopyrigarnite	58	Hand-specimen 94-E2-105: tourmaline-bearing muscovite-chlorite-garnet-schist 67
Hand-specimen 95-A4-230: garnet-(pyroxene)-amphibolite	59	General remarks about the albite fabrics 67
Hand-specimen 95-A4-205: pyroxene-amphibolite	60	Literature 68
Hand-specimen 95-A3-175: blastomylonitic amphibolite	60	Samenvatting 68
Hand-specimen 95-E4-230: blastomylonitic pyroxene-amphibolite	60	References 69
The results of petrofabric analyses fitted into the structural framework	61	3 Enclosures (in back flap).

CHAPTER I

INTRODUCTION

GEOGRAPHY

The investigated area is situated around the ancient city of Santiago de Compostela in northwestern Spain, the ultimate destination of pilgrims in the past and today the goal of a modern kind of Crusader – the tourist. The topographical data, necessary for preparing the geological map, were obtained mainly from the 1:25,000 maps, edited by the Cartografía Militar de España: Sheet 94 (Santiago de Compostela), quadrants I and II; Sheet 95, quadrants III (el Pino) and IV (Enfesta); Sheet 120 (Padron), quadrant I. In addition Sheet 121 (La Estrada), edited by the Instituto Geográfico y Catastral, Madrid, (scale 1:50,000) was used. The topographical data, incorporated in the geological map, have been restricted to prevent distraction from the geological information. The accessible roads are indicated on the map; however except for the paved roads, I cannot guarantee that all are always passable by car.

GEOLOGICAL SETTING

The area around Santiago de Compostela forms part of a large belt of crystalline rocks in northwestern Spain and northern Portugal. In this predominantly Hercynian orogene, the presence of several units could be established of which the composition, the structural features and the type of metamorphism invite the assumption that these rocks do not occur in their original tectonic position. Some important characteristics of these units are the abundance of mafic rocks and their tectonic contact with the adjacent rocks. Units of the above-mentioned type include the Cabo Ortegal massif, the Ordenes 'basin' and two massifs in northern Portugal, viz. the Morais massif and the Bragança-Vinhais complex. The area dealt with forms part of the Ordenes 'basin'. Since this region is not entirely mapped in detail, it is premature to state that this elliptically shaped 'basin' is really a unit. The possibility exists that this 'basin' consists of

separate massifs; in places the discrepancies between the basic rocks are striking, specifically the grade of metamorphism and the diversity of metabasic rocks vary at different places. It appears that the basic massif, east of Santiago de Compostela, contains only a few varieties of basic rocks as compared with the Mount Castelo area described by Warnars (1967) and the area around Mellid: both are part of the Ordenes 'basin'. The remaining part of the area under discussion contains low-grade metasediments partially migmatized, orthogneisses and two-mica granites.

PETROLOGICAL INVESTIGATION BY THE UNIVERSITY OF LEIDEN

Since 1956, the western part of Galicia has been the subject of petrological study by staff and students of the Department of Petrology, Mineralogy and Crystallography, Leiden University.

The investigation was initiated along the Galician coast and gradually extended into inner Galicia. The catazonal to mesozonal rocks of the Cabo Ortegal massif are an exception in that they extend beyond the proper area of investigation (see Fig. I-1). The western part of the Ordenes 'basin' and the adjacent schists and gneisses, halfway between Santiago de Compostela and Carballo, have been described by Warnars (1967). He especially studied the petrographical and chemical aspects of the rocks found in this region.

The southern part of the area under discussion (Encl. I) was originally mapped by B. H. Hazelhoff Roelfzema. His geological map provided a good guide to the structural and petrological work. The geological map of the northern area was prepared by the author during his graduate study. The field work was done during the summer months of 1965, 1966 and 1967. An additional short visit followed in the spring of 1968.

The scope of this study was to describe the rocks present in the area and to investigate their mutual relationships (Chapter II). The accent however was placed on the structures in these rocks. First the mesoscopic structural features are described in Chapter III and subsequently microscopical fabric analyses were carried out and are explained in Chapter IV. The idea underlying the tectonic analysis was to unravel the structures in the intermediate-grade rocks from part of the Ordenes 'basin' and finally to compare these

results with data obtained from the predominantly low-grade rocks in the western part of the area. This area was investigated because the structures have not been as intensively disturbed by younger fault movements as those of the adjacent eastern area.

PREVIOUS WORK

A review of publications dealing with geological investigations in Galicia has been presented by Parga-Pondal (1966). The 'Mapa petrográfico estructural de Galicia' by Parga-Pondal (1963) is of importance and provided beforehand some insight into the structural problems of the region in question.

A general account of the geology of Galicia was given by Carlé (1945).

A conference in Santiago de Compostela (1965) dealt with the geology of Galicia and northern Portugal. The papers contributed are recorded in volume 36 of the 'Leidse Geologische Mededelingen'.

The area near Cabo Ortegal, containing catazonal to mesozonal rocks, has been studied by Vogel (1967). The area around Mt. Castelo, between Santiago de Compostela and Carballo, has been analysed by Warnars (1967). A petrological study of mainly felsic rocks in southern Galicia was carried out by Floor (1966).

EXPLANATION OF SYMBOLS AND TERMS USED

Sample numbers

All samples collected have a figure-letter combination as sample number. The prefix denotes the numbers of the topographical sheet (scale 1:50,000) on which the sample locality occurs. The suffix is composed of one of the letters A-E followed by a number (1-4), indicating one of the 20 quadrants in which a topographical sheet has been subdivided. In each quadrant numbers were assigned to the samples that correspond with the numbers indicated on Enclosure II. The number and letter of the quadrant are also shown on this map.

The hand-specimens described will be kept at the 'Rijksmuseum van Geologie en Mineralogie' in Leiden. The X-ray powder photographs are kept and registered at the Department of Petrology, Mineralogy and Crystallography, Leiden University.

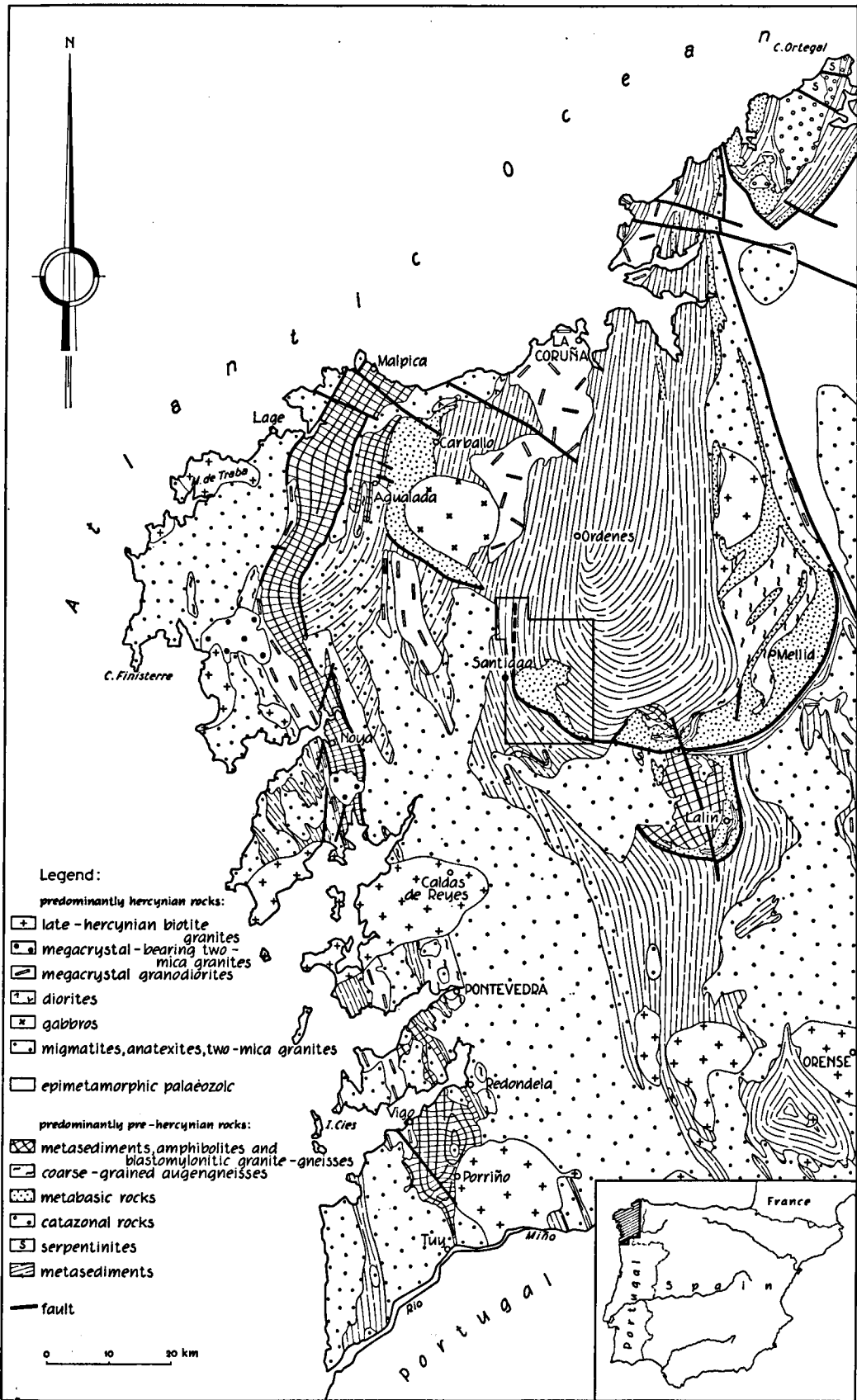


Fig. I-1. Simplified geological map of western Galicia, from Parga-Pondal (1963) and mainly unpublished data from the Department of Petrology and Mineralogy and Cristallography, Leiden University.

Terms and abbreviations

Grain size is classified as follows:

> 3 cm	very coarse-grained	
3 cm – 5 mm	coarse-grained	
5 mm – 1 mm	medium-grained	
1 mm – 0.33 mm	fine-grained	
0.33 mm – 0.01 mm	microcrystalline	} aphanitic.
< 0.01 mm	cryptocrystalline	

The crystallographic axes of minerals are denoted by a , b and c whereas the indicatrix axes are denoted as α , β and γ for biaxial minerals and ω and ϵ for unaxial minerals; Δ stands for the birefringence ($n_\gamma - n_\alpha$; $n_\omega - n_\epsilon$; $n_\epsilon - n_\omega$). The structural symbols and terms will be explained in Chapter III.

ACKNOWLEDGEMENTS

The author wishes to record his appreciation of the many valuable suggestions made by Professor E. den Tex during the preparation of this thesis. I should like to acknowledge Professor H. J. Zwart, who commented upon the problems of structural geology in the area, and Professor W. R. van Zwet for his critical reading of those parts of the manuscript dealing with statistics. I am grateful to Mr. H. Koning, who accompanied me during several field trips and provided useful information concerning the petrography.

Dr. I. Parga-Pondal of the *Laboratorio Geológico de*

Lage gave valuable advice during the field work in Spain.

I am especially grateful to Dr. J. R. Möckel for fruitful discussions and suggestions related to statistics and for his kindness in placing at my disposal the computer programmes he had written. Dr. P. Hartman offered many suggestions on crystallographic problems. The microprobe analyses were carried out by Dr. F. W. Warnaars at the Laboratory for Analytical Chemistry, State University, Utrecht.

Special appreciation must be expressed to my petrofabric associate Mr. J. P. Engels, who gave valuable advice on several problems dealing with petrofabric analysis; together with Mr. C. E. S. Arps and Mr. E. van Scherpenzeel, we enjoyed our stay in the back-loft of the Geological Institute. I wish to thank Dr. P. Floor, Dr. B. H. Hazelhoff Roelfzema, Mr. C. F. Woensdregt and Mr. R. O. Felius for their helpful discussions.

The proficiency of Mr. J. Bult manifests itself in his excellent drawing of the figures and enclosures. The photographic illustrations were made by Messrs. J. Hoogendoorn, W. C. Laurijssen and W. A. M. Devilée. The preparation of X-ray photographs was carried out by Mr. A. Verhoorn. Messrs. M. Deyn and C. J. van Leeuwen made the thin sections.

Thanks are also due to Mrs. G. P. Bieger-Smith for correcting the English manuscript and to Mr. B. van Hoorn for translating the abstract into Spanish. Finally I am indebted to Misses C. C. Zuiderduin, J. C. Koning, Mrs. B. J. Veldhuizen-Goosen and my wife for typing the manuscript.

CHAPTER II

PETROGRAPHY

INTRODUCTION

The area studied lies in the neighbourhood of Santiago de Compostela, and forms part of the crystalline rocks of NW Spain. The rocks, present in the investigated area, have been divided into three major units, viz.:

- A. The Ordenes Complex
- B. The Complex of Santiago de Compostela
- C. Intrusive rocks.

A. The Ordenes Complex is composed of intermediate-grade metasediments, partially migmatized, and meta-

basic rocks which underwent M_1 -metamorphism and subsequent retrogressive metamorphic phases (see Table II-1). The rocks are situated on the eastern side of the large thrust zone which separates the Ordenes Complex from the Complex of Santiago de Compostela (see Encl. I).

B. The Complex of Santiago de Compostela is mainly composed of low-grade schists and migmatized rocks. This complex comprises the metasediments west and south of the thrust zone. The reasons for separating this complex from the Ordenes Complex are:

- a. the high- to intermediate-grade rocks *versus* the

low-grade series of the Complex of Santiago de Compostela.

b. the manifold occurrence of basic rocks *versus* only a few minor bodies and dykes in the Complex of Santiago de Compostela.

c. the prevailing greywacke-type composition of the Ordenes metasediments *versus* the preponderance of pelites in the Complex of Santiago de Compostela.

d. the intricate structural pattern of the Ordenes Complex *versus* the rather simple structures of the Complex of Santiago de Compostela.

C. The intrusive rocks are located in both complexes; this group embraces all the rocks which intruded after M_1 .

In order of assumed development we may discern: (a) metagabbroic rocks in the metabasites of the Ordenes Complex, (b) orthogneisses occurring in both complexes, (c) metadiorites found in both complexes, (d) megacrystal-bearing two-mica granites in the Complex of Santiago de Compostela and (e) a widely spread group of rocks of varying age composed of hornblende-pegmatites, pegmatites, dolerites and quartz veins.

In the following description of the above-mentioned rocks, symbols indicating metamorphic phases and folding phases are used. A simplified scheme is presented in Table II-1, which makes reading this chapter easier. A more extended treatment is accorded the subject in Chapter III, Tables III-1 and III-2.

Table II-1. A simplified scheme indicating the relationship between metamorphic and folding phases.

folding phases	pre-Hercynian			Hercynian			phyllonitization mylonitization
	F ₁	F ₂	F ₃	F ₄	F ₅	F ₆	
regional metamorphic phases	} M ₁ M ₂			M ₃	M ₄	—————→	
axial-plane cleavage or schistosity (i.e. s_1 developed during F ₁)	s_1	s_2	s_3	s_4	s_5	s_6	

A. THE ORDENES COMPLEX

The rocks of the Ordenes Complex form part of *le bassin d'Ordenes*; a geotectonic unit defined by den Tex (1966). In this part of the 'basin' high- to intermediate-grade rocks occur but elsewhere the author also found low-grade rocks. The Ordenes Complex was subjected, during a first phase (M_1), to an inter-

mediate-pressure amphibolite facies (according to the classification of facies series by Miyashiro, 1961), more specifically the kyanite-almandine-muscovite subfacies of the almandine-amphibolite facies according to Winkler (1967). In several localities in the metabasic rocks however, the metamorphism approximates the granulite facies. This kind of metamorphism is characteristic of the Barrovian type: a rather low geothermal gradient and intermediate pressure. The difference in grade of metamorphism between the metasediments (kyanite-almandine-muscovite subfacies of the almandine-amphibolite facies) and the metabasites may be the higher level of the metasediments in this complex.

A second phase of metamorphism (M_2) is a mesozonal retrogradation. In the metabasites it gave rise to a strong amphibolization of the original hornblende-clinopyroxene-garnet rocks. The pegmatoid injections composed of plagioclase-hornblende-epidote-calcite (\pm garnet \pm scapolite) are probably related to M_2 . In the northern part of the metabasic rocks, the amphibolites have been partly recrystallized as shown by the linear growth of hornblende crystals parallel to the axial direction of F_2 .

In the schists and gneisses, this metamorphism induced a second generation kyanite (?) and the growth of biotite in bands and streaks.

Perhaps the occasionally well-marked zoning of the garnets is an indication of plurifacial¹ metamorphism. This may also explain the increase in the albite component in rims of plagioclase.

At the eastern and western edges of the basic massif, the main metamorphic phase of the Hercynian orogeny (M_3) induced the recrystallization of green or blue-green hornblende in subvertical foliation planes striking N-S (see Photograph II-1). On a microscopical scale the imprint of this phase is very well expressed as a tectonic banding (Photograph III-12). In the blastomylonites of the amphibolites, near the Coto de Viso, this phase gave rise to the formation of epidote and tiny needles of blue-green hornblende in the groundmass.

An ensuing migmatization in the metasediments led to the destruction of many older structures and a partial recrystallization of quartz and plagioclase.

¹ A term proposed by de Roever & Nijhuis (1964) indicating rocks which underwent metamorphism in two or more different facies; it does not necessarily imply that the rocks were affected during two or more orogenic cycles.



Photo II-1. Recrystallization of hornblende on subvertical planes, striking N-S, in the neighbourhood of Monte Alboya. The newly formed dark streaks (parallel to the white match) crosscut an older fold.

Nevertheless, in the non-migmatized sections, one can observe the formation of new biotite and muscovite on subvertical schistosity planes striking N-S. It is possible that the microcrystalline garnets belong to this main phase because in the non-migmatized rocks of the Complex of Santiago de Compostela, west and south of the amphibolites, the same microcrystalline garnets are widespread. Where the temperature was high enough and sufficient water was available, a migmatite front intersected the rocks. This process involved a separation of the rock into a leucocratic and a melanocratic type. If the transport of material takes place over short distances and external supply is excluded, the process of partial melting is called *anatexis* as defined by Mehnert (1957).

In the basic rocks near the Coto de Viso, at the western extremity of the metabasic massif, are hornblende-quartz-diorite-pegmatites composed of quartz, plagioclase and green amphibole, which are regarded as segregations belonging to this anatexis phase.

Strong tectonization of amphibolites as well as metasediments was accompanied by a retrograde metamorphism of lower greenschist facies (M_4). In the metabasic rocks, this phase gave rise to decomposition of green hornblende into blue-green or nearly colourless amphibole and the chloritization of the mafic minerals.

In the metasediments biotite and garnet are partly converted into chlorite. Staurolite and kyanite are replaced by sericite.

The successive metamorphic stages from granulite facies to greenschist facies point to changes in temperature and pressure conditions. These changes are often interpreted as differences in the depth at which these processes took place. In the next chapter, it will be shown that active movement brought the intermediate-grade rocks from deep levels up to their present position, adjacent to the low-grade rocks.

Position of the non-migmatized rocks

All the paragneisses and schists east and north of the prolongation of the thrust zone, which borders the metabasic rocks in the south and divides the monometamorphic rocks (Complex of Santiago de Compostela) from the probably polyorogenic complex, belong to this formation. The rocks in this part of the area are poorly exposed. Therefore it is difficult to get a precise impression of the paragneiss/schist ratio.

North of the mafic rocks, the strike of the schistosity in the metasediments varies greatly between N-S and E-W directions and the dip is moderately inclined toward the north. This is in consequence of Hercynian folding which folded the rocks in large-scale antiforms and synforms. East of the amphibolites, the N-S directions predominate but here too some structures of the above-mentioned type occur.

Petrography of the non-migmatized rocks

Kyanite-staurolite-garnet-two-mica-gneisses. – Directly on the easternmost border of the basic massif there are gneisses containing a mineral assemblage of kyanite (\pm staurolite)-almandine-biotite-muscovite. This zone proceeds to the east but to the north-northeast kyanite diminishes (see Fig. II-1). The sequence almandine, staurolite and kyanite is a progressive one and characteristic of the Barrovian-type metamorphism. Den Tex (1965) has shown that this sequence belongs to his intermediate- to high-pressure lineage of metamor-

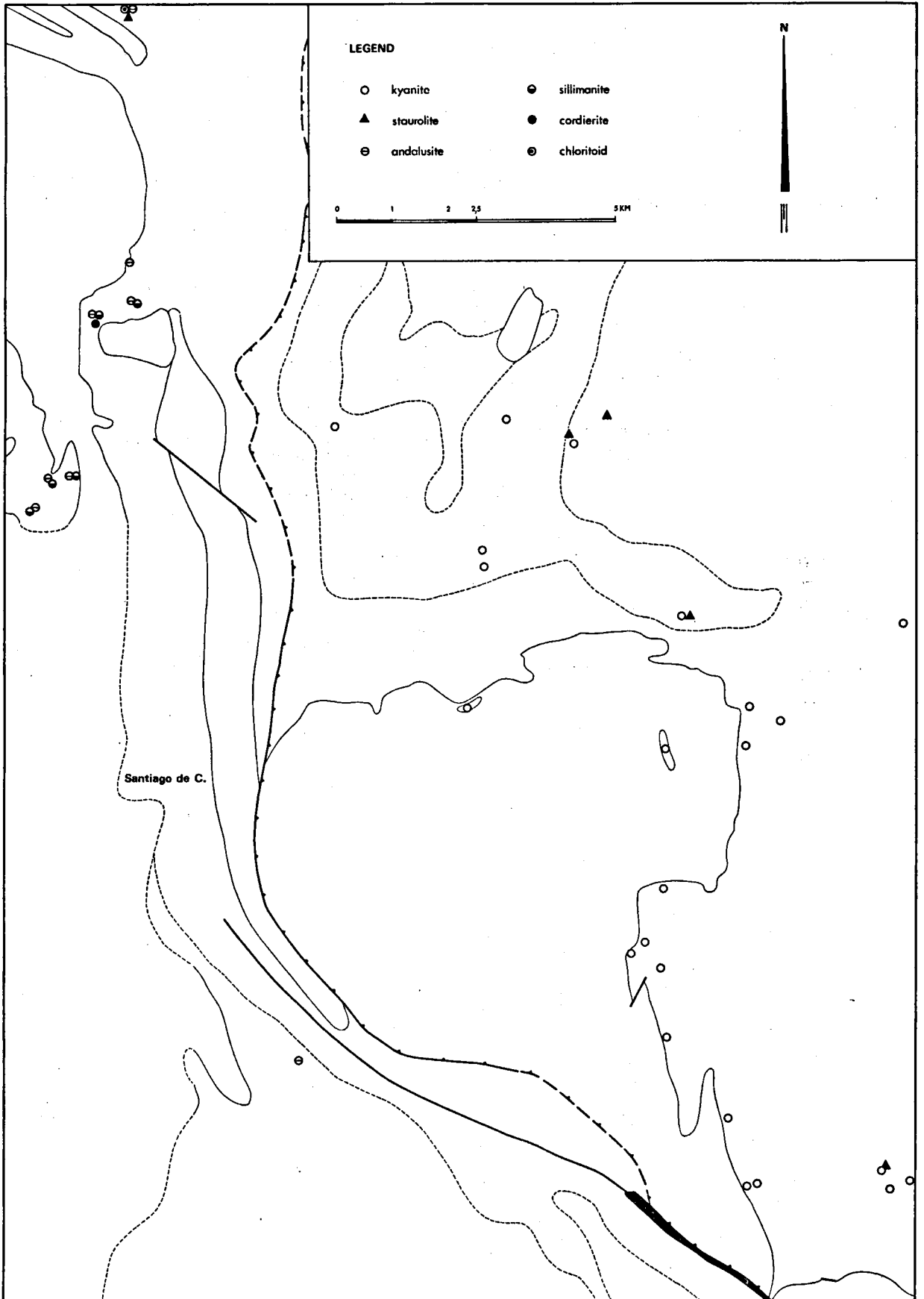


Fig. II-1. The distribution of mainly diagnostic minerals in the supposed polyorogenic complex and the Hercynian metamorphic part of the mapped area.

phism. The garnet-clinopyroxene subfacies of the granulite facies has been placed in the same trend, although at a higher grade.

Zwart (1967) has implied that the distribution of kyanite-staurolite parageneses is rather scanty in Hercynian orogenes in Europe. This is consistent with our concept that the main phase of metamorphism (M_1), which affected the metasediments of the Ordenes Complex, is of pre-Hercynian age. The occurrence of mineral assemblages including biotite, almandine, staurolite, kyanite (?) and sillimanite found in the metamorphosed Paleozoic rocks around Lugo (NW Spain) does not fit this hypothesis (Capdevila, 1967 and 1968). Kyanite however has also been found in series of Precambrian age and therefore the possibility of a pre-Hercynian age for this mineral should not be excluded. A microscopical investigation of the rocks follows below; their position is indicated on Enclosure II.

Macroscopically the *kyanite-staurolite-garnet-two-mica-gneisses* are heavily linedated by a postcrystalline deformation. The grey to reddish-brown colour is due to the biotite. Garnet is nearly always macroscopically visible.

Mineralogy. – Quartz has an average grain size approximately 0.03–0.08 mm. The grains are usually undulose and xenomorphic, sometimes elongated parallel to the schistosity. Equidimensional crystals of quartz occur in interlocking grains; they have been slightly strained and are often present in micro-folded veins.

Plagioclase (20–30% An.) is sometimes normally zoned; the crystals are rarely twinned but some of them show polysynthetic twinning along the {010}-planes. An exceptional simple twin along {010} has been found.

Muscovite as fine flakes is micro-folded by a crenulation cleavage; another type of coarse muscovite is sometimes undeformed. The growth of the latter around garnet is striking. Locally, coarse muscovite has recrystallized in patches without preferred orientation and is always distinctly bent and crinkled.

Biotite has a peculiar appearance recurring in all the non-migmatized metasediments of the Ordenes Complex. It is present as fine-grained reddish-brown flakes around quartz and plagioclase and has a distinct preferred orientation with its {001}-planes parallel to the schistosity. A second generation of biotite has been noted in the pressure shadows of garnets and as streaks in the axial planes of microfolds; the grain size is somewhat coarser and a distinct preferred orientation is generally lacking (thin section 95-A2-122). Sometimes the grains show an intergrowth with muscovite and partial alterations to chlorite.

Potash feldspar contains a large number of inclusions of muscovite and quartz. The medium-grained crystals carry small quantities of fine vein perthite (thin section 95-B3-50).

Potash feldspar is a mineral which does not fit in the paragenesis kyanite-almandine-muscovite. It might have resulted from a higher grade of metamorphism.

Garnet (\varnothing 0.5–1.5 mm) has irregular outlines and contains many inclusions of rutile and kyanite. Occasionally the crystals have a crumbled appearance and are tectonically flattened in the schistosity plane. Inclusions of rutile and opaque minerals are in parallel alignment and form a distinct internal structure (s_i), which is sometimes aligned with the external schistosity (s_e). Nevertheless in most cases, the s_i -direction is not parallel to s_e proving a postcrystalline rotation of the garnets (thin section 95-A2-122).

One garnet, half enclosed in staurolite, has a rim of kyanite although there are also many observations of kyanite enclosed in garnet. Probably the garnets developed before and after the formation of staurolite, i.e. the crystallization was not restricted to a specific phase (thin section 121-B1-306). Advanced alterations to chlorite, biotite and sericite are common, leaving only a few relics of the original mineral.

Kyanite is frequently situated in randomly oriented sericite aggregates (\varnothing 1–3 mm). The grain size varies greatly, a fibrous variety has even been observed in biotite and muscovite. The medium-grained, occasionally deformed, crystals in nearly monomineralic random aggregates have to be deemed an older generation. Except in micas, the younger generation also occurs as fringes of microcrystalline needles around feldspar. Due to the minute dimensions of the crystals, it is difficult to differentiate between sillimanite and kyanite although the large $2V_x$ indicates kyanite (thin section 95-B3-50).

Vogel (1967) described a comparable rock in his Chimparragneiss Formation.

Staurolite is a scarce mineral with an s_i -pattern similar to that of the garnet (see Fig. II-2). Around the staurolite, a rim of kyanite and biotite has occasionally been noted. This is an indication of a progressive replacement of staurolite by kyanite and biotite (thin section 121-B1-306). Rims of kyanite around staurolite have been described by Felius (1967) and Warnaars (1967) in similar rocks. Staurolite is converted, at a higher grade of metamorphism during M_1 , into kyanite, biotite and almandine when sufficient iron is present (Tröger, 1967). The above-mentioned aggregates of kyanite may be pseudomorphic after staurolite, because (see thin section 121-B1-306) relics of staurolite are common in these aggregates.

Accessories: *Tourmaline* in small prisms with a yellowish-brown rim and a blue core; *rutile* enclosed in garnet as needles as well as rounded grains; *chlorite* around biotite; *zircon* sometimes as rounded crystals; *apatite*; *clinozoisite* and opaque minerals.

Graphite-bearing schists. – Many bands of a rock with a distinct, nearly black, colour have been encountered concordant in the gneiss-series; the bands never exceed a width of 10 cm. The result of a qualitative analysis on manganese was negative; the black material was in-

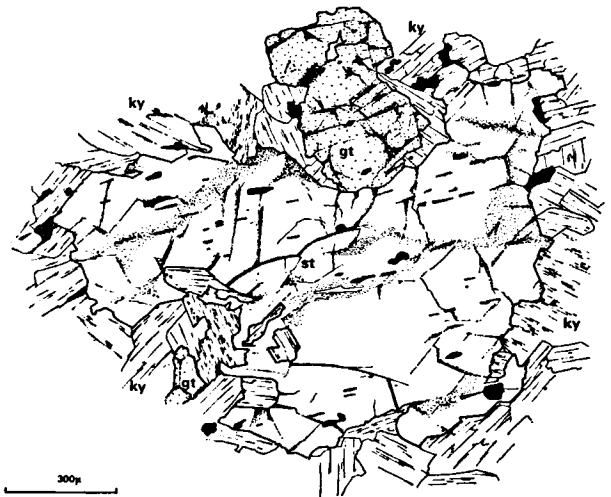


Fig. II-2. Rim of kyanite around staurolite; the garnets also have a border of kyanite. Note the straight s_i -pattern within the staurolite. Thin section 121-B1-306.

soluble in concentrated acids. Graphite seems to be the most probable mineral for the black grains in the rock.

Microscopically it is evident that 90% of the rock is quartz with some flakes of muscovite, biotite and chlorite. The amount of graphite seems very low (thin section 95-A2-322).

Amphibole-bearing schists. – In a few localities in the Ordenes-gneiss-schist series are outcrops of a grey to blue-grey rock with a yellowish-grey film along veins and in cracks. These rocks are more common in the northern part of the area. In larger exposures one can see that the rocks form discontinuous lenses about 10 m or less in length. They are indicated on the geological map (Encl. I) with the letters AM (amphibole).

A microscopical investigation of specimen 95-A2-3 shows that the rock is mainly composed of slightly strained quartz, muscovite, amphibole and opaque minerals. The amphibole is pale-green to nearly colourless. The optic sign is negative with $2V_{\alpha} \approx 80^{\circ}$ and $c \wedge \gamma = 17-20^{\circ}$. Occasionally plagioclase is present.

Retrograded gneisses and mylonites. – The retrograded gneisses are found as bands about 30 cm thick. Macroscopically they have an almost white colour. The rocks are totally converted into an aphanitic mass of sericite and quartz. There are however patches which look like pseudomorphs to garnet (thin section 95-A2-108).

The mylonitic rocks are restricted in their occurrence to distinct horizons. Under the microscope, the mylonitic texture of the rocks can be observed. Quartz is smeared out into a cryptocrystalline paste. Occasionally strongly deformed, long, flat grains are left which are again affected by a younger deformation (crenulation cleavage). Both muscovite and biotite are crumbled. Cataclastic grains of plagioclase have partially fallen to pieces. Chlorite is present converted from biotite.

Calc-silicate rocks. – West of the Castro, east of Santiago de Compostela, one hand-specimen has been found of a calc-silicate rock. Macroscopically the rock has a greyish to black colour with pink dots of garnet (\varnothing 0.5–2 mm). The rock is banded due to differences in the mineralogical composition of the separate bands. In thin section, the rock is rich in quartz and plagioclase (78% An.). The subhedral spongy garnet is profuse in quartz and plagioclase inclusions. The clinopyroxene is nearly colourless. The hornblende is green

pleochroic and occurs secondary after clinopyroxene and garnet. The clinozoisite has a low birefringence ($\Delta = 0.004-0.006$) and shows twinning along {100}. Sphene, calcite, zircon, apatite and opaque minerals are minor constituents.

General description of the migmatized metasediments

In the metasediments of the Ordenes Complex, there are rocks which have been migmatized. The age of this anatexis is presumably Hercynian. On the geological map, the rocks are indicated according to the classification of Mehnert (1957). In the sequence of increased anatexis, we can distinguish respectively metablastic paragneisses, which are not differentiated on the map, metatectic gneisses, diatectic gneisses and occasionally inhomogeneous diatexites. The original schistosity has been disturbed by segregation of pegmatoid and granitoid material. Often injections of pegmatites have also been noted, although strictly speaking they do not belong to the process of anatexis. The outlines of the anatectic rocks are irregular, all the boundaries are approximated and the transitions of the anatectic sequence are not exposed.

For more details about migmatization in Galicia, the reader is referred to the description of the area near Cabo Finisterre by Woensdregt (1966).

Petrography of the migmatized metasediments

Macroscopically the separation of the rocks into a leucocratic and a melanocratic type is distinct. In the leucocratic streaks, quartz, feldspar and minor biotite have been noted. These rocks, with an approximate granitoid composition in the segregation component, are classified as diatectic gneisses (Photograph II-2).

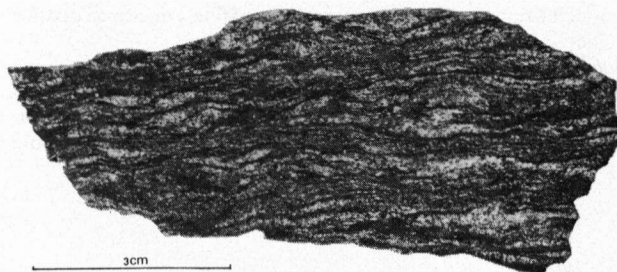


Photo II-2. Diatectic gneiss at location 95-A2-9 A. The segregation veinlets are composed of quartz, feldspar, muscovite and biotite.

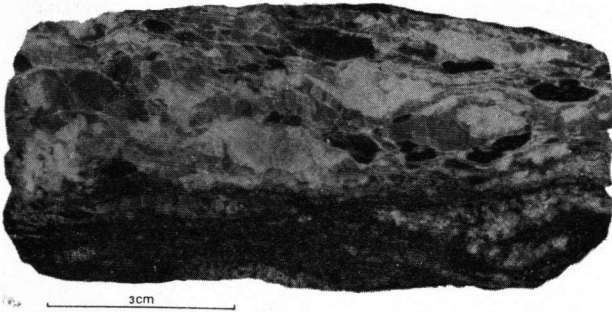


Photo II-3. Sample 95-A2-10. Metatectic gneiss, the leucocratic part consists of quartz and feldspar, the dark specks within this part are booklets of coarse muscovite.

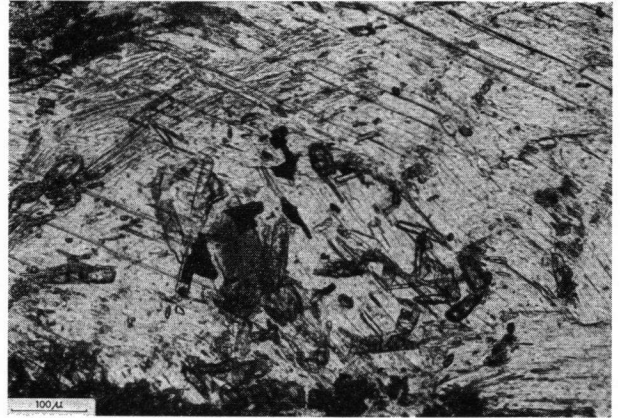


Photo II-4. Thin section 95-B3-53. Incipient growth of sillimanite as tiny needles in muscovite (-nic).

Where the original schistosity has been obliterated, the rocks are indicated as inhomogeneous diatexites. If the anatectic melt consists of feldspar and quartz, the composition is pegmatitic and the name becomes metatectic gneiss (Photograph II-3).

Anatectic gneisses. – The rocks have a dark colour caused by the abundance of biotite and white flames of quartz, feldspar and micas.

Quartz is usually medium-grained and occurs in bands and veins together with feldspar. Quartz is often present in recrystallized mortar bands.

Plagioclase (albite-oligoclase) shows twinning along {010} and {001}, and sometimes inverse zoning. It is found together with quartz in veinlets. Myrmekite has been noted where potash feldspar is adjacent to plagioclase.

Potash feldspar is fine- to medium-grained with a cross-hatched twinning, although simple {010}-twins have also been observed. Occasionally a rim of potash feldspar around plagioclase has been found. Perthite in many configurations is often present.

Muscovite occurs mostly as fine crystals intergrown with biotite but there are also large, thick flakes which are crinkled.

Biotite with a reddish-brown colour is a common mineral. Alterations of garnets produce a coarser variety of biotite which is also greatly deformed.

Chlorite has an anomalous blue interference colour as well as a yellowish colour. Chlorite often grows as rims around biotite.

Garnet (\varnothing 0.5–1.5 mm) as well as *kyanite* has been noted as relics. Kyanite has been rimmed by sericite. It appears that all the sericite masses could have been crystals of kyanite (thin section 95-A3-54).

Sillimanite (?) appears as minute needles in coarse muscovite (Photograph II-4) in thin section 95-B3-53.

Accessories are brown-yellow *tourmaline*, with a grain size of about 0.8 mm, rounded *zircon*, *apatite* and finely dispersed opaque minerals.

Inhomogeneous diatexites. – These rocks have lost their distinct schistosity and the distribution of the leucocratic and melanocratic streaks is irregular. Their mineralogical composition is about the same as that of the anatectic gneisses. Kyanite and garnet occur here too as relics (thin section 95-A2-127).

Metabasic rocks

Introduction. – All the metabasic rocks, with exception of the metagabbros, belong to this formation. They are

found mainly in the lower level of the sequence of the Ordenes Complex. The only exposure of ultramafic rocks has been found southeast of the Coto de Viso.

All the rocks were probably affected by a granulite-facies metamorphism (M_1). The subsequent retrogressive metamorphic phases (M_2 , M_3 and M_4) altered the rocks to amphibolites or greenschists. The metabasic rocks, the gabbroic composition of which has been questioned by Warnaars (1967), contain some relics of granulite-facies rocks, garnet-amphibolites, lineated amphibolites, epidote-amphibolites, greenschist-facies rocks and calc-silicate rocks.

Striping or banding is a common feature of the granulite-facies rocks and garnet-amphibolites. The width of the individual bands is variable and alternates from 0.5 cm to 10 cm (Photograph II-5). The banded rocks consist of layers of different mineralogical composition. Hornblende-garnet-plagioclase-(\pm clinopyroxene) streaks are interchanged with plagioclase-clinopyroxene-clinzoisite-(\pm garnet \pm hornblende) bands. The bands were folded by F_1 -deformation. This implies that before deformation took place, the banding was already present. The origin of this banding is not clear. There are many suggestions varying from rhythmic layering in the original intrusive, metamorphic segregation (Bowes & Park, 1966; Evans & Leake, 1960) to tectonic banding; however evidence for either is lacking. The prevailing direction of the foliation in the central part of the metabasites is E-W with a subhorizontal foliation plane. The strike changes to N-S at the easternmost and westernmost border zones and the dip is steep towards the east.

There is confusion regarding the nomenclature for rocks affected by granulite-facies metamorphism. Scheumann (1961) restricts the name granulite to fine-



Photo II-5. Banded amphibolites on the southern slope of the Coto de Viso. The plagioclase-rich clinopyroxene-epidote bands have a white to greyish colour.

grained blastomylonitic rocks with mineral associations of low-pressure granulite facies. Vogel (1967) has suggested the name *pyrigarnite* for those rocks in which garnet (pyralmandine) and clinopyroxene are a stable association and with a chemical composition of gabbros or diorites. Vogel's definition has the advantage that the textures of the rocks may be either granoblastic, gneissic or granulitic.

The subdivision of the granulite facies according to de Waard (1965) will be used in this paper.

Hornblende-plagiopyrigarnites. – The plagiopyrigarnites are always amphibolized by younger retrogressive metamorphism. But the classification of the granulite facies according to de Waard (1965) indicates that within this facies hornblende is co-stable with clinopyroxene and garnet in the hornblende-clinopyroxene-garnet subfacies. The difficulty arises when determining which of the hornblende generations might be stable with garnet and clinopyroxene since subsequent amphibolization makes the relationships obscure.

Macroscopically the rocks are fine-grained and have a striped appearance.

Mineralogy. – Microscopically a minor amount of quartz is found occurring interstitially.

Plagioclase (20–30% An.) is usually zoned. Locally plagioclase has been replaced by saussurite due to retrograde metamorphism. The crystals have been deformed; this can be observed on the curved traces of the planes of twinning.

Clinopyroxene ($2V_\gamma = 57\text{--}60^\circ$) has a pale-green colour. The spongy crystals often have rims of blue-green hornblende which replaced the diopsidic pyroxene – especially near the contacts with pyroxene and garnet.

Garnet (\varnothing 0.1–2 mm) has a pale pink colour. The anhedral to subhedral grains have a pitted appearance and contain many inclusions of pyroxene, sphene, quartz and sometimes brownish-green hornblende.

Hornblende occurs as at least two generations. The oldest variety ($2V_\alpha = 78\text{--}85^\circ$; $c \wedge \gamma = 15\text{--}18^\circ$) has a greenish-brown γ -colour. The rims are often green. This generation is thought to be co-stable with clinopyroxene and garnet. The second variety, although the above-mentioned green rims may perhaps be an intermediate phase, has a blue-green γ -colour. The subhedral greenish-brown hornblende, as well as the clinopyroxene, has been converted into this blue-green variety (thin sections 121-B1-304 and 305).

Accessories: Veins are filled with *clinozoisite*, *garnet* and *calcite*. Good examples of *scapolite*-bearing hornblende-plagiopyrigarnites come from the Pena Mayor, situated in the central part of the metabasites. The fine-grained scapolite ($\Delta \approx 0.03$) shows a mosaic pattern. Probably this variety is calcic-rich and approximates meionite. The scapolite occurs in leucocratic streaks but is also dispersed throughout the rock (thin section 95-A4-217 B). Scapolite-bearing assemblages in granulite-facies rocks are described by v. Knorring & Kennedy, 1958; Lovering & White, 1964; Hapuarachchi, 1967; and Vogel, 1967.

Zircon, *sphene*, *chlorite* and opaque minerals occur as minor constituents.

Garnet-bearing amphibolites. – This type of amphibolite has a widespread distribution in the metabasic formation. These amphibolites are in part probably retrogressive plagiopyrigarnites. This is suggested by the occurrence of brownish-green hornblende which we have already noted in the plagiopyrigarnites. It is however possible that the granulite-facies metamorphism (M_1) was restricted to certain localities and that the majority of the amphibolites were affected by almandine-amphibolite-facies metamorphism.

The rock is macroscopically characterized by the abundant presence of garnet. The laminated rocks are mostly fine-grained.

Mineralogy. – Quartz occurs in minor amounts or is absent.

Plagioclase (20–35% An.) has recrystallized in a mosaic pattern. Twinning along {010} and {001} was frequently noted.

Garnet (\varnothing 0.5–1.5 mm) has a pink colour and a spongy appearance. The crystals are usually crowded with plagioclase and sphene. Evidence of zoning in the garnets is seen in the occurrence of atoll-like shapes (see Photograph II-6). The core has been filled with plagioclase or epidote. Along cracks the garnet has been replaced by epidote and chlorite (thin section 95-A4-215).

Hornblende has a hypidiomorphic habit and a green γ -colour. In contact with garnets the colour becomes bluish-green.

Accessories are rutile with a rim of *sphene*, *saussurite*, *epidote* and opaque minerals.

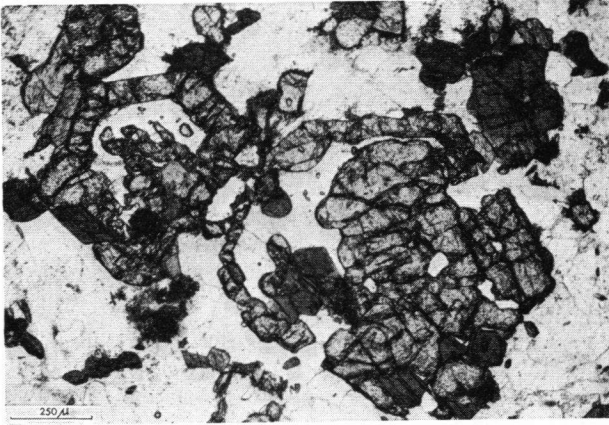


Photo II-6. Atoll garnets from amphibolized plagiopyrigarnites. The core is filled with plagioclase, epidote and hornblende. Thin section 95-A4-215.

Lineated amphibolites. – In the field these rocks are recognizable by the parallel alignment of the hornblende crystals. Their occurrence is restricted to the northern border zone and the thrust zone, east of Santiago de Compostela, of the metabasic massif. The development of the hornblende porphyroblasts is closely connected with F_2 -folding. The c -axes of the hornblendes are parallel to the axial direction of F_2 , viz. WNW, and gently plunging. We must assume a second pulse of metamorphism (M_2) during or after F_2 . From the recrystallization of the above-mentioned green hornblende and plagioclase, it can be deduced that the grade of metamorphism falls within the amphibolite facies.

Mineralogy. – Only some salient characteristics will be described.

Hornblende occurs as two generations. The oldest one forms a microcrystalline groundmass, in which the foliation is well-marked by parallel orientation of elongated opaque minerals.

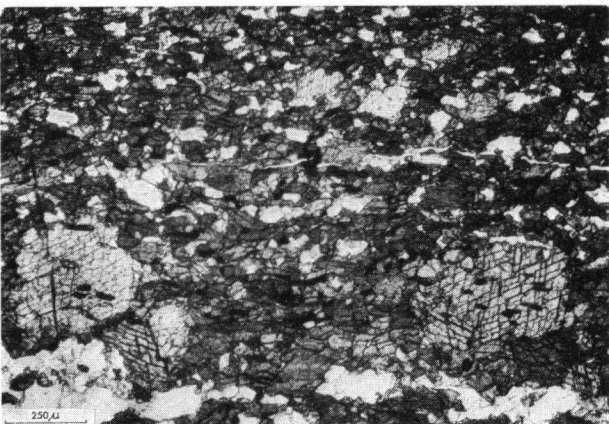


Photo II-7. Porphyroblastic growth of hornblende from a lineated amphibolite, the s_2 -pattern is adopted by s_4 without disruption. Thin section 95-B3-212 (-nic).

The probably younger generation consists of porphyroblastic green hornblende ($2V_\alpha = 78-83^\circ$ and $c \wedge \gamma = 15-17^\circ$). Evidence of the porphyroblastic growth of this hornblende (length about 1.5 mm) can be derived from the parallelism of the s_4 -fabric with s_2 (Photograph II-7). In contrast to the hornblende in the groundmass, the [010]-direction of many porphyroblasts is normal to the foliation plane (thin section 95-B3-212). Frequently the porphyroblasts have been observed in a mylonitized aphanitic groundmass (thin section 95-B3-101). Therefore it has been assumed that the lineated amphibolites are restricted to zones of blastomylonitization.

The widespread occurrence of segregation veins and streaks in the banded amphibolites is presumably related to this metamorphism.

In the neighbourhood of Bando, an incipient migmatization has been observed in the amphibolites (Photograph II-8), involving segregation of predominantly plagioclase (32% An.). Perhaps a comparable expulsion of leucocratic minerals occurs in the striped hornblende-plagiopyrigarnites near the Pena Mayor. The streaks here are composed of plagioclase, clinopyroxene, epidote, scapolite, calcite and small amounts of accessory amphibole.



Photo II-8. Migmatization of an amphibolite; especially the leucocratic minerals have been segregated. Hand-specimen 95-A3-209 ($\times \frac{1}{2}$).

Epidote-bearing amphibolites. – Locally, near the eastern and western borders of the metabasic formation, the rocks have been partially recrystallized during an amphibolite-facies metamorphism (M_3). The banded garnet-bearing amphibolites have been converted into banded epidote-bearing amphibolites. The formation of hornblende in stripes and bands in the axial planes (s_4) with their c -axes parallel to the fold axis (B_4) is especially visible on a limited scale in the field (Photograph II-1).

It is clear from the preceding that this metamorphism was closely connected with F_4 : the Hercynian main phase deformation. This penetrative deformation gave rise to transposition structures; thus the differentiation between the original and the newly formed foliation is difficult. Comparison of structural data for the amphibolites and the adjacent orthogneisses near Santiago de Compostela makes it clear that this deformation phase in the metabasic rocks is consistent with the main deformation phase in the orthogneisses. The resemblance between our orthogneisses and those described by Floor (1966) in South Galicia is striking. The orthogneisses of Floor have yielded Rb/Sr whole rock ages of 486 ± 24 to 500 ± 25 m.y. (cf. Floor, 1966). The transformation of the original granites into orthogneisses is regarded as the main phase of the Hercynian orogeny and therefore it seems to be an obvious conclusion to couple this phase with N-S structures in the adjacent amphibolites.

Mineralogy. – *Hornblende* is fine- to medium-grained and has a green or blue-green γ -colour. It is concentrated in the previously mentioned bands and streaks together with opaque minerals, which are rimmed with sphene. The subhedral to anhedral hornblende crystals are preferentially oriented.

Clinopyroxene occurs as porphyroblasts which are probably relics of an older metamorphism.

Plagioclase ($\approx 30\%$ An.) has been saussuritized and *epidote* has been formed (thin sections 95-A4-235 and 95-A4-252).

Greenschist-facies rocks. – The metabasites suffered local greenschist-facies retrogradation (M_4). In zones of intense deformation the amphibolites have been converted into greenstones. Near or on the thrust zone, some lenses have been found in which the plagioclase has been replaced by epidote. Phyllonitization and mylonitization promoted retrogradation of these rocks. It is impossible to place the M_4 -phase in a distinct time-interval. The process of retrogressive metamorphism probably started after the intrusion of the two-mica granites in the western part of the area, and was connected in time and space to the younger Hercynian deformations.

Macroscopically the fine-grained retrograded amphibolite has a distinct green colour caused by the decomposition of plagioclase into epidote. Microscopical investigation reveals occasionally zoned yellowish *epidote*. The blue-green *hornblende* is rimmed with a colourless *amphibole*. Specks of *chlorite* and *epidote* are presumably pseudomorphs after garnet.

Minor constituents are *quartz*, *muscovite*, *sphene*, *zoisite* and opaque minerals (thin sections 94-E3-23 and 95-A3-58).

Calc-silicate rocks. – These rocks are described under the heading 'metabasic rocks' since they form part of

the basic massif. Their occurrence is restricted to the northwestern border zone of the metabasites where these rocks have been observed interstratified between amphibolites. The banded rocks have greenish stripes with an epidote-clinopyroxene-garnet composition alternating with black streaks abundant in hornblende. Opaque minerals are mainly dispersed in the clinopyroxene-epidote-garnet-rich bands. The cause of the bands is not clear; it may be due to either original differences in the non-metamorphosed rock or to later injections of Ca-rich material.

Mineralogy. – The subhedral *hornblende* has a brownish-green core and a green rim. Colourless amphibole has also been noted. The subhedral *garnet* (\varnothing 0.2–1.0 mm) has zonally arranged inclusions of sphene and epidote. The zoning of the garnet is well-marked by atoll- and barrier reef-like shapes. Furthermore, the garnet includes *biotite*, *chlorite* and *rutile* with a rim of *sphene*. Fig. II-6 shows that the garnet of the calc-silicate bands has a grossularite-rich composition. Koning (1966) distinguished between three types of garnet in the metabasic rocks east of Santiago de Compostela. His third type is consistent with the above-mentioned.

Plagioclase ($\approx 35\%$ An.) has been heavily saussuritized.

The pale-green *clinopyroxene* does not seem to be stable and has been replaced by hornblende. *Sphene*, *calcite* and opaque minerals occur as minorities.

Ultramafic rocks

An individual body of ultramafic rock has been encountered in the metabasic formation which was metamorphosed during the granulite-facies metamorphism (M_1). The garnet-amphibolites, south of the Coto de Viso, contain a lens of spinel-peridotite. The contact with the amphibolites appears concordant. The mode of emplacement is unknown but because they were exposed to granulite-facies conditions, it may be concluded that the emplacement occurred before the M_1 -metamorphism. The rocks are usually greatly weathered but one fresh hand-specimen was taken by Hazelhoff Roelfzema and is described as follows:

Spinel-amphibole-peridotite. – About 70% of the rock is composed of euhedral colourless to pale-green *amphibole* ($n \approx 1.67$). The hypidiomorphic crystals enclose, in addition to flakes of *hematite*, clouds of tiny needles and droplets (*rutile* or *spinel*?).

Orthopyroxene (\varnothing 0.1–2 mm) is colourless and has an optic axial angle of about 70–80°. The birefringence is rather low ($\Delta \approx 0.010$). The crystals have a pitted appearance and include small grains of amphibole.

Olivine (\varnothing 1–4 mm) occurs as *phenoclasts*, at least in the larger broken grains. Along cracks the grains have been altered into *serpentine*.

Spinel has a conspicuous green colour. It may be included in amphibole and orthopyroxene.

Accessories are *chlorite*, with twinning along {001} and a positive optic sign, *zircon* and opaque minerals (thin section 95-A4-115).

Comparable occurrences of intermediate- to high-pressure rocks in western Europe

A number of metamorphic areas have been listed below in order to compare rocks which are, roughly speaking, similar to those described in this chapter.

Vogel (1967) has reported similar rocks in the area around Cabo Ortegal (NW Spain). According to him, the rock complex is polymetamorphic. The metabasites of the Capalada Complex, and particularly the Candelaria Amphibolite Formation, are closely akin to the metabasites east of Santiago de Compostela. The Candelaria amphibolite body contains some relics of plagiopyrigarnite and part of the formation is made up of metagabbroic rocks (Vogel, *op. cit.*, p. 185).

In the Ibero-Hesperian zone, Portugal V. Ferreira (1965, 1968) described amphibolites and gneisses in northern Portugal which have been metamorphosed in pre-Hercynian times under high-pressure conditions. These rocks are overthrust on a Silurian sequence. Similar rocks are described by Anthonioz (1966) in the Morais region of northeastern Portugal. A nearly circular occurrence of a sequence of amphibolites, serpentinites, pyroxenites and amphibole-schists is discordantly underlain by slightly metamorphosed Silurian.

In Brittany, a geotectonic unit has been described by Cogné (1960 and 1966) as Brioverian. The Brioverian contains at its base meta-ophiolites which are followed in sequence by pelitic material and greywackes. During the Cadomian orogeny, which took place between the *Briovérien moyen* and the *Briovérien supérieur*, the basic rocks were converted into amphibolites or eclogites while the sediments were sometimes converted into high-grade schists and gneisses. Folding at the end of the Brioverian closed the Cadomian orogeny. A probably structural hiatus in the sequence then followed. Later sediments of Cambrian-Ordovician age were deposited, which suffered Hercynian metamorphism along with the Brioverian sequence.

B. THE COMPLEX OF SANTIAGO DE COMPOSTELA

Introduction

Roughly speaking, this complex comprises rocks found west and south of the thrust zone, which borders the metabasites and related rocks. The complex is composed of garnet-(staurolite)-muscovite-(biotite)-chlorite-schists, porphyroblastic albite-schists, talc-schists, migmatized gneisses, superimposed contactmeta-



Photo II-9. Thin section 94-E2-105 (-nic). Transposition of the s_4 -plane into the s_5 -schistosity. The section is cut normal to the longitudinal direction of bluish tourmaline.

morphic schists and inliers of basic rocks. The metasediments suffered greenschist-facies metamorphism (M_3) during Hercynian orogeny; an incidental occurrence of staurolite points to amphibolite-facies metamorphism. In general, the mineral assemblage muscovite-chlorite-quartz-(\pm garnet) is most often found. Traces of the main deformation (F_4) are partly obliterated by a deeply penetrating younger deformation (F_5). F_5 gave rise to isoclinal folding and occasionally a total transposition of the original schistosity (s_4) into s_5 (Photograph II-9). During and after F_5 -folding, porphyroblasts of albite were formed. The zone of porphyroblastic albite-schists is a continuous band beginning in the north, west of the thrust zone, and ending southwest of the Pico Sacro. The locally developed F_5 -folding, presumably associated with the albite growth, has a subvertical to steeply plunging axial direction. The axial planes (s_5) strike N-S and dip steeply to the east, except west of the Pico Sacro where the strike changes to NW-SE.

The dominant N-S and NW-SE structures, west of the Pico Sacro, have been disturbed by a process of migmatization (cf. p. 7). Products of partial crystallization of melts from the metasediments are quartz and feldspar. Because the rocks were not only affected by anatexis but also by the introduction of pegmatitic material along veins and dykes, the name migmatites seems to be more correct than anatexites.

At a later stage, granitic magma intruded into the schists, forming new minerals such as sillimanite, andalusite, chloritoid, cordierite (?), biotite, chlorite and muscovite. The distribution of these minerals is indicated in Fig. II-1; at the same time, the relation between the two-mica granites and the above-mention-

ed minerals is also shown. A period of dislocation, phyllonitization and mylonitization terminated Hercynian movement activities. Veins and fractures in the schists have filled up mainly with quartz and minor opaque minerals.

Petrography

Garnet (spessartine-rich)-(staurolite)-muscovite-(biotite)-chlorite-schists. – Among the metasediments, the occurrence of garnet-bearing schists has been observed. The chemical composition of the garnet has not been determined, but cell edge size (a_0) and refractive index (see Fig. II-6) indicate a probably Mn-rich variety. Folded veinlets of quartz are common.

In several localities and concordant with the schist-series, graphite-bearing schists have been noted. The contact with other rocks is razor-sharp and identification is easy because of the conspicuous dark colour of the rocks. The isoclinal folding of the s_4 -plane is rather common. The thickness of the individual bands does not exceed a value of approximately 15 cm.

Mineralogy. – Quartz occurs as equidimensional grains in veinlets as well as elongated grains parallel to the schistosity. The grains are slightly undulose.

Muscovite is often found as deformed plates, frequently intergrown with *chlorite*.

Subhedral to euhedral *garnets* (\varnothing 0.12–2.5 mm) sometimes include tiny needles of *rutile*. In pressure shadows of garnet, *chlorite* has grown and corroded the garnet.

Small amounts of greenish *tourmaline*, *biotite*, *zircon*, *apatite*, *sphene* and opaque minerals are present (thin section 94-E1-192). Strings of *graphite* indicate the trend of the s_4 -plane, which has been folded by F_5 (thin section 94-E1-29).

Staurolite occurs as irregular grains and has been converted into *chloritoid* during contactmetamorphism. It was found in only one locality (94-E1-189).

Talc-schists. – In the zone of thrusting, several localities of talc-schists have been exposed. The lenses are sometimes 20 m long and 1–5 m thick. The mode of emplacement of these rocks is uncertain but they were probably pinched into planes of dislocation. The rocks are composed mainly of talc and minor amounts of quartz in veins, and opaque minerals.

Porphyroblastic albite-schists. – The zone of porphyroblastic albite-schists is a continuous band beginning in the north and ending west of the Pico Sacro. The regional schistosity strikes N-S but southeast of Santiago de Compostela, it swings toward a NW-SE direction. The plane of schistosity has a subvertical attitude and dips steeply to the east-northeast. Many observations in the field as well as microscopical investigation have

shown that the prominent schistosity plane is s_5 (Photograph II-9). The s_4 -plane has been concealed except in fold hinges. The schists have a predominantly albite-muscovite-chlorite-quartz (\pm spessartine-rich garnet) composition. The albite-porphyroblasts are macroscopically recognizable and have a grain size of 0.3–3 mm. The s_5 -plane has a greenish-black colour due to chlorite. The rocks are heavily lineated by a crenulation cleavage (s_6). The lineations ('Runzungen') are subhorizontal with N-S directions in the s_5 -plane. Conjugate planes, intersecting this plane, have been formed by late-Hercynian phyllonitization.

Literature. – Many investigators have tried to explain the presence of albite-porphyroblasts in such schists.

Albite-gneisses in the Loch-Lomond district in Scotland have been reported by Cunningham-Craig (1904). He states that the albite-gneisses are a result of metamorphism of greywacke-shales. The albite was already present as feldspar pebbles in the greywacke series. This suggestion has been adopted by Bailey (1923). According to Bailey, the albite-schists of the Cowal anticline have albite pebbles with lamellar twinning and albite-porphyroblasts in which this characteristic is absent.

In contrast to these investigations in the Scottish Highlands are the results of work done by Goldschmidt (1921) in the Stavanger district of Norway and Sobhen Ray (1967) in the Singhbhum district (India). Goldschmidt is of the opinion that the formation of albite-porphyroblasts is related to intrusions of trondjemite. The porphyroblasts are however not really of albitic composition but have anorthite contents varying between 10–28%. Ray points out that the albite-blasts have resulted from sodium metasomatism. The blasts have grown postkinematically and after the main metamorphism.

The occurrence of porphyroblastic albite-schists in the Otago province in New Zealand has been described by Turner & Hutton (1941). The albite-schists are believed to be metamorphosed greywackes.

It is argued by Tobi (1959) in his discussion of the St. Hugon schists in the Belledonne massif (France) that indication of the injection of sodium from outside these schists is lacking. He has shown that the Na_2O content in certain clays does not exceed the amounts of Na_2O for the St. Hugon schists. The albite-schists of the Complex of Santiago de Compostela closely resemble those described in Scotland, New Zealand and France. The distribution of the albite-porphyroblasts is not limited to a definite horizon. The same feature is recognized by Tobi (1959). He points out that albite-rich pore solutions must have circulated on a limited scale.

Microscopical appearance. – Quartz has undulose extinction and is fine-grained. Sometimes the quartz grains are elongated with their long dimension parallel to the foliation. The quartz inclusions in the albite-blasts have sutured boundaries (thin section 94-E1-67 g).

Albite (\varnothing 0.3–3 mm) has oriented inclusions of quartz, chlorite and dusty strings of possible graphite. The kernels of the porphyroblasts are crowded with these inclusions whereas the rims are often devoid of these minerals. The same phenomenon has been noted by Bailey (1923), Turner & Hutton (1941) and Tobi (1959). The albite has an anorthite content between 0–5%. The blasts are sometimes twinned. With the aid of the universal stage, the kind of twinning has been determined using the method of Tobi (1959). The $\{010\}$ -plane was always the plane of twinning. Twin types of the albite law are frequently found ($a \wedge a'$ for albite

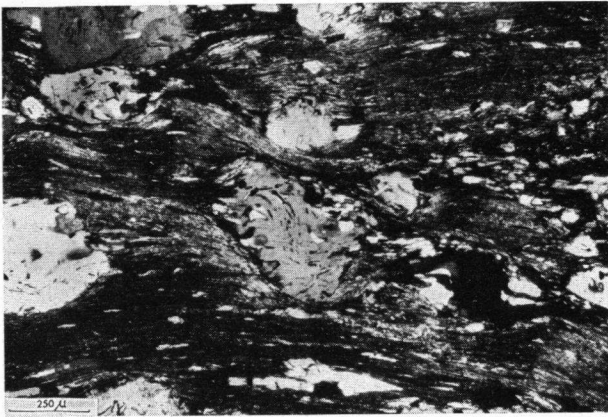


Photo II-10. Synkinematic growth of albite-blast. The rotation took place on subvertical B-axes and is counter-clockwise in the field. Thin section 94-E4-140 A (+ nic).

0–2°). In a few cases, twins according to the Carlsbad law have been measured ($\alpha \wedge \alpha'$ for albite 8–21°; see graphs by Köhler, 1942). S-shaped inclusions could be discerned in the albite-blasts present in thin section 94-E4-140 A (Photograph II-10). The blasts have grown synkinematically with F_5 . They are embedded in a fine-grained matrix of *muscovite* intergrown with *chlorite*. Post-kinematic growth of lepidoblastic *muscovite* with straight opaque inclusions parallel to s_6 are frequently found.

Microcrystalline *garnets* (\varnothing up to 0.08 mm) are totally converted into aggregates of *chlorite*.

Rutile, *tourmaline*, *garnet* and *clinozoisite* (?) needles are arranged in straight lines indicating the s_5 -plane. The orientation of the inclusions in the rims however differs from those of the kernels of albite (Photograph II-11). Therefore it may be possible that two stages of albite-growth have taken place.

Migmatized metasediments. – The migmatization in the Ordenes Complex (cf. p. 11) is presumably of the same age as that which affected the metasediments of the Complex of Santiago de Compostela. Therefore it is not necessary to describe the different rocks in detail. Diatectic and metatectic gneisses closely resemble their counterparts in the Ordenes Complex. The

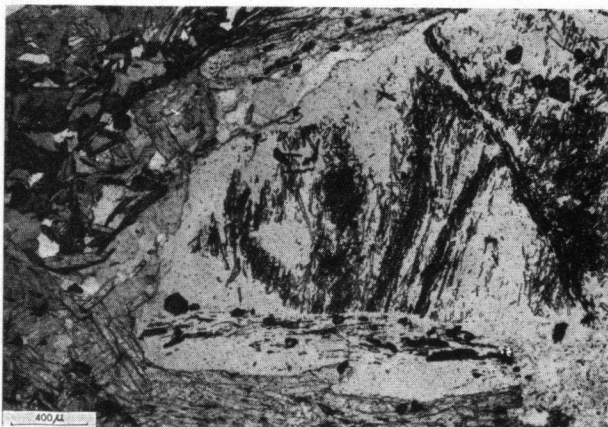


Photo II-11. Thin section 94-E2-177 (—nic). Albite-blast with rutile, tourmaline and garnet inclusions. The s_5 -direction of the kernel deviates from that of the rim.

rocks are generally found southeast of Santiago de Compostela. The strike of the schistosity, sometimes rather vague, is NW-SE. The migmatization must have taken place after the Hercynian main phase of metamorphism (M_3), because the structures belonging to this phase are partially obliterated by the melting of some of the minerals of the metasediments. The close association of the migmatites and granites in this area suggests an increase in temperature and pressure which induced melting of the metasediments and later on the introduction of granitic magma. The difficulty arises when trying to separate the process of anatexis from the alterations due to intrusion of granitic magma.

Metablastesis, one of the successive stages in the process of anatexis according to Mehnert (1957), has not been described in the foregoing. Metablastic paragneisses are present in the Complex of Santiago de Compostela. The gneisses have plagioclase-blasts with a grain size of about 1 mm. The rocks are often situated near the outcrop of the two-mica granites. The relative age of the growth of the plagioclase-blasts is uncertain.

In thin section the oval *plagioclase*-blasts contain numerous inclusions of quartz and micas. The quartz inclusions are sometimes elongated grains in parallel alignment with s_6 .

Lamellar twinning of the plagioclase is often interrupted by irregular spots of *potash feldspar*.

Fine flakes of *muscovite* surround the plagioclase-metablasts and lie parallel to each other, forming a distinct schistosity.

Coarse *muscovite* as well as *biotite* has grown crosswise through the schistosity and could be attributed to the increase in temperature during the intrusion of granitic magma in the neighbourhood.

Equidimensional *quartz* grains outside the metablasts are larger than the quartz inclusions in the blasts.

Apatite, rounded *zircon*, *sphene* and opaque minerals are the accessories.

Superimposed contactmetamorphic schists. – Along the boundaries of the outcrop of the two-mica granites in the western part of the area, evidence of contact-metamorphism in the adjacent schists has been found. The minerals involved are *chlorite*, *muscovite*, *biotite*, *chloritoid*, *cordierite* (?), *andalusite* and *sillimanite*. The reasons for assuming contactmetamorphic growth for these minerals are their distribution (Fig. II-1) and their time-relationship with the previously formed schistosity planes. All these minerals crosscut the schistosity and a preferred orientation is lacking. The occurrence of *chloritoid* in contact zones around granites is rather scarce. Hoschek (1967) has pointed out that for the formation of this mineral a specific rock composition is required. Therefore the scarceness seems to be explained.

The width of the aureole on the eastern side of the granites seems smaller than that which borders the granites farther west. The granites in the westernmost part of the area are concealed by a thin cover of metamorphic rocks. Small outcrops of granites here are actually domes which intersect the schists.

Chloritoid-(staurolite)-andalusite-garnet-chlorite-muscovite-schist. - The rocks have a greenish-grey colour and macroscopically recognition of chloritoid is easy. The same rocks are extensively described by Warnaars (1967).

In thin section, it is interesting to distinguish between those minerals resulting from the greenschist-facies regional metamorphism (M_3) and those which are closely related to the two-mica granites.

Mineralogy. - *Muscovite*, *chlorite*, *garnet* and *staurolite* are probably the minerals belonging to the regional metamorphism (M_3). Except for *staurolite*, the assemblage is widely distributed beyond the contact aureoles in the Complex of Santiago de Compostela. *Garnet* (\varnothing up to 0.3 mm) is euhedral and encloses trails of opaque material.

Staurolite occurs as a relic often embedded in chloritoid. The formation of *chloritoid* (grain size up to 3 mm) and *andalusite* is without doubt related to contact metamorphism. These minerals have grown porphyroblastically crosscutting the schistosity. Both minerals show helicitic inclusions of quartz and opaque minerals. Sometimes they are broken by a late-Hercynian dislocation deformation, especially in this zone. Chloritoid is twinned along the {001}-plane. Andalusite as well as chloritoid encloses idiomorphic garnet. Chloritoid and garnet are partly converted into *chlorite*. The microcrystalline *quartz* is slightly strained and the grains form a mosaic pattern (thin section 94-E1-189 a).

Cordierite (?) - andalusite-sillimanite-hornfels. - *Plagioclase* (20% An.) has grown as porphyroblasts.

Cordierite (?) is totally converted into sericite and a quasi-isotropic product (pinitite?).

Sillimanite needles are embedded in *biotite* and *muscovite*.

Andalusite occurs as small grains but sometimes pink pleochroic blasts have also been noted (thin section 94-E2-85).

Inliers of basic rocks. - According to the definition, inliers are older rocks surrounded by younger rocks. In the metasediments of the Complex of Santiago de Compostela, conformable amphibolite lenses are most frequently found in the northern part of the area. The amphibolite bodies vary between 1-800 m in length. The rocks are probably derived from the metabasic rocks of the Ordenes Complex. They are sometimes entirely recrystallized as plagioclase-blast-bearing amphibolites although barely altered garnet-amphibolites are also present. Similar lenses of albite-blast- or plagioclase-blast-bearing amphibolites are described by Rijks (1968) and Warnaars (1967) near the continuation of the basic complex to the north, in the neighbourhood of Carballo (NW Spain). The mode of emplacement of these large lenses is enigmatic but their occurrence in a zone of intensive movement indicates a tectonic origin. Small bodies (\varnothing 0.5-1 m), how-

ever, may possibly have been emplaced simultaneously with the surrounding sediments. The lenses may also be boudinaged basic dykes but evidence is lacking.

Plagioclase-blast-bearing epidote-amphibolites. - The plagioclase blasts in these rocks are macroscopically visible as oval white spots (\varnothing up to 1 mm). The rock is fine-grained to microcrystalline.

Mineralogy. - The *plagioclase* (26% An.) forms blasts with numerous inclusions of blue-green colourless fibrous *amphibole*. The s_1 -pattern is often parallel to s_0 . The blasts also contain myrmekite and are greatly saussuritized whereby the anorthite content decreases.

Elongated *quartz* grains, parallel to a well-developed foliation, are slightly undulose.

The *hornblende* is microcrystalline and has a bluish-green colour. Chloritization of the hornblendes indicates a strong retrogradation of these rocks.

Garnet enclosed in plagioclase, *biotite*, *sphene*, *adularia* in veinlets and opaque minerals are minor constituents (thin section 94-E1-4).

C. INTRUSIVE ROCKS

This group of rocks is treated separately since their distribution is often not restricted to one of the complexes described. The rocks will be discussed in order of supposed age.

Metagabbroic rocks

Renewed basic activity probably took place after the granulite-facies metamorphism (M_1); evidence for this is the large amount of metagabbroic rock in the basic massif, east of Santiago de Compostela. Its relationship with the well-foliated amphibolites is not clear. The conservation of palimpsest structures and the absence of relics of granulite-facies rocks indicate a probably younger basic suite during the pre-Hercynian orogenic cycle. The growth of rims of garnet around hornblende and the alteration of clinopyroxene into hornblende point to amphibolite-facies metamorphism (M_2).

The gabbroic structure of the rock is recognized by the unoriented texture of the plagioclase laths. Striking is the lack of foliation and the poor orientation of the hornblende crystals.

Microscopical appearance. - The *plagioclase* (76-70% An.) is normally zoned and has a palimpsest gabbroic texture (Photograph II-12). Sometimes the crystals have been recrystallized into aggregates of fine grains; the anorthite content is then about 45%. The green *hornblende* has been tectonized and has vermicular inclusions of plagioclase. Rims of pale-green amphibole have been observed. A younger generation of pale-green tinged fibrous amphibole occurs in the plagioclase. The above-mentioned deformed medium-grained hornblende crystals are frequently brown to brownish-green, often with dusty clouds of tiny inclusions.

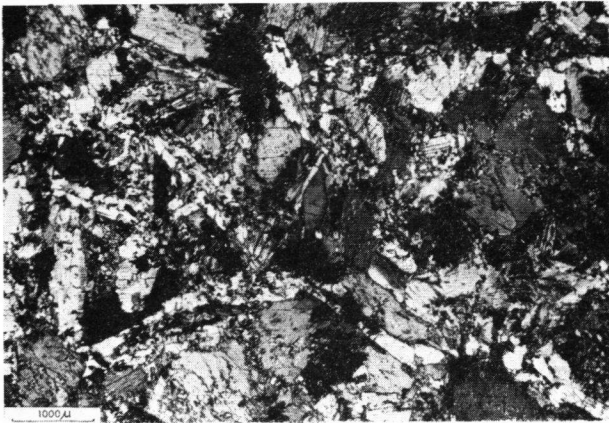


Photo II-12. Thin section 95-B3-88 (+ nic). Gabbroic palimpsest texture in a metagabbro. Hornblende is embedded between plagioclase laths.

Tröger (1967) described the possibility of replacement of pyroxene by hornblende and the segregation of ilmenite flakes or sphene into the hornblende crystal. In addition to the usual {110}- and {100}-cleavages, the hornblende also shows a peculiar kind of parting along {001} and the growth of a colourless lamellar amphibole, which has a higher birefringence than the brown variety, along the {001}-planes (Photograph II-13).

Clinopyroxene is pale-green and is converted in patches into green hornblende.

Chlorite occurs in shearzones replacing hornblende along cracks. *Accessories* are muscovite, quartz, rutile cores in sphene, and opaque minerals (described thin sections: 95-A3-149, 150, 157 and 174).

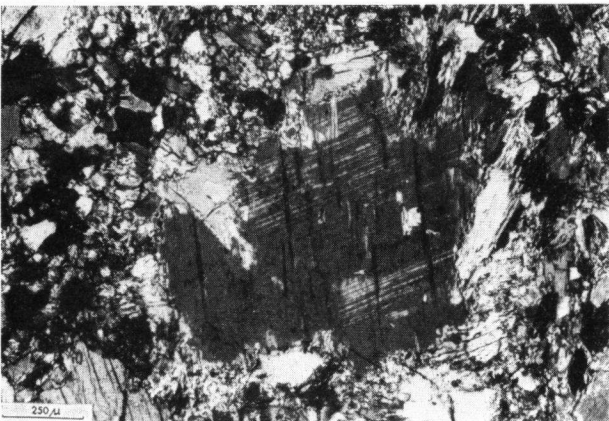


Photo II-13. Thin section 95-A3-184 (+ nic). Lamellar growth of colourless amphibole within green hornblende according to {001}.

Orthogneisses in the Complex of Santiago de Compostela

A formation of planar or planolinear orthogneisses has been mapped in the Complex of Santiago de Compostela. The width of the N-S striking band varies greatly. The outcrop of these gneisses forms N-S running ridges. The eastern part of the city of Santiago de Compostela has been built upon this rock type. The N-S strike and the subvertical east-dipping folia-

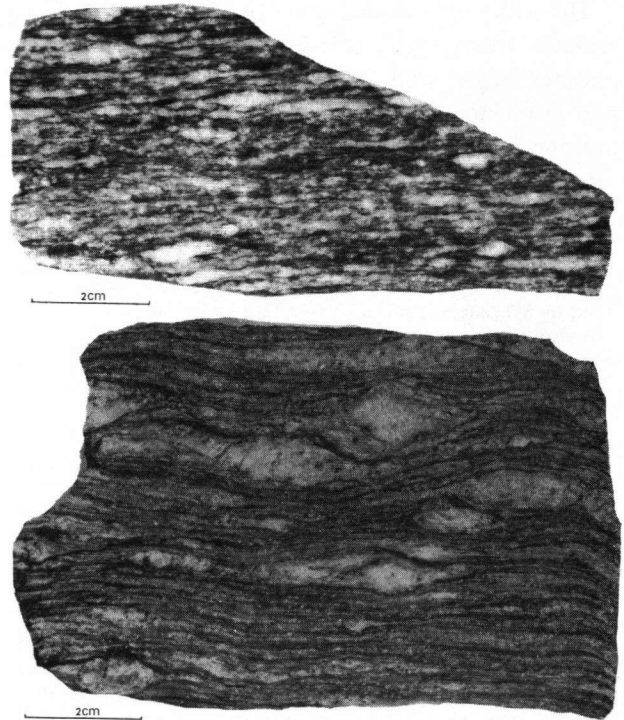


Photo II-14. Two types of orthogneisses: a. the planar type (sample 94-E3-10), b. planolinear augengneiss type with porphyroclasts of potash feldspar (sample 94-E2-28).

tion planes are constant, except to the south of Santiago de Compostela. Here the strike swings to the NW-SE. This aberration could be explained by accommodation of the structures in the orthogneisses to the shape of the competent basic massif during late-Hercynian phyllonitization and dislocations.

In the field various types of orthogneisses could be distinguished. Sometimes the rocks are planar but a planolinear augengneiss type is also present (Photograph II-14a and 14b). Mineralogically we can discern a biotite-rich and a muscovite-rich type. The distribution of these types is irregular. Inclusions of amphibolites and interstratifications of porphyroblastic albite-schists have been observed. The porphyroblastic albite-schist horizons are concentrated at the border zone of the orthogneiss body. Floor (1966) has described such rocks in southern Galicia. He states that the rocks are pre-Hercynian granites (intruded during the transition from Cambrian to Ordovician) which were foliated by the Hercynian orogeny. The rocks have a distinct blastomylonitic structure. The orthogneisses also have a greenschist-facies assemblage similar to the adjacent schists.

Macroscopically a well-developed foliation is visible in the leucocratic rock. The flattened eyes are aggregates composed predominantly of plagioclase, potash feldspar and quartz.

Microscopical appearance. – The undulose quartz grains are arranged in a mosaic pattern.

Plagioclase (3–8% An.) is poikiloblastically developed and contains a profusion of inclusions. Polysynthetic twinning and simple twins along {010} are common.

Potash feldspar occasionally has a cross-hatched twinning. The clasts frequently enclose plagioclase and quartz.

Muscovite has pale-green tinges. The flakes are slightly deformed.

The occurrence of green and brown *biotite* is striking.

Small crystals of *garnet* (\varnothing up to 0.05 mm) are present in the greenish *biotite* and in *muscovite*.

Minor *sillimanite* needles in *muscovite* are probably due to the influence of the two-mica granites.

Epidote rims around *allanite* have been observed. The metamict cores of *allanite* have an orange colour.

Zircon in pleochroic haloes in *muscovite*, *apatite* and opaque minerals are minor constituents (thin sections 94-E3-10 and 94-E1-16).

Orthogneisses in the Ordenes Complex

Original granitic sills are also observed in the basic rocks of the Ordenes Complex, north of Bando. The foliation of these rocks is concordant with the direction found in the metabasites.

In the metabasic rocks on the Castelo de Vigo Hill, a foliated pegmatitic dyke has been found, crosscutting the structures in the metabasites (Photograph II-15). It seems therefore justifiable to regard these acid rocks as younger than the adjacent amphibolites. A correlation between these rocks and those found in the Complex of Santiago de Compostela cannot be proven.



Photo II-15. Foliated pegmatite on the crest of the Castelo de Vigo Hill, cutting the metabasites discordantly.

Small bodies of orthogneisses have been noted on the southern slope of the Formaris Hill in the Ordenes Complex. The foliation has a N-S direction.

The rocks are macroscopically planar and fine-grained.

Microscopical appearance. – Deformed xenomorphic quartz

grains are often elongated parallel to the trace of the foliation plane.

Plagioclase (8–13% An.) often displays a normal zoning. The plagioclase-clasts are bent.

The *potash feldspar* has a cross-hatched twinning. This mineral frequently grows interstitially.

Brownish *biotite*, as well as *muscovite*, has been deformed.

Zircon, occurring as tiny prisms but also in pleochroic haloes in *biotite*, *apatite* and opaque minerals are minor constituents (thin section 95-A2-318).

Metadiorites

North of Santiago de Compostela, several metadioritic bodies have been mapped including several small massifs near or along the thrust zone. The age of these rocks is uncertain but the absence of high-grade metamorphic relics points to a monometamorphic rock. In that case, an approximate Lower-Paleozoic age of intrusion has been assumed and the rocks are taken to have suffered only Hercynian metamorphism.

In the field the metadiorites show all the transitions from undeformed rocks with palimpsest gabbroic textures to rocks with a well-developed foliation.

Microscopical appearance. – Fine-grained quartz crystals have been slightly deformed.

Plagioclase is totally saussuritized. The grains are up to 4 mm long.

Hornblende often has a brownish-green core with a green rim. Probably two types are present: one type includes clouds of opaque minerals and the other shows polysynthetic twinning.

Chlorite occurs as large flakes which probably are alterations of *biotite*.

Clinzoisite is often observed as altered plagioclase crystals.

Accessory minerals are *zircon* in pleochroic haloes in *chlorite*, *apatite*, *muscovite*, (*sericite*), *sphene* and opaque minerals (thin section 95-A2-93).

Megacrystal-bearing two-mica granites

As stated previously, the two-mica granites are located in the western extremity of the area; Warnars (1967) described these rocks as the two-mica granites of Villardoa. The granites are inequigranular fine- to medium-grained rocks. The contacts with the schists are sharp and only a few xenoliths have been observed. Laths of potash feldspar have a preferred orientation (Photograph II-16). The orientation is probably due to a parallel arrangement of the potash feldspar megacrysts during the intrusion of magma. In some localities, the rocks underwent phyllonitization due to a late-Hercynian deformation phase on a subvertical B-axis.

Macroscopically the granites are medium-grained holocrystalline rocks with potash feldspar megacrysts of about 1 cm.



Photo II-16. Preferred orientation of potash feldspar laths (parallel to ballpoint) in a two-mica granite northwest of Santiago de Compostela.

Microscopical appearance. – The xenomorphic quartz grains have undulose extinction. Plagioclase (3–5% An.) is sometimes hypidiomorphic. The cores of the crystals are often turbid, owing to sericitization.

Potash feldspar with a cross-hatched twinning also has simple twins along the {010}-planes. Sometimes it shows the formation of vein and patch perthite.

Muscovite flakes are often found in booklets and are sometimes deformed.

Brown and green biotite are frequently intergrown with muscovite.

Sagenite needles are embedded in most of the biotite flakes.

Zircon in pleochroic haloes in micas, apatite, chlorite (an alteration from biotite), fluorite, anatase and opaque minerals are minor constituents (thin section 94-E1-17).

Dolerites, pegmatites and quartz veins

Dolerites. – In the Ordenes Complex, a swarm of dykes is found with a gabbroic or dioritic composition. The rocks are non-porphyrific and fine-grained. The dykes are frequently located in the metasediments, but north of Bando an olivine-dolerite dyke has been found in the metabasites. Because of their well-preserved appearance, it is possible that their emplacement was later than the acid intrusions. Some of the hypabyssal rocks are epidioritized by hydrothermal solutions. The dykes are discordant with regard to all the rocks in the Ordenes Complex.

Macroscopically the rock is fine-grained to microcrystalline and has a distinct ophitic texture.

Microscopical appearance. – The hypidiomorphic plagioclase (65–70% An.) has polysynthetic twins along {010} and {001}. The lath-shaped grains embay mafic minerals such as olivine and clinopyroxene.

Rounded olivine is colourless and sometimes has inclusions of greenish-brown spinel and opaque material. Olivine shows a corona texture. The grains are surrounded by a colourless orthopyroxene rim and the outer rim consists of pale-brownish clinopyroxene. Occasionally the outer rim of clinopyroxene has a border of fibrous greenish hornblende (see Fig. II-3).

Clinopyroxene is xenomorphic with Schiller inclusions and brownish tinges. At the borders, the brown colour is somewhat darker. Alterations to uraltic amphibole have been observed. Accessory minerals are spinel, a reddish-brown alteration product of olivine (*iddingsite?*), and opaque minerals (thin section 95-A3-153).

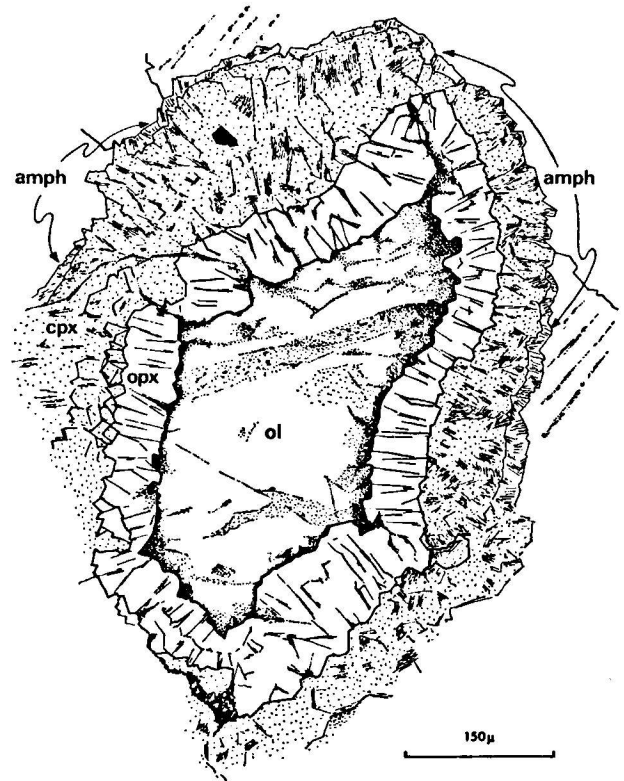


Fig. II-3. Corona around olivine of orthopyroxene and clinopyroxene; the latter has been replaced by amphibole. Thin section 95-A3-153.

Hornblende-quartz-diorite-pegmatites. – As previously mentioned (cf. p. 8), at the western border of the metabasites the occurrence of hornblende-quartz-diorite-pegmatites has been noted. The hornblende crystals are sometimes 3–4 cm long in the direction of the *c*-axis.

Garnet-tourmaline-pegmatites. – Closely associated with migmatites and two-mica granites are pegmatites which have been injected into the metasediments. The rocks consist essentially of quartz, potash feldspar, plagioclase, muscovite, tourmaline and garnet. The pegmatitic dykes are frequently parallel to the regional schistosity.

Quartz veins. – Quartz veins are widely distributed over the area. At certain localities, especially in dislocation zones, they occur as large veins. Examples are the

Pico Sacro quartz vein and two veins in the two-mica granites with NW-SE direction.

CONCLUDING REMARKS

From the preceding petrographic investigation, the following conclusions can be drawn:

1. The Ordenes Complex underwent intermediate- to high-pressure metamorphism during a probably pre-Hercynian orogeny
2. The rocks of the Complex of Santiago de Compostela and the Ordenes Complex have suffered low-pressure metamorphism during the Hercynian orogeny. Therefore, the Ordenes Complex is considered poly-metamorphic
3. The growth of albite-porphyroblasts took place after the Hercynian main phase metamorphism (M_3)
4. Migmatization followed after the main phase of Hercynian metamorphism and destroyed many older structures
5. Contact metamorphism around two-mica granites gave rise to the formation of muscovite, chlorite, biotite, andalusite, chloritoid, cordierite (?) and sillimanite.

MINERALOGY

Hornblende

Hornblendes from amphibolites and hornblende-plagiopyrigarnites of the metabasic massif have been investigated for their trace-elements. The samples were prepared by passing the crushed rock through a sieve. A fraction (100–50 μ) of the crushed rock was chosen for separation; an isodynamic separator was used. Further purification was obtained by applying gravitative methods. Methylene iodide and tetrabromoethane were used as separation liquids.

The results of the quantitative spectographic analyses are presented in Table II-2. The discrepancies between the results of duplicate analyses of one sample are sometimes striking. In general a toleration of 10–20% is acceptable. Inspection of Table II-2 points perhaps to an increase in the amounts of Ti, V, Zn and Co with increasing grade of metamorphism. In this case it is impossible to make statistical inferences on the basis of the present results, since the number of observations is too small. Engel, Engel & Havens (1961) reported the same trend for amphibolites from Emeryville to hornblende-granulitic rocks in the Colton area, except for the amount of Zn which decreased in the high-grade hornblendes.

Table II-2. Trace element analyses (carried out at Imperial College, London) of hornblende from pyrigarnites and amphibolites (quantitative spectographic analyses in parts per million; each sample was determined in duplicate).

	plagiopyrigarnites				amphibolites							
	95-A4-218		95-A4-205		95-A4-253		95-A3-158		95-A3-99		95-A3-182	
Ag	0.8	0.6	1.6	1.6	1.3	1.6	0.8	0.8	0.3	0.2	1.3	1.6
Bi	5	5	5	5	5	5	5	5	5	5	5	5
Co	160	130	85	85	85	85	60	85	60	60	60	60
Cr	600	400	600	600	600	600	600	600	600	400	600	1000
Cu	4	2	30	30	8	8	2	2	3	3	8	16
Ga	20	16	30	20	20	16	20	20	30	16	13	16
Ge	300	300	400	300	400	300	300	400	300	300	300	300
Mn	1300	1300	1300	1300	1300	1300	1300	1300	1300	1000	850	1000
Mo	2	2	2	2	2	2	2	2	2	2	2	2
Ni	300	350	300	300	400	400	300	400	300	300	200	300
Pb	8	8	13	13	8	10	8	8	8	6	6	10
Sn	5	5	5	5	5	5	5	5	5	5	5	5
Ti	5000	4500	8500	8500	8500	8500	6000	6000	5000	4000	3000	3000
V	1600	1300	1600	1300	1000	1000	850	850	850	600	600	850
Zn	300	200	200	150	50	60	85	60	85	60	50	60
	green hornblende (core brownish-green)		brownish-green hornblende		brownish-green hornblende		brownish-green hornblende		bluish-green hornblende		bluish-green hornblende	

95-A4-218 green hornblende from a hornblende-plagiopyrigarnite of the Pena Mayor.

95-A4-205 brownish-green hornblende from a hornblende-plagiopyrigarnite of the Coto de Viso.

95-A4-253 brownish-green hornblende from an amphibolite south of the Coto de Viso.

95-A3-158 brownish-green hornblende from a metagabbro near Bando.

95-A3-99 bluish-green hornblende from an amphibolite north of Bando.

95-A3-182 bluish-green hornblende from an amphibolite west of Bando.

Garnets

Procedures. – For measuring the refractive indices and the unit cell size (a_0), the samples were prepared using an isodynamic separator and gravitative separation with the help of methylene iodide and Clerici solution. The refractive index was determined by using the Cargille set of index liquids. The cell edges (a_0) were obtained from X-ray powder photographs. Quantitative analyses were carried out with an electron-microprobe analyzer following the methods of Atherton & Edmunds (1966).

Computation of garnet-endmembers. – The analyses were calculated by using the formula $X_3Y_2Z_3O_{12}$. The cations were calculated on the basis of 12 oxygens. In the above-mentioned formula X stands for Ca^{2+} , Mg^{2+} , Mn^{2+} , Fe^{2+} and sometimes Fe^{3+} cations, Y for Al^{3+} and Fe^{3+} cations and Z for Si^{4+} and Al^{3+} cations.

In those cases where the number of cations to 12 oxygens is less than 8, vacancies in the lattice are assumed (cf. Vogel, 1967, p. 195).

Quantitative chemical analyses. – The results of quantitative analyses of two specimens of garnet from retrograde hornblende-plagiopyrigarnites and two from high-grade kyanite-garnet-biotite-muscovite-gneisses are listed in Table II-3.

Inspection of Table II-3, considering only the garnets of the metabasites, suggests a close similarity to the results obtained by Warnars (1967, p. 112) from garnet-bearing amphibolites. The higher Py-content in our rocks indicates a transition to granulite-facies conditions. The garnet are grossularite-rich, probably due to the composition of the host rock. A graphic presentation of the chemical compositions is shown in the triangular diagram (Al+Sp)–(Gr+An)–Py (Fig. II-4).

For purposes of comparison, the composition of garnets from garnetiferous amphibolites (Warnars, 1967) and from plagiopyrigarnites from Cabo Ortegal (Vogel, 1967) is plotted. The threefold division of metamorphism (den Tex, 1965) can be incorporated in the diagram. From the plottings, it can be seen that the composition of our garnets and those from Cabo Ortegal falls within the range of the high-pressure lineage field.

Yakovlev's (1966) analyses of garnets are shown as two domains. The value indicating such a field is relatively poor since the composition of garnets depends not only on metamorphic grade but also on

Table II-3. Chemical analyses (performed by F. W. Warnars) of garnets from metasediments and metabasites of the Ordenes Complex.

	metabasites		metasediments		
	B1-304	A4-215	B3-2	B2-10 core	B2-10 rim
wt.% SiO ₂	38.4	37.8	37.0	37.0	38.0
Al ₂ O ₃	20.7	21.1	21.0	21.0	20.8
Fe ₂ O ₃	1.6	0.6	?	?	1.1
FeO	22.5	26.1	32.4	31.3	32.0
MnO	13.7	10.9	1.2	6.1	1.5
MgO	3.0	2.7	3.5	1.9	3.0
CaO	0.6	0.5	3.4	2.5	5.2
	100.5	99.7	98.5	99.8	101.6

Calculation of cations on the basis of 12 oxygens

Z	Si	3.02	3.12	3.12	3.12	2.90
	Al	–	–	–	–	0.10
Y	Al	1.91	1.98	2.10	2.10	1.85
	Fe ³⁺	0.09	0.02	–	–	0.15
	Fe ³⁺	1.46	1.75	2.21	2.13	1.96
	Fe ²⁺	–	–	–	–	–
X	Mn	0.04	0.03	0.08	0.42	0.10
	Mg	0.35	0.32	0.42	0.23	0.34
	Ca	1.15	0.92	0.29	0.22	0.43

Computation of the endmembers

Py	11.7	10.7	14.0	7.7	11.3 ²
Al	48.7	57.7	73.7	71.0	65.3
Sp	1.3	1.0	2.7	14.0	3.3
An	4.5	1.0	–	–	7.5
Gr	33.8	29.7	9.7	7.3	6.8

² A deficit of 5.7% is present in this analysis.

the oxidation ratio of the rock (Hsu, 1968; Hounslow & Moore, 1967, p. 16), the bulk chemistry and sometimes the different affinities of one element for certain minerals.

All these phenomena should be kept in mind when interpreting composition fields for garnets derived from compilation work. In spite of these restrictions, the presentation of such diagrams can be illuminating when only garnets from one area are used where the physical conditions are well-known and the bulk chemistry of the different metamorphic rocks is the same.

The composition of the garnets from metasediments recalculated to their endmembers is shown in Fig. II-5. The high almandine content is remarkable. The garnets are derived from kyanite-garnet-biotite-muscovite-gneisses of the Ordenes Complex. Zoned garnets are often observed in metamorphic areas. Garnets from sample 95-B2-10 display such a symmetrical zoning. The spessartine content varies from 14% at the core to 3.3% at the rim, whereas the pyrope content in-

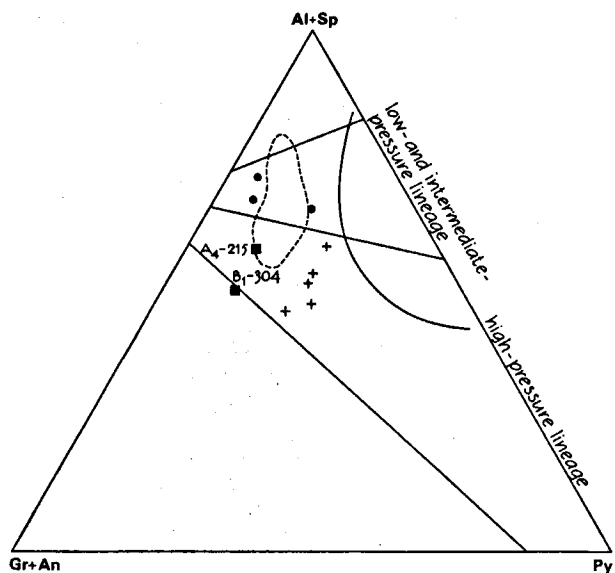


Fig. II-4. Composition of garnets from metabasites indicated in the (Al + Sp)-(Gr + An)-Py triangular diagram.

- garnetiferous amphibolites (Warnaars, 1967);
- + plagiopyrigarnites from Cabo Ortegal (Vogel, 1967);
- hornblende-plagiopyrigarnites from the Ordenes Complex; Yakovlev's (1966) composition fields for garnets from amphibolites (dashed lines) and from mafic granulite-facies rocks (solid line) are drawn.

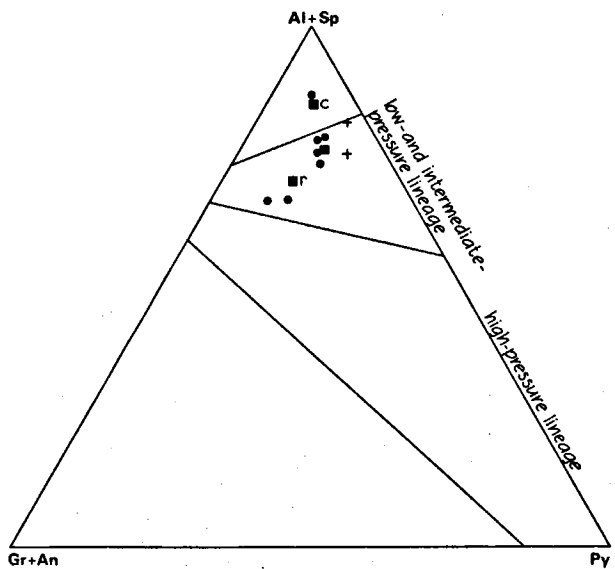


Fig. II-5. Composition of garnets from metasediments indicated in the (Al + Sp)-(Gr + An)-Py triangular diagram.

- Grenville schists (Hounslow & Moore, 1967);
- + garnets from paragneisses at Emeryville, Adirondacks, Engel & Engel (1960);
- garnets from high-grade gneisses of the Ordenes Complex (c = core, r = rim).

increases towards the rim. The same features are described by Atherton & Edmunds (1966) for garnets from Zermatt (Switzerland). In a later paper, Atherton (1968) states that zoned garnets from the Dalradian schists are due to segregation. Concisely rendered, he emphasizes the importance of the distribution coefficient for elements during growth. A decrease in MnO and CaO during growth is due to a decrease in the distribution coefficient values for these elements. Garnets occurring in high-grade Grenville schists (Hounslow

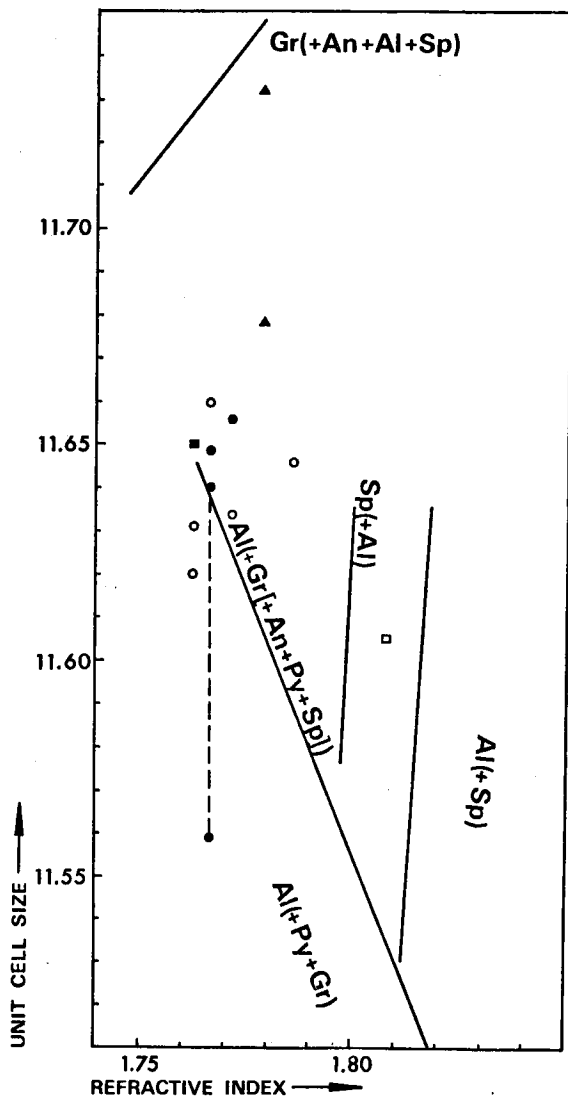


Fig. II-6. a_0-n_D diagram derived from Frietsch (1957).

- garnets from hornblende-plagiopyrigarnites (dashed line indicates a zoned garnet);
- garnets from garnetiferous amphibolites;
- garnet from a high-grade gneiss;
- garnet from a low-grade schist;
- ▲ garnets from calc-silicate rocks.

Cell edge values and n_D are listed in Table II-4.

& Moore, 1967) from the staurolite and kyanite zone are plotted together with the results of Engel & Engel (1962) at Emeryville, Adirondack Mountains. Metamorphism goes from amphibolite facies at Emeryville to granulite facies at Colton. As stated previously (p. 7), the metasediments are metamorphosed in the kyanite-almandine-muscovite subfacies of the amphibolite facies.

Physical properties of garnets. – The graphic representation of a_0 and R.I. for garnets according to the method of Frietsch (1957) is used in many papers containing descriptions of regional metamorphic areas. The absolute meaning of such a diagram is of little importance since the chemical composition of the garnets can only be derived approximately. As previously mentioned, the composition of garnets is not dependent on metamorphic grade alone. Nevertheless one can see the differences within one area, for instance between amphibolite-facies rocks and granulite-facies rocks, when plots of the different types are grouped. Overlapping of the fields due to retrogradation or transition to higher grade rocks often makes the diagrams rather vague (cf. Vogel, 1967, p. 197).

The results of determinations of a_0 and R.I. for garnets from hornblende-plagiopyrigarnites, garnet-bearing amphibolites, calc-silicate rocks, high-grade gneisses of the Ordenes Complex and low-grade schists of the Complex of Santiago de Compostela are listed in Table II-4 and graphically represented in Fig. II-6.

Table II-4. Cell edge values and indices of refraction for garnets plotted in Fig. II-6.

Registration number of X-ray photograph	Sample number	n_{Na} (± 0.002)	\bar{a}_0	
3887	95-A4-218	1.773	11.656	} hornblende-plagiopyrigarnites
3885	95-A3-112 ^c	1.767	11.648	
3889	95-B4-226	1.767	11.558 11.640	
3673	95-A3-126	1.767	11.660	} garnetiferous amphibolites
3526	95-A3-108	1.787	11.645	
3671	95-A3- 82	1.763	11.620	
3882	95-A3- 86	1.767	11.633	
3883	95-A3- 95	1.763	11.631	
3744	95-B3- 50	1.763	11.650	high-grade gneiss
4186	94-E1-192	1.807	11.605	low-grade schist
3886	95-A3-127	1.777	11.678	} calc-silicate rocks
3525	95-A3- 61 ^a	1.777	11.731	

The grossularite-rich garnets from the calc-silicate rocks are conspicuous because of their high a_0 -values. There exists a striking difference between the values for the high-grade and low-grade gneiss-schists. It seems possible that the latter has a higher manganese content.

CHAPTER III

TECTONICS

INTRODUCTION

General remarks

The unravelling of the structures of the complexes described is the main scope of this study. The relationship between structural development and metamorphism has been investigated and it will be shown that the study of this connection is indispensable for the relative dating of the structural events.

The examination of the major and minor structures in the area is completed with the petrofabric analysis of specific minerals in the next chapter. Petrofabrics

should be applied to those problems where structural field investigation fails and it should also support the results of tectonic analysis from field observations.

During the last twelve years, the mapping of several crystalline areas in Galicia has been completed (Floor, 1966; Vogel, 1967; Warnaars, 1967; and many internal reports). The emphasis was placed on petrography and therefore the structural aspects lagged behind. One exception is a paper by Avé Lallemant (1965) in which a structural account of an area around Muros (NW Spain) has been given. A thesis under preparation by

J. P. Engels deals with the structures near Cabo Ortegal (NW Spain). Since the area under discussion is a relatively small part of the Galician-Castilian zone³, large-scale structures are difficult to recognize. For this reason, only a local structural development could be established. The rocks are poorly exposed in the area and this restricts structural investigation to measurements at scattered localities. Therefore it was almost impossible to avoid extrapolations of structural trends and this must be kept in mind when evaluating the structural map (Enclosure III) and cross-sections.

As mentioned in the foregoing chapters, the rocks were divided into two complexes: (a) the intermediate-to high-pressure series of the Ordenes Complex and (b) the low-pressure series of the Complex of Santiago de Compostela. There are not only petrographical but also structural reasons for separating these complexes. The structural study has shown that older structures occur in the rocks of the Ordenes Complex. The possibility that some crystalline parts of Galicia underwent polymetamorphism has been discussed by others, such as den Tex (1966). Absolute evidence for a polyorogenic history can be derived only from radiometric age-determinations or from the presence of an unconformity between a basement and a younger sequence. Neither of these are available and therefore one could formulate two hypotheses: (a) the rocks in the mapped area have suffered only Hercynian metamorphism which implies that the rocks of the Ordenes Complex are part of an Hercynian infrastructure or (b) the mapped area contains some rocks which have been metamorphosed during more orogenies and are polymetamorphic. It will be shown that the latter interpretation is preferable.

Nomenclature

The terminology of rock deformation has been chiefly adopted from Ramsay (1967).

X, Y, Z – measured ellipsoid axes of a deformed sphere with radius r^4

a, b, c – axes defining direction of translation by simple shear

A, B, C – axes of fabric symmetry

For the terminology for planar and linear structures, we have partly used Sander's connotation (1948) which is also advocated by Turner & Weiss (1963, p. 131).

³ The Galician-Castilian zone of the Hesperian massif is defined by Lotze (1945) as a part of the crystalline rocks of NW Spain and N Portugal up to the Guadarrama Mts.

⁴ Flinn (1962) denotes the major axes of the deformation ellipsoid as $Z \geq Y \geq X$, conforming to the practice in mineralogy for indicatrix axes. Ramsay (1967) designates the axes $X \geq Y \geq Z$.

ss sedimentary stratification
s₀, s₁, s₂, etc. *s*-surfaces including foliations, schistosity, cleavages and axial planes; the subscripts denote the chronological order
l₁, l₂, l₃, etc. lineations; the subscripts give the chronological order; the intersection of the sedimentary stratification and *s₁, s₂, etc.* is designated $\delta_1, \delta_2, etc.$ or *l₁, l₂, etc.*
F₁, F₂, F₃, etc. phases of folding in chronological order

In contrast to the usage of Turner & Weiss, we do not use capital letters for linear and planar structures.

Applied methods

Subareas. – In order to provide the reader an insight into the structural pattern, the area has been divided into twelve subareas or domains (Encl. III). Structural homogeneity determines the size and shape of each subarea. Thus in each subarea, poles to schistosity or foliation planes have been plotted on an equal-area net (lower hemisphere) and the densities have been contoured. Directions of linear structures have been indicated in the same diagrams. In spite of the fact that the distribution of the measurements in a subarea is unfortunately dependent upon the localities where the rocks are exposed, this method makes it still possible to resolve an intricate structural pattern into simple structures in which the relationship between minor and major folds on the one hand and between lineations and folding on the other, can be detected.

Constructions. – The geometry of deformed linear structures has occasionally been investigated. For large-scale structures, we could derive the kind of folding from the results of such an analysis because often such folds cannot be studied in detail. In stereograms of deformed lineations (by similar folding), the translation direction *a* could be constructed. The construction procedures and theory have been extensively described by Ramsay (1960 and 1967).

PRE-HERCYNIAN STRUCTURES (?)

As previously mentioned, the structures in the Ordenes Complex are more complicated than those in the Complex of Santiago de Compostela. Subtracting the structures occurring in the low-pressure rocks from



Photo III-1. F_1 -folds at the Pena Mayor. The stratified retrogressive plagiopyrigarnites have been folded and the development of an amphibole lineation, approximately parallel to the fold axis, was apparent (looking N).

those found in the intermediate- to high-pressure rocks, several older tectonic phenomena may be resolved. The fold structures discovered in the low-pressure series are supposed to belong to an Hercynian orogenic cycle. The fold geometry of the F_1 -folds in the metabasic rocks and metasediments will be discussed separately.

F_1 -folding

Metabasic rocks. – A glance at the structural map (Encl. III) reveals that the structures in the western and eastern extremities of the metabasites are closely aligned to the contiguous metasediments. The central and northern sections show a different structural picture. The general structural trend in West Galicia is approximately N-S.

In order to determine Hercynian structural trends we should investigate rocks which were metamorphosed only during the Hercynian orogeny. The orthogneisses are rocks which, one can be sure, were gneissified only during the Hercynian orogeny (cf. p. 20). Logical reasoning therefore, leads to the identification of the N-S structures of the orthogneisses as representing the

most important Hercynian direction. The central and northern sections of the metabasites (with predominantly E-W structures) enable us to investigate structures without a dominating, superimposed N-S system.

Before F_1 -folding, a certain layering already existed in the rocks and is marked by differences in colour and in the mineralogical composition. This surface is designated s_0 . Inhomogeneous strain and homogeneous strain of the rocks have induced a folding (F_1) of s_0 . The asymmetric folds are of a similar⁵ type (Photographs III-1, III-2). The isoclinal to tight recumbent folds (nomenclature of folds according to Fleuty, 1964) have been overturned to the east as well as to the west although the former direction predominates.

At the centre of the metabasites, on the crest of the Pena Mayor, some of these F_1 -folds are exposed (Photograph III-1). Poles to foliation planes of this subarea are plotted on diagram 10 (Encl. III). Because of the tightness of the folds under discussion, the axial

⁵ The descriptive term 'similar fold' has been used to avoid the expression 'shear fold' which has a genetic connotation.

planes are, except in the fold hinges, parallel to s_0 . The axial planes (s_1) have an horizontal attitude or dip slightly to the north. The axial direction varies between north and north-northwest (diagram 10, Encl. III).

The position of the F_1 -folds to the north (subarea 8) has been influenced by younger fold movements. The strike of the axial planes remains rather constant (E-W) but the dip becomes steeper to the north. The fold axes also plunge therefore more steeply to the north (Photograph III-2).



Photo III-2. F_1 -folds at Castro which have developed in garnet-bearing amphibolites. The axial planes (E-W) have been steepened by later folding (looking at an horizontal plane).

The F_1 -deformation was accompanied by hornblende clinopyroxene - almandine - subfacies metamorphism (M_1). The formation of amphiboles gives the rocks a mineral lineation (l_1) parallel to the fold axis (Fig. III-1). These mineral lineations have been plotted in diagrams 8 and 10 (Encl. III).

The time-relationship of deformation and metamorphism seems to be such that the climax of metamorphism postdated that of deformation. It has not been possible to establish whether the above-mentioned mesoscopic structures are related to major folds.

The absence of markerbeds and the small number of observations prevented the detection of such major structures.

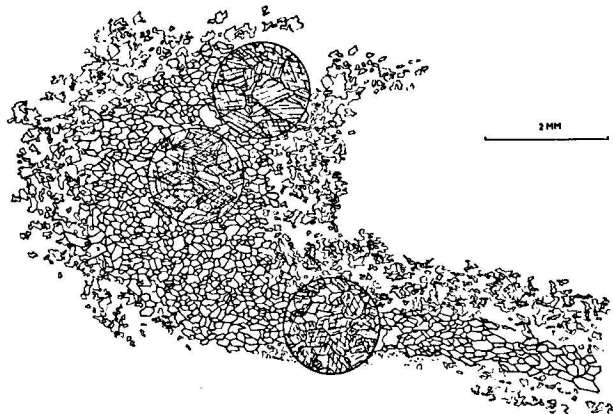


Fig. III-1. Drawing of thin section 95-A4-300, a detail of Photograph III-1. The c -axes of hornblende are parallel to the B-axis of the F_1 -fold. The orientation of the {110}- and {100}-planes can be seen in the circular enlargements.

Metasediments. - The difference in physical properties between the metabasic rocks and metasediments is expressed in the preservation of the pre-Hercynian (?) structures. It appears that in the incompetent metasediments, the younger movements have completely overprinted the older structures. Only some relic structures are left, which will be discussed later.

North of Berdia, near the Santiago-La Coruña Railroad, some recumbent folds have been found with a meridional axial direction and subhorizontal plunge

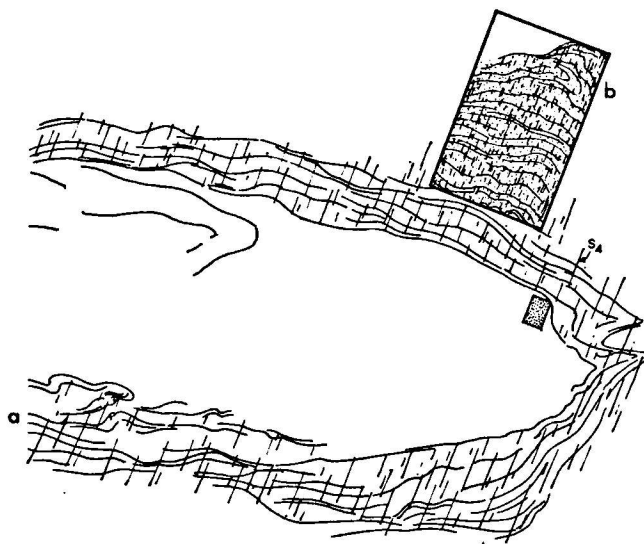


Fig. III-2. a. Recumbent F_1 -fold in metasediments of the Ordenes Complex. The exposure is situated north of Berdia. A second schistosity (s_4), with a N-S strike, has been superimposed (looking S). b. The inset shows on a microscopical scale the relationship between the schistositities.

(diagram 3, subarea 3). The structures of the first Hercynian folding (F_4) cut across these folds with subvertical N-S striking axial planes (Fig. III-2a and 2b).

SSW of Berdia, where the Santiago-La Coruña Rail-

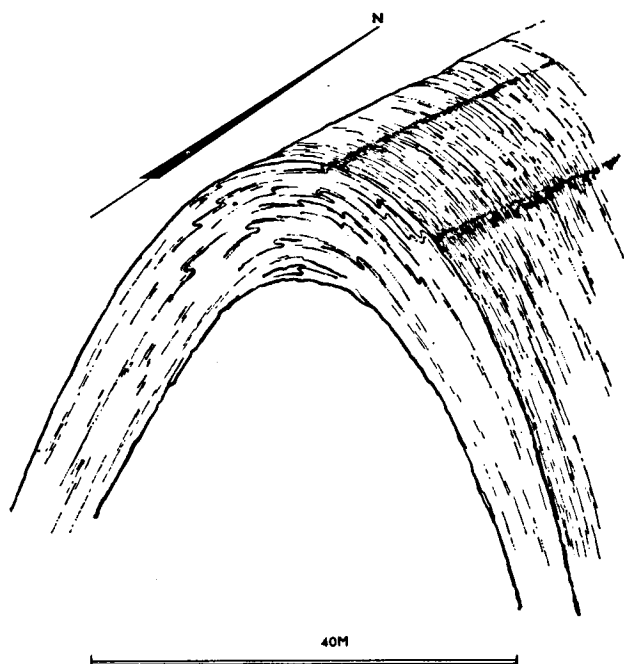


Fig. III-3. Interference pattern between supposed recumbent F_1 -folds and a large-scale N-S antiform of Hercynian age (F_4 ?). Location is about 1 km south of Berdia.

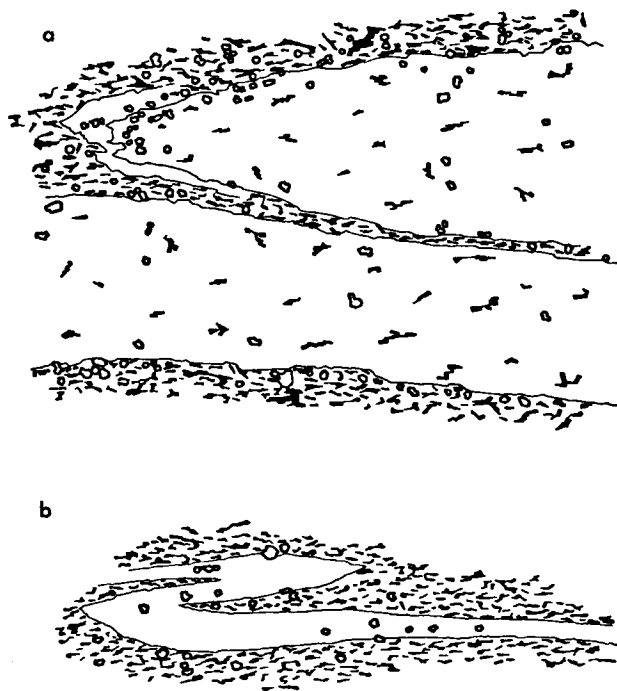
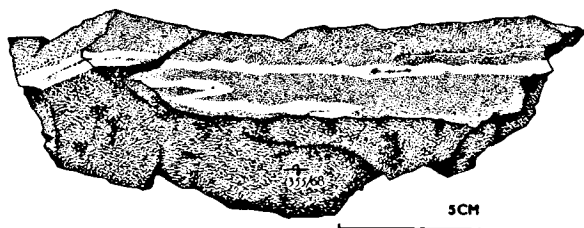


Fig. III-4. a. Drawing of hand-specimen 95-A2-312 and its thin section. b. Another specimen taken from locality 95-A3-300. Both drawings show the development of the s_1 -schistosity parallel to the axial planes of the F_1 -folds. The main constituent of the recrystallized minerals is biotite; some garnets are visible.

road crosses a tributary of the Tambre River, one can observe the aspect of F_1 -folds. The major structure is an antiform; the axis plunges slightly to the north. The geometry of this large-scale Hercynian fold will be discussed on p. 37. In the hinge zone, asymmetric minor folds, which are not related to the major fold, are overturned to the west (Fig. III-3). The axial direction of these small folds is to the north, almost coincident with the major folds (diagram 3, Encl. III). The axial planes (s_1) became curvilinear by refolding on a subvertical axial plane.

F_1 minor folds have been observed on a microscopical scale. Some drawings have been made and are shown in Fig. III-4a and 4b. The s_0 -plane, forming the limbs of the F_1 -folds, could not be identified with certainty as *ss*. The layering is marked by an alternation of bands with micaceous minerals and quartz-feldspar-bearing streaks. The F_1 -folding was accompanied by staurolite-almandine-subfacies metamorphism culminating in kyanite-muscovite-almandine-subfacies metamorphism of the almandine-amphibolite facies. The kyanite-staurolite assemblage is a diagnostic mineral-pair in the intermediate- to high-pressure series of regional metamorphism (Zwart *et al.*, 1967).

The growth of staurolite was postkinematic as shown by the straight inclusions in this mineral. This is illustrated in Fig. II-2, p. 10.



F₂-folding

The second set of folds in the Ordenes Complex are often situated in zones of intense movement. The rocks were mylonitized and later recrystallization gave rise to the formation of blastomylonites. Three zones of thrusting have been recognized: 1) the boundary zone between the two complexes 2) the thrust zone in the central part of the metabasites near the Castelo de Vigo 3) the blastomylonite zone near the northern boundary between the metabasites and metasediments of the Ordenes Complex. The thrust planes dip moderately in varying directions.

The attitudes of the first and third thrusts have been reoriented by later folding. These thrusts appear to have been steepened during younger movements. The thrust zone near the Castelo de Vigo is poorly exposed; the foliation of the rocks dips subhorizontally toward the north, whereas the fault plane dips more steeply to the northwest. A schematic N-S cross-section is depicted in the geological map (Encl. I). The entire structure in the metabasites seems to be an imbricate structure in which overlapping slices occur. From the growth of green hornblende and the recrystallization of plagioclase, we can deduce an amphibolite-facies metamorphism (cf. p.14) penecontemporaneous with F₂.

Boundary zone between the two complexes. – On the structural map (Encl. III), the position of the boundary zone is indicated as a N-S trending zone of movement. To the southeast of Santiago de Compostela this zone turns toward the NW-SE. The attitude of the thrust plane varies from steeply to moderately inclined to the east or northeast.

At a number of localities in the thrust zone which borders the metabasites, the amphibolites have been blastomylonitized. On petrographical grounds (see p.14), it could be deduced that neomineralization took place during, but especially after, the deformation. Laminated mylonites have been formed during Hercynian phases of deformation. The texture of these rocks is cataclastic. The younger movements, causing mylonitization and dislocation, disoriented the older linear structures in such a way that their directions form a disorganized picture. The thrust outcrop in the metasediments was chiefly established using petrographical data.

The thrust zone near the Castelo de Vigo. – In the vicinity of this thrust zone, many recumbent folds with monoclinic symmetry were found which are overturned to the S or SSE (Photograph III-3). The foliation of the mylonitic rocks, north of the thrust,



Photo III-3. Recumbent F₂-folds, on the crest of the Pena Mayor, in metabasic rocks. The folds are overturned to the S or SSE (looking E).

is subhorizontal. The general trend of the thrust varies between NE-SW near the Castelo de Vigo to nearly E-W south of the Pena Mayor.

Diagram 10 of subarea 10 shows the axial directions of the folds which plunge anywhere between ENE and E. The minor folds have been thickened in the hinges and attenuated at the limbs (Photograph III-4). The irregular form and the spread of the axial directions of the folds could be explained by the plastic condition of the rocks during deformation. This kind of folding was recently described by Howard (1968). He indicated that the flow direction is rather constant while the fold axes are irregularly oriented.



Photo III-4. Specimen of a folded blastomylonitic metabasic rock, indicating the strong plasticity of the rocks during deformation. Hand-specimen 95-B4-221 A.

The translation direction a could be determined at the Pena Mayor. The ENE plunging fold axes are rather constant in direction here. Since the N-S trending, linear structures (l_1) have been affected by this folding, the translation direction a could be deduced. Because the plane, containing the deformed lineations, is almost normal to the axial plane, we obtain approximately a N-S direction as movement direction. The sense of vergence to the S or SSE appears to be in the translation direction a .

Thrust zone at the northern outcrop of the metabasites. – The amphibolites are partly developed as blastomylonites along this thrust zone. The foliation in the blastomylonites is parallel to that of the undisturbed amphibolites in the vicinity. The dip is moderately inclined towards the north, but later large-scale folding induced a slight spread in this direction. The style of folding suggests strong flow during deformation. The folds have been disrupted and have become rootless (Photograph III-5). Only a few folds could be found and

the axial direction is gently plunging approximately to the WNW (diagram 8, Encl. III). Hornblende prisms are aligned parallel to the fold axes. This mineral lineation (l_2) is well-developed in the northern part of the metabasites (see diagram 8, Encl. III).



Photo III-5. Specimen of folded blastomylonitic amphibolite taken from the northern border of the metabasic body. The F_2 -folds are disrupted and became locally rootless. Hand-specimen 95-A3-307.

Interference pattern. – Interference patterns resulting from F_1 - and F_2 -folding have not been found. Locally a remarkable elliptical configuration of a fold structure could be distinguished. At first sight one is inclined to consider this an interference pattern, formed by the superimposition of two fold-systems. On the other hand, differential flattening during F_2 -folding might easily explain such a pattern. The effects of the mechanism of differential flattening in the ab -plane have been described by Ramsay (1962). The fold axis becomes a curve, and a profile parallel to the BC-plane shows the above-mentioned configuration (Photograph III-6).



Photo III-6. Elliptical section of an F_2 -fold produced by differential flattening in the ab -plane by which the fold axis developed a curved configuration.

F₂-structures in the metasediments. – The results of *F₂*-folding are rather scarce in the metasediments. Near the Coto de Son, north of Santiago de Compostela, subhorizontal E-W trending fold axes occur. The folds are overturned to the south. The postkinematic rotation of staurolite and garnet is probably associated with *F₂*-folding. Thin section (121-B1-306) displays subhorizontal folds with an E-W axis and a vergence toward the south in a kyanite-staurolite-garnet-gneiss. The formation of *s₂*-schistosity could be locally demonstrated in the hinges of *F₂*-folds (Photograph III-7).

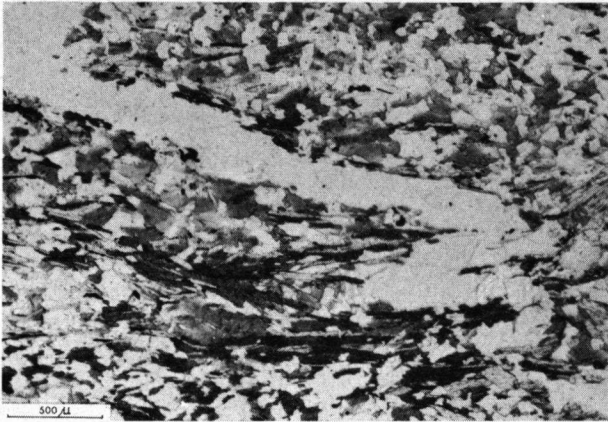


Photo III-7. The development of *s₂*-schistosity in the hinge zone of an *F₂*-fold. Especially biotite has recrystallized along *s₂*-planes in these kyanite-staurolite-garnet-gneisses. Thin section 121-B1-306.

F₃-folding

F₃-folding differs markedly in style from the previous folds. The axial planes are steeply inclined and have an E-W strike. The fold axes plunge subhorizontally E or ENE (see Fig. III-5). Large-scale folding as well as minor structures has been recognized. The problem of the time-relationship with other structures is difficult. The arguments for placing *F₃*-folding *post-F₂* and



Fig. III-5. *F₃*-folding in garnet-amphibolites ENE of Bando. The subvertical axial planes have an ENE-WSW strike.

pre-F₄ in time are not conclusive. It is mainly based upon their occurrence in the northern part of the metabasites and a few indications of their relationship with older and younger structures. As stated on p. 28, the older structures in the metabasites are well-preserved in the central and northern part of the metabasic rocks. This fact together with the slight deflections of the axial traces of the *F₃*-synform and -antiform on Mt. Castro (subarea 8), which are probably caused by Hercynian movements, is the reason for placing *F₃*-folding in a pre-Hercynian orogene. The folds are post-metamorphic since they crenulated the existing foliation or schistosity (Photograph III-8) without the formation of new minerals.

A few examples of refolding of *F₂*-folds have been found (Photograph III-9, Fig. III-6) but they do not demonstrate whether *F₃*-folds were *pre-* or *post-F₄*. ENE of Bando, in the northern section of the metabasites, minor folding with an axial direction plunging subhorizontally ENE has been found (Fig. III-5). The axial planes are subvertically or steeply inclined to the

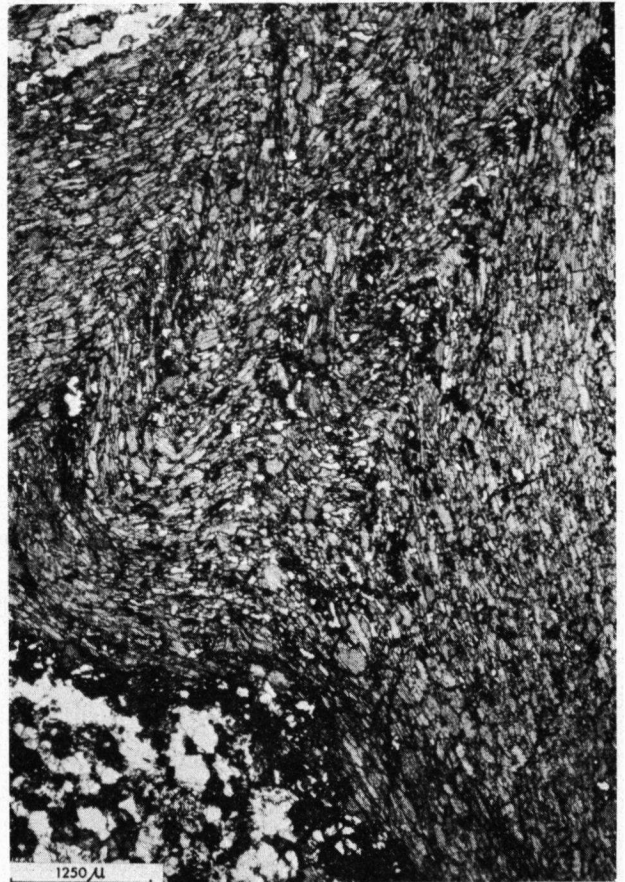


Photo III-8. Crenulation cleavage, likely due to *F₃*-folding, in a garnet-bearing amphibolite. The axial plane dips steeply to the N (looking ENE). Thin section 95-A3-186.

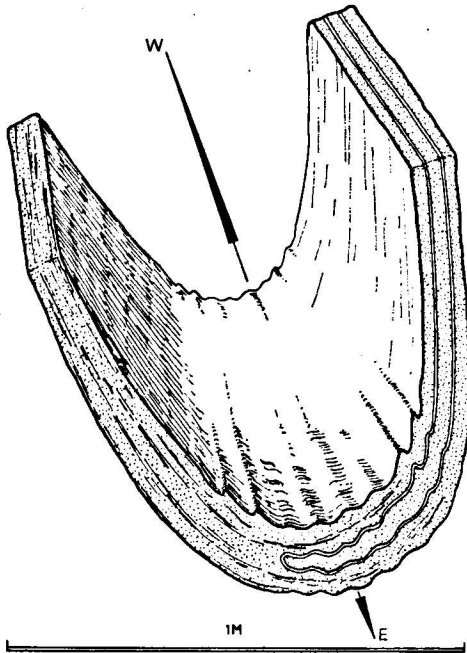


Fig. III-6. A schematic section of an interference pattern (type 3 of Ramsay's classification of interference patterns, Ramsay, 1967, p. 520-537). A minor F_2 -fold has been refolded on a steeply inclined axial plane (s_3).

NNW (diagram 13, Encl. III). The folds corrugated the older planar structures and the associated linear structures.

On the southern slope of the Coto do Espiño, the same structures occur. The crenulation cleavage sometimes induced an E-W lineation on the foliation planes (diagram 13, Encl. III).

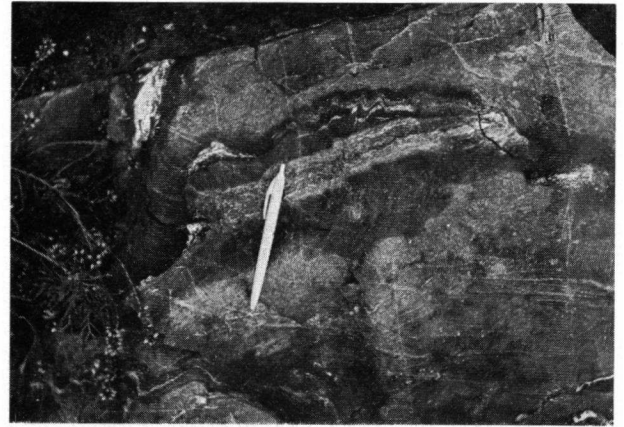


Photo III-9. Flat F_2 -structures refolded by F_3 on subvertical axial planes at the Coto do Espiño. In the darker, amphibole-rich streaks, a new cleavage may be observed as thin lines cross-cutting the darker parts (looking E).

Conclusions

A synopsis of structural and metamorphic events is presented in Table III-1. Three folding phases have been recognized in the Ordenes Complex which are absent outside this complex. The F_1 -folding is typical of the deep-seated levels of an orogene. According to de Sitter & Zwart (1963), such structures often occur in the infrastructures of orogenic belts. Depth of burial appears to influence the type of folding, as shown by Oele (1966) in the Central Pyrenees and by Escher (1967) in the Precambrian rocks of South Greenland. Tectonic thickening buried the rocks at the deep-seated levels necessary for intermediate-pressure con-

Table III-1. Synopsis of pre-Hercynian (?) structures and metamorphism.

Folding phases	F_1	F_2	F_3
Structural and metamorphic data			
axial direction	NNW to N with varying plunge	ENE or WNW with varying plunge	E to ENE with subhorizontal plunge
inclination of axial plane	subhorizontally to moderately inclined	subhorizontally to moderately inclined	subvertically to steeply inclined
strike of axial plane		E-W with slight variations	E-W
translation direction		between SSW and SSE	
grade of metamorphism	metasediments metabasites	ky-alm-ms subfacies of almandine amphibolite facies hbl-cpx-alm subfacies of granulite facies	amphibolite facies amphibolite facies
some important minerals	metasediments metabasites	staurolite + kyanite + garnet clinopyroxene + hornblende + almandine ± scapolite	garnet + biotite + kyanite (?) hornblende ± scapolite

ditions, as deduced from the postkinematic growth of hornblende, pyroxene, garnet, staurolite and kyanite. F_2 -folding is only locally developed. The association of these folds with zones of movement leads to the suspicion that F_2 -folding is connected with upthrusting. Upthrusting gave rise to mylonitization of the rocks in these zones. The rocks were brought to a higher level and the grade of metamorphism, i.e. amphibolite facies, decreased with regard to (M_1). The recrystallization of hornblende porphyroblasts, where the c -axes are aligned with B_2 , can be observed.

A subsequent F_3 -folding has been placed before F_4 although conclusive arguments are lacking.

Perhaps the Ordenes Complex forms part of an Hercynian infrastructure. An explanation, however, for the E-W structures within an Hercynian orogene, with a predominantly N-S trend, then becomes difficult. The pronounced overprinting by N-S structures on the steeply inclined axial planes in the western and eastern extremities of the metabasites indicates rather an older inheritance for the structures in the central part. This together with the previously described petrographical evidence leads to a plausible hypothesis of a pre-Hercynian orogenic cycle to explain the structures and metamorphism of the Ordenes Complex.

The mode of emplacement of this high-grade metamorphic complex is a difficult problem. Before the onset of the Hercynian orogeny, the basement rocks were upthrust during F_2 . An imbricate structure has been proposed for the complex. Overthrust wedges overlap each other; but the question remains whether the slices are associated with a nappe or with an autochthonous conical basement diapire, which was squeezed upwards.

The planes of thrusting were without doubt steepened during F_3 and the Hercynian deformations.

HERCYNIAN STRUCTURES

Hercynian deformations have affected nearly all the rocks in the described complexes. The metasediments and orthogneisses, which belong to the Complex of Santiago de Compostela, are assumed to have been deformed and metamorphosed only during the Hercynian orogeny. This in contrast to the rocks of the Ordenes Complex which are polyorogenic. In part, the structures in the Ordenes Complex and the Complex of Santiago de Compostela will be discussed separately.

F_4 -folding

Complex of Santiago de Compostela. – The metasediments from this complex were folded during the main phase (F_4) of Hercynian orogeny, but the direction of the fold axes and the attitude of the axial plane could not be established. A locally developed intense folding (F_4), on subvertical plunging axes and N-S subvertical to steeply inclined axial planes, prevents the determination of the original orientation of the F_4 -folds.

F_4 -folds occur in this zone of F_5 -folding. As illustrated on Photograph II-9 (p. 16), the s_4 -plane has been transposed into s_5 . In fold hinges of F_5 -folds, one can, however, observe that before F_5 , a schistosity was already present. The accompanying greenschist-facies metamorphism gave rise to the formation of quartz-chlorite-muscovite-(\pm spessartine-rich garnet) assemblages.

The pre-Hercynian granites (cf. p. 20) underwent penetrative deformation during F_4 , which caused cataclasis of the rocks. Recrystallization of quartz and feldspar, and the parallel alignment of newly formed micas, changed the rocks into blastomylonitic *orthogneisses*. The foliation planes are steeply inclined to the east and have a N-S direction. Sometimes we can discern a lineation on the foliation plane which plunges subhorizontally to the north (diagrams 1 and 2, Encl. III). The orthogneisses are barely folded and it is likely that the above-mentioned lineation also resulted from F_4 -folding. Avé Lallemand (1965, p. 166) found the same structural picture for the main phase of the Hercynian orogeny, near the Ria de Noya (NW Spain).

Ordenes Complex. – Hercynian structures in the metasediments and metabasic rocks are locally well-developed in this area. On the structural map (Encl. III), lines are drawn which illustrate the changes in the strike of foliation planes or schistosities. In this part of the Ordenes Complex, it is assumed that s_1 is often coincident with s_2 . Thus it will be sufficient to draw only the s_1 -pattern, particularly since s_2 does not have a widespread distribution. If axial planes or schistosities have been encountered which are associated with F_4 -folding, this is indicated on the structural map.

The structures in the *metasediments*, which developed during F_4 , are found sporadically in exposed parts of the Ordenes Complex. Some localities where F_4 -folds could be distinguished are described below.

South of the hamlet Enfesta, the gneisses have been

folded on subvertical to steeply inclined axial planes. In this N-S trending axial plane, the fold axis plunges gently to the north (diagram 4, Encl. III).

The minor folds, with amplitudes up to 1 m, are related to the major structures which are shown on the structural map. In these minor structures, the development of a new schistosity (s_4) parallel to the N-S trending axial planes could be observed (Photograph III-10). Biotite, muscovite and perhaps quartz have been formed during F_4 . The fold limbs are often crenulated by F_6 -folding (Fig. III-7); the axial plane of the F_6 -folds is not coincident with s_4 .

The attitudes of the pre-Hercynian planar structures have influenced the plunges of the younger F_4 -folds. The difference in inclination of the E-W trending schistosities, caused by F_2 - and F_3 -folding, is expressed in the variable attitudes of the F_4 -folds. For this reason perhaps, the isoclinal folds on the Formaris plunge moderately to the NNE (see Photograph III-11).

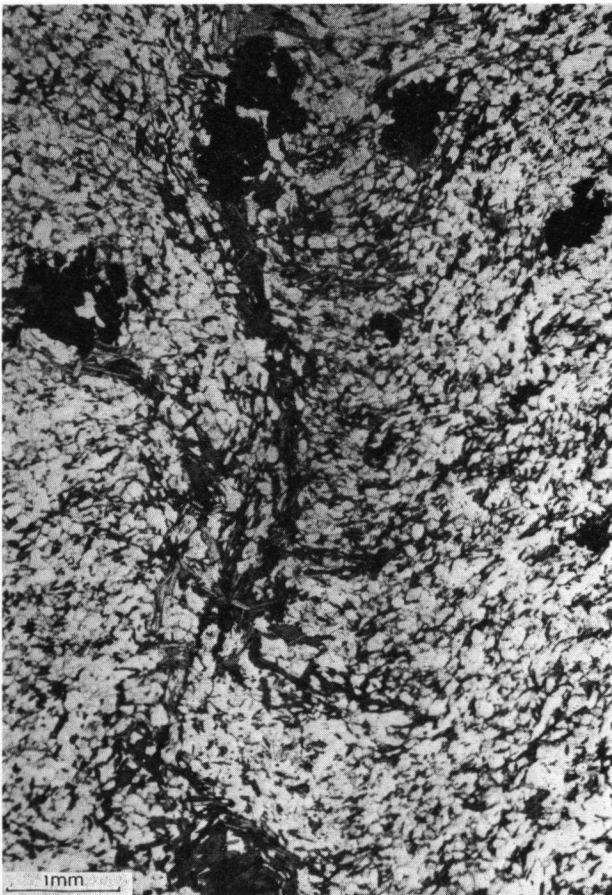


Photo III-10. The results of Hercynian main-phase metamorphism (M_3) can be studied in metasediments, southeast of Enfesta. Coarse biotite has grown along N-S striking subvertical planes, whereas tiny flakes of biotite and muscovite belong to an older metamorphism just as the garnets do. Thin section 95-B2-13.

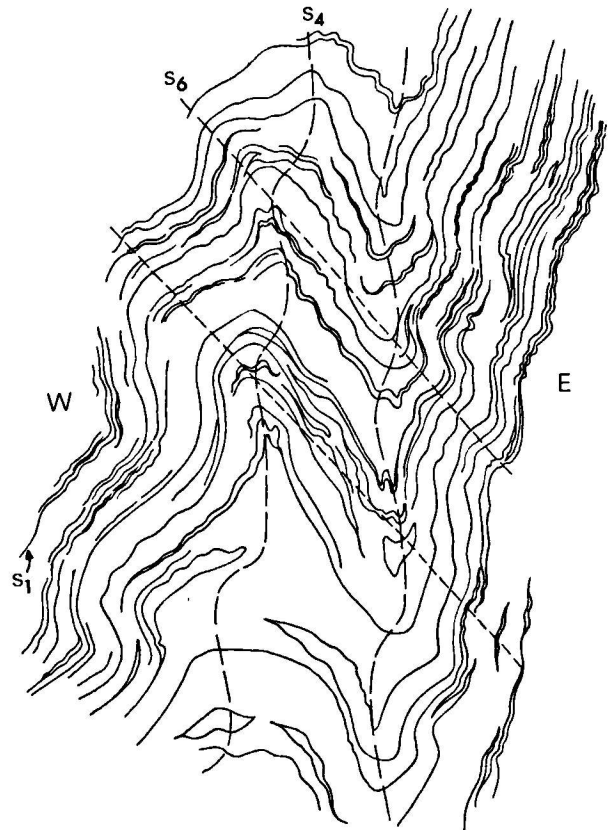


Fig. III-7. Large thin section 95-B2-6. The axial planes of F_4 -folds may be observed as curved lines caused by superimposed F_6 -folding in garnet-biotite-muscovite-gneisses, SE of Enfesta (true size).

The folds on the Formaris Hill are minor structures related to a large-scale antiform of which the axial trace has a NNE-SSW direction.

On a microscopical scale, the new axial-plane schistosity s_4 can be shown in thin sections from hand-specimens 95-B3-53, 95-B3-33 and 95-B2-13.

The *metabasites* were subjected to the same F_4 -deformation as the metasediments. The eastern and the western extremities of the basic block are especially suited for the investigation of F_4 -structures. The structural map shows that N-S trending foliations are dominant (subareas 7 and 9, Encl. III) in these domains. Superimposed F_4 -folding upon F_1 -folds could be demonstrated near the crest of the Alboya (see Photograph II-1, p. 8). In thin section, it can be shown how coarse hornblendes are recrystallized approximately on the N-S striking axial planes of F_4 -folds (Photograph III-12). The *c*-axes of hornblendes are aligned with the fold axis, which is subhorizontally inclined to the north. Asymmetric isoclinal minor folds indicate a sense of vergence to the east but they are



Photo III-11. Pinched F_4 -folds in garnet-biotite-muscovite-gneisses on the Formaris. The isoclinal folded quartz veins show a well-developed axial-plane schistosity. The plane of exposure is almost horizontal and the sharp edge of the chisel indicates NNE.

perhaps related to major structures (Photograph III-13), since overturned minor folds to the west have been found elsewhere. The axial planes are steeply inclined to the east and the fold axes plunge gently to the NNW (diagram 9, Encl. III). At the western extremity of the mafic rocks, a well-developed antiform, near the Coto de Viso, could be discovered from aerial photographs. Fortunately the Santiago-La Coruña Railroad cuts across this large-scale structure which enables us to observe some details of the major fold. These large-scale structures were probably initiated during the main phase of the Hercynian orogeny (F_4) and later reactivated by younger deformations for which the direction of compression was the same. The type of folding can tentatively be derived from the projected loci of the deformed lineations (l_2) (Ramsay, 1960). The lineations are mineral lineations produced by the parallel arrangement of hornblende crystals. The crystallization of these hornblendes seems to be related to F_2 . The deformed lineations are plotted in diagram 7 (Encl. III). For the sake of convenience we have rotated the fold axis of the antiform to an horizontal position. The deformed lineations have also been

rotated through an angle equal to the angle between B_4 and B'_4 (Fig. III-8a). The angle between the fold axis B'_4 and the deformed lineation is not always constant. It appears that the locus of lineation displays an affinity for a flexural-slip fold which was later flattened, because the locus roughly forms a partial small-circle with slight deviations (Ramsay, 1967, p. 466). The deviation from a small-circle pattern could be explained by subsequent flattening of the fold. Indications for such a flattening process have been found in the hinge zone of the antiform as major tension joints. Tension cracks can also be demonstrated on a microscopical scale (thin section 95-A3-310). The previously mentioned rotation procedure was also used for the l_2 -lineations of amphibole prisms deformed during F_4 , northeast of Bando (Fig. III-8b). This diagram is consistent with that obtained for the deformed lineations of the Coto de Viso antiform.

Together with F_4 , the metamorphism (M_3) reached its culmination in the amphibolite facies involving epidote-bearing amphibolites. This could be deduced from the recrystallization of green to blue-green hornblende, plagioclase and epidote.



Photo III-12. Detail from Photograph II-1. Coarse amphiboles, forming a new N-S striking subvertical foliation, may be observed. The F_4 -folding is well-marked in the leucocratic bands in which the above-mentioned amphiboles have grown along the axial planes. Large thin section 95-A4-235.

F_5 -folding

The distribution of F_5 -structures is restricted to a narrow zone which runs from the north, about 1 km east of Puente Albar, along the eastern boundary of the orthogneisses toward the eastern side of Santiago de Compostela. The zone continues further toward the south, approximately following the strip containing porphyroblastic albite-schists. The folds have amplitudes varying from 0.2 to 50 cm. They are of similar type and, in general, they have steeply inclined axial planes with a N-S strike (Photograph III-14). The fold axes plunge subvertically to steeply to the east, although a spreading of the fold axes can be observed (cf. diagram 14, Encl. III). The folds are easy to recognize on a mesoscopic scale because veins of milky quartz are involved. The folded quartz veins have been disrupted by shearing along the axial planes which gave rise to

transposition structures (Photograph II-9, p. 16) and the formation of rootless folds. Locally the direction of movement could be established, but lack of conclusive evidence for the entire strip prevents determination of the movement direction on a larger scale. Nevertheless, the assumption that subhorizontal movements were active seems to be justified.

Rotation of albite-porphyroblasts. – As already noted, albite-porphyroblasts are often found in the schists where F_5 -folds occur but their presence is not restricted



Photo III-13. F_4 -folding in laminated garnetiferous amphibolite at the eastern border of the metabasic body. Metamorphism gave rise to recrystallization of amphiboles, found mainly in fold hinges, but an axial-plane foliation is lacking. Large thin section 95-B3-86.

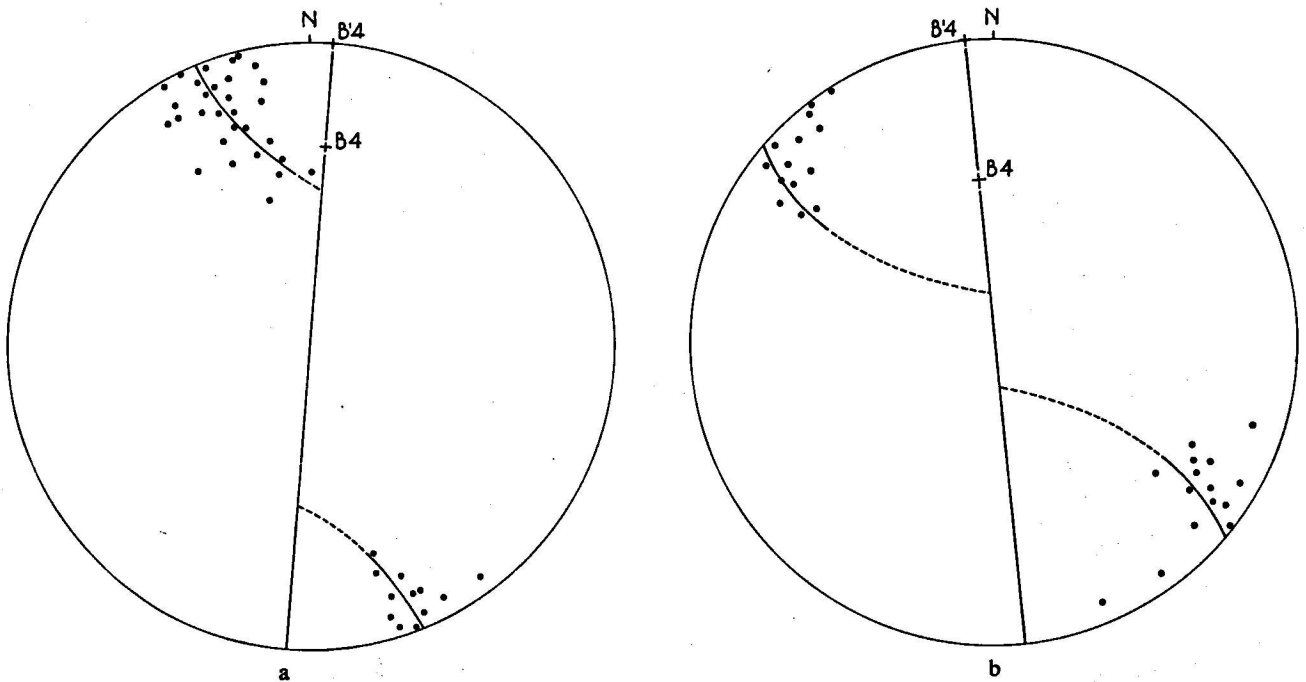


Fig. III-8. a. Plots of deformed lineations (l_2) measured on the Coto de Viso antiform. For the sake of convenience, the fold axis B_4 has been rotated to an horizontal position (B_4') lying on the circumference of the projection net and the l_2 -measurements have been rotated through the angle between B_4 and B_4' . The locus of the deformed lineations has tentatively been drawn and the picture apparently indicates flexural-slip folding with a component of flattening (a deformed small-circle girdle). b. The same procedure has been followed for a structure northeast of Bando. The antiform was less tight here, causing the occupation of the locus to be less complete.



to this zone. The blasts have interesting internal structures due to their synkinematic growth, although other s_1 -patterns are also present which point to post-kinematic growth. Some s_1 -patterns have been drawn and are shown in Fig. III-9a, b, c and d. The origin of the folded inclusions (Fig. III-9d) could not be ascertained; they might be relics of either F_4 - or F_5 -folds. The growth of a clear rim of albite around blasts, otherwise crowded with inclusions, has already been discussed (cf. p. 17). Without doubt it can be postulated that the blasts were rotated after their growth (Fig. III-9b and d). Paracrystalline rotation of albite-blasts (Fig. III-9c) has been observed in thin sections from hand-specimens, collected south of Santiago de Compostela to the west of the orthogneisses. The sense of rotation and the orientation of the rotation axis have been established. Powell & Treagus (1967) have analysed the S-shaped inclusion trails in garnets from a Norwegian schist. On the basis of this study, they argued that fixing the spatial orientation of the rotation

Photo III-14. Relationship between s_4 and s_5 in a muscovite-chlorite (\pm garnet)-schist, northeast of Son de Abajo. The sub-vertical s_5 -planes are N-S striking shear planes, parting the rock in microlithons. The plane of exposure is horizontal and the pushbutton of the ball-point indicates N.

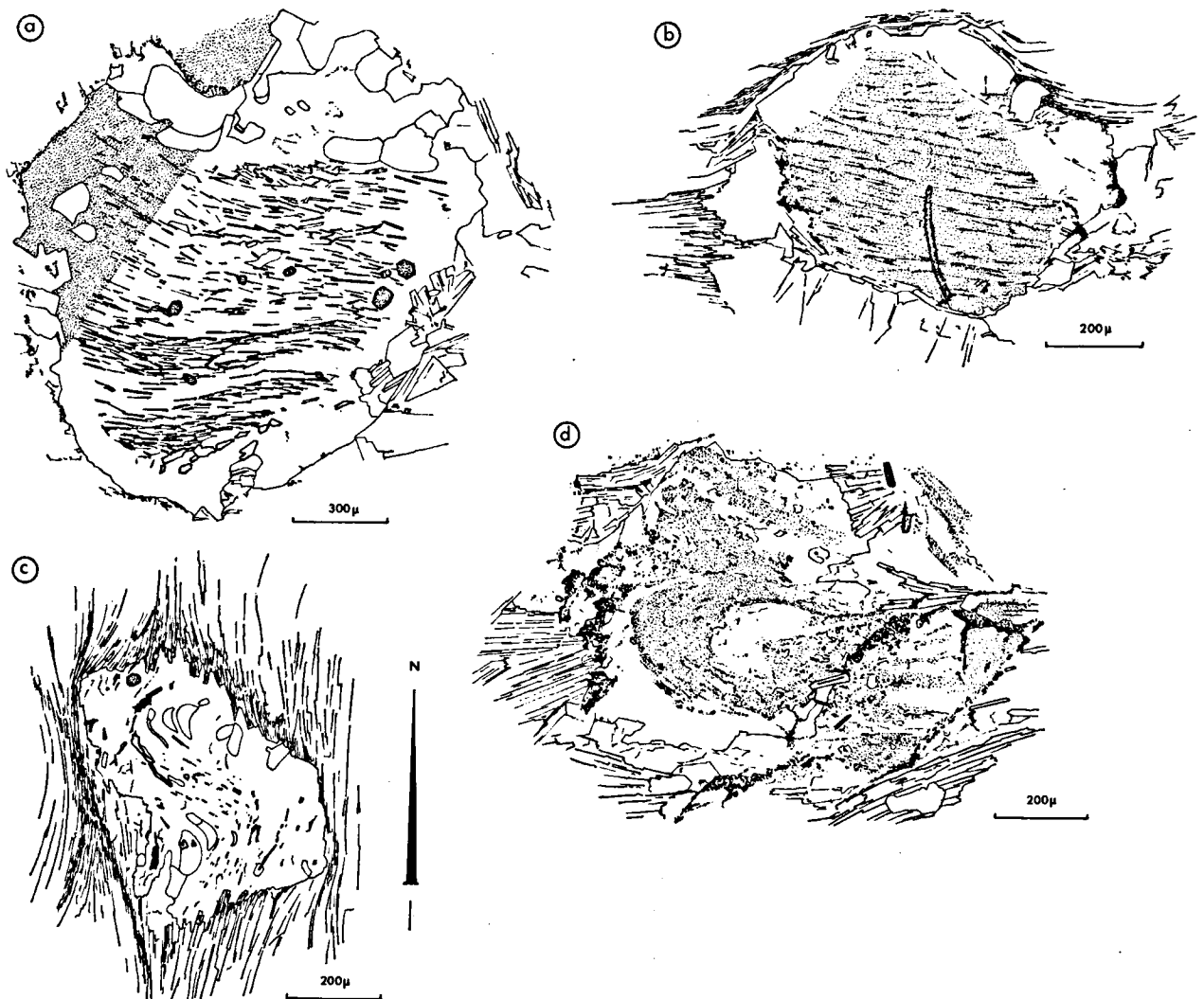


Fig. III-9. Inclusion patterns in porphyroblastic albites. a. Straight to slightly curved inclusions formed by subidiomorphic garnets and tiny needles of epidote or tourmaline (?) in a simple albite twin. b. Albite-blast crowded with dusty inclusions in the core; note the clean rim. c. Synkinematic growth of albite during F_5 ; the rotation is counter-clockwise. The plane of drawing is the horizontal plane. d. Helicitic inclusions in an albite-blast; the folds might be F_4 or F_5 because these blasts formed after the F_5 -deformation.

axis only from thin sections with S-patterns in blasts is rather doubtful. Additional sections in other directions must be made, since S-shaped inclusions can also occur in planes intersecting the rotation axis at angles up to 45° .

In our case the rotation axis is almost subvertically oriented, lying in the schistosity plane ($s_4 = s_5$). A counter-clockwise sense of rotation, looking downward upon the horizontal plane, predominates but cases have been found where clockwise rotation also occurs (Fig. III-10). We shall try to incorporate these observations in the structural framework. It is reasonable to assume that the rotation axes of the albite-blasts correspond with fold axes with the same orientation, i.e. F_5 -fold axes. Rotation of crystals has often been



Fig. III-10. Opposite senses of rotation of albite-blasts. It is possible that, in a specific domain of a fold (e.g. a fold hinge), both rotations occur although there is no evidence for this – neither in the field nor on a microscopical scale. Thin section 94-E4-146 A.

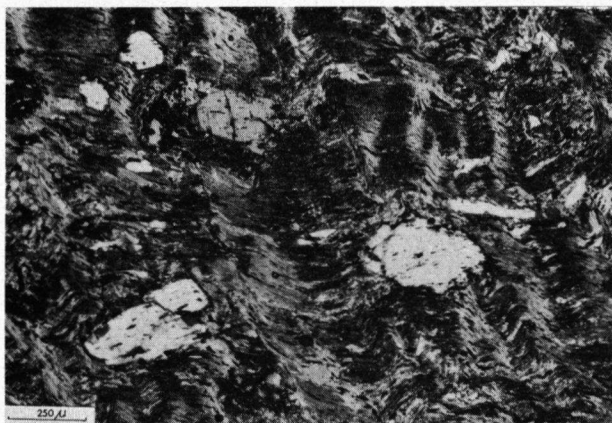


Photo III-15. Porphyroblastic albites with straight inclusions lying in a matrix which was crenulated during F_6 . Thin section 94-E4-104 (+ nic).

connected with similar folding (Langheinrich, 1964; Zwart & Oele, 1966). The predominance of counter-clockwise rotation indicates a simple shear (or laminar flow) mechanism with a preference for a sinistral movement couple or asymmetric folding pointing to the same rotation.

F_6 -folding

The effects of F_6 -folding can be studied mainly in the metasediments from both complexes. The deformation had little influence upon the rigid metabasic rocks, as far as could be determined from field observations. The structures dealt with are to be seen on a mesoscopic scale either as fold-axis lineations or as a lineation formed by intersecting planes. On a minor scale, they compare with those microstructures, described by Matte (1968) in eastern Galicia as second Hercynian phase structures. Large-scale structures, initiated during F_4 (Hercynian main phase), were probably reactivated since both deformations are nearly homaxial (cf. p. 37).

The spatial orientation of l_6 -lineations has been plotted in diagrams 1-6 and 12 of the corresponding subareas (Encl. III). Except in diagram 12, a N-S trending lineation is present; the plunges are dependent upon the attitudes of the existing schistosity or foliation plane. The deflections of the lineations in subarea 12 to the NW-SE were probably due to late-Hercynian flattening of the metasediments around the competent metabasic rocks. According to the classification of cleavages by Knill (1960), this kind of structure belongs to the *crenulation-cleavage* type.

It is apparent that E-W compression has resulted in upthrusting of the metabasic rocks to the west, along a pre-existing thrust plane which was already inclined to the east. Evidence for the mechanism has been found

in the formation of asymmetric folds along the thrust zone in the metasediments, which are overturned to the west (Fig. III-11). The axial plane of the microfolds is more steeply inclined than the present schistosity.

Occasionally the sense of movement during this phase could also be established with the aid of the nearly postcrystalline counter-clockwise rotation of the porphyroblastic albites; see Fig. III-11. The subhorizontal rotation axis seems to be aligned parallel to the crenulation lineation (l_6). The postcrystalline nature of this deformation with regard to the growth of the albite-blasts is seen on Photograph III-15; note that the crenulations are visible outside the blasts, whereas inside the inclusion trails are straight. In a few cases, the relationship between F_5 - and F_6 -folding could be investigated. Thin section 94-E2-105 (Photograph II-9) shows a refolding of F_5 -folds on subvertical N-S striking axial planes. The F_5 -structures deviate from the general pattern here because they have NW-SE striking axial planes. The time-relationship with migmatization differs in the two complexes. F_6 -folding in

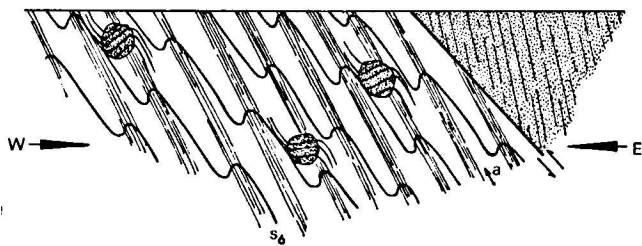


Fig. III-11. Schematic E-W cross-section (south of Santiago de Compostela) through the metabasic rocks (stippled) and the metasediments of the Complex of Santiago de Compostela. E-W compression resulted in upthrusting of the metabasic rocks; a new cleavage has developed in the axial planes of the asymmetric F_6 -folds and the postcrystalline counter-clockwise rotation of the albite-blasts (N-S subhorizontal rotation axis) is in accordance with the translation direction a during F_6 -folding.

the Ordenes Complex took place after migmatization since the segregation veins have been folded (Photograph III-16). In contrast to this phenomenon are the observations of polygonal arcs of biotite and muscovite around the hinges of F_6 -folds in the migmatized rocks of the Complex of Santiago de Compostela. Yet, deformed micaceous minerals have also been found so that syn- to postkinematic growth of these minerals must be assumed. The explanation for these discordant observations is found in the fact that a relationship is being sought between two processes, which migrate both in time and in space; therefore the relationship will not be constant. The crenulation cleavage in the metabasic massif is poorly developed



Photo III-16. Folded segregation streaks of pegmatoid composition in migmatized gneisses, south of Sionlla. The subvertical axial planes (s_6) have a NNW-SSE strike (looking W).

except in a few localities near the eastern extremity where amphibolites show a distinct corrugation of the foliation plane.

The crenulation cleavage in the non-migmatized metasediments from the Ordenes Complex gave rise to interference with F_4 -structures. The patterns are similar to type 3 of Ramsay's classification of interference patterns (Ramsay, 1967, p. 520). Small-scale F_4 -structures were refolded such that the axial planes of the F_6 -folds, although they have almost the same strike (N-S) as the F_4 -folds, crosscut their limbs (Fig. III-7). The newly formed axial planes are usually moderately inclined to the east (see Fig. III-7).

Investigations outside the area dealt with, but within the Ordenes Complex, revealed that in addition to the N-S trending crenulation lineation, an ENE-WSW lineation is also present. As far as could be determined, they do not form a conjugate set and the ENE-WSW lineation is probably older.

Phyllonitization, mylonitization, wrench faults and kink banding

A period of flattening and dislocation was active at the

end of the Hercynian orogeny. This style of deformation is characteristic of high-level structures. The rocks have been retrograded under greenschist-facies conditions.

Phyllonitization. – During phyllonitization the rocks have been subjected to a penetrative flattening, often accompanied by the development of a conjugate set of shear planes and by retrogressive metamorphism. The results of phyllonitization could be studied in the strip containing porphyroblastic albite-schists.

Locally the two-mica granites have also been phyllonitized. The conjugate shear planes intersect each other such that their intersection is subvertical (Fig. III-12). The direction of maximum compression (σ_1) is approximately ENE-WSW. The direction of minimum principle stress (σ_3) is about NNW-SSE; this could be established from the maximum length of the pressure-shadow tails (Fig. III-12) on both sides of the albite-blasts.

Mylonitization and wrench faults. – Along faults, the rocks are sometimes mylonitized. On the western margin of the metabasic block, the rocks underwent block

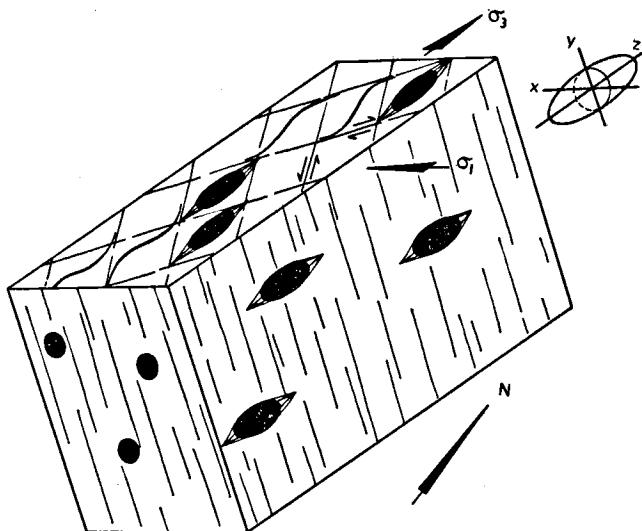


Fig. III-12. Block diagram showing the phyllonitization of rocks lying in the zone of albiteblast-bearing schists. A conjugate set of shear planes can be observed and the direction of the stresses could be derived, using the maximum length of the pressure-shadow tails as an indicator for the minimum stress (σ_3) orientation as well as for the determination of the direction of maximum elongation (Z). The maximum compressive stress (σ_1) is parallel to the bisector of the obtuse angle between the shear planes.

faulting resulting in rocks with pseudo cross-bedding (Fig. III-13), similar to the structures described by Dimroth (1966) in metabasic rocks from the Grenville Province (Canada). The NW-SE striking foliations in the amphibolites in the southern part of the basic

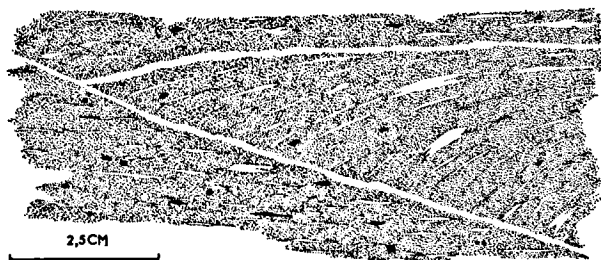


Fig. III-13. Pseudo cross-bedding in a blastomylonitic amphibolite on the northern slope of the Coto de Viso. Porphyroclasts of hornblende as black spots. Hand-specimen 95-A3-176.

rocks (diagram 11, Encl. III) can be tentatively explained as adaptations of these directions to a stress field, as indicated in Fig. III-14. The sinistral component of the wrench fault system in the NW-SE direction is ascertained from the two-mica granites and orthogneisses; its dextral counterpart with a N-S direction was active in the metabasic rocks near Monte Sar. The faults were filled at a later stage, during relaxation, with quartz, e.g. the Pico Sacro fault and

two faults within the two-mica granites. In the zone of maximum curvature of the banana-shaped competent metabasic body, SSE of Santiago de Compostela, tension joints have developed in the outer arc; further to the east in the inner arc, gentle folding with roughly E-W trending axes is present. These structures are probably related to this deformation.

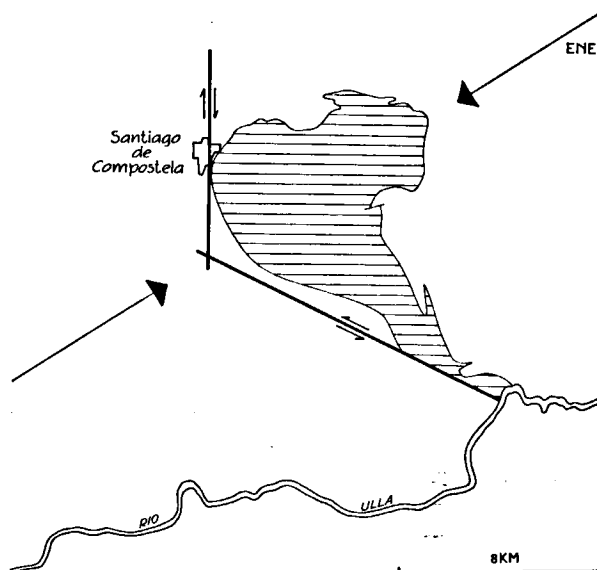


Fig. III-14. Wrench fault system near the metabasic complex. The direction of maximum compression is ENE-WSW.

Kink banding. – When the structures in the metasediments to the southeast of Santiago de Compostela, in the vicinity of the major NW-SE fault, were examined in detail, kink banding was found. The sinistral movement, associated with the NW-SE wrench fault, involved kink banding in the adjacent rocks. The sinistral movement is confirmed by the sense of rotation of the kink bands.

Concluding remarks

The hypothesis that the rocks in the area investigated were deformed and metamorphosed during two (or more) orogenies is chiefly based upon both petrographical evidence and structural analysis. The petrographical investigation gave rise to the assumption that the Ordenes Complex was subjected to a different kind of metamorphism (i.e. high- to intermediate-pressure metamorphism) before the Hercynian orogeny partially converted these rocks to low-pressure mineral assemblages. The structural analysis supported the above-mentioned assumption that part of the area is polyorogenic.

The Hercynian structures could be identified in orthogneisses which bear many similarities to dated granitoid rocks (cf. p. 15) elsewhere in Galicia, which were gneissified during the Hercynian orogeny. This affords an important criterion for the recognition of Hercynian structures in the rocks of the Ordenes Complex. The results of Hercynian main-phase deformation (F_4) in the orthogneisses could be correlated with similar structures in the adjacent rocks of the Ordenes Complex. A brief summary of the essential structural events is provided in Table III-2. Resolution of different folding phases during an orogeny as in Table III-2 creates the impression that deformation took place during restricted intervals. In fact, however, each time we ascertain a finite state of strain in the rocks preceded by infinitely small increments of strain. In reference to this, Flinn (1962) outlined that rocks follow a *deformation path* during distortion.

The regional metamorphism (M_3) started synchronously with F_4 or was post-deformation (F_4). Meta-

morphism went on and a considerable quantity of heat was introduced and resulted in partial melting of the rocks in scattered localities.

After the migmatization, a period of intrusion of two-mica granites followed. Through this, the formation of contact aureoles was induced in the country rocks and was accompanied by the growth of new minerals.

The distribution of polyorogenic areas in Galicia in their present locations was in essence probably already established during the pre-Hercynian orogenic cycle. These polyorogenic massifs were incorporated in the Hercynian orogeny and squeezed upwards. As previously mentioned (cf. p. 41), massifs were upthrust after the Hercynian main-phase metamorphism. This might explain the difference in grade of metamorphism between the two complexes, viz. amphibolite facies giving rise to epidote-bearing amphibolites in the Ordenes Complex *versus* greenschist facies in the Complex of Santiago de Compostela.

Table III-2. A synopsis of Hercynian structures.

Deformation phases structural data	F_4	F_5	F_6	Phyllonitization, mylonitization wrench faults
axial direction	to N with subhorizontal plunge	To E with subvertical to steep plunge	To N with subhorizontal to gentle plunge	subvertical
inclination of axial plane	subvertically to steeply inclined (?)	subvertically to steeply inclined	subvertically to steeply inclined	subvertical
strike of axial plane	N-S	N-S	N-S (NW-SE, subarea 12, Encl. III)	variable
translation direction			to W (see Fig. III-11)	

CHAPTER IV

PETROFABRIC ANALYSES

INTRODUCTION

As a complement to the mesoscopic analysis in the foregoing chapter, microscopical fabric analyses were carried out for *amphibole*, *clinopyroxene* and *scapolite* in the metabasic rocks and for *albite* and *tourmaline* in the low-grade schists of the Complex of Santiago de Compostela. The results of the statistical analysis of the optical and crystallographic orientation of several minerals will be compared with the field observations.

APPLIED METHODS

Measurements of amphibole and clinopyroxene orientations with the aid of a four-axis universal stage

When this petrofabric work was initiated, the method of electronic data processing developed by Möckel (1969, pp. 91–93) for measurement of mineral orientations was not yet available. Therefore part of the diagrams, obtained from the measured orientation of

a 'better' sample than a parallel section does (i.e. the former is more representative of the entire hand-specimen).

Once the thin section has been selected, a random sample of a specific mineral must be obtained. Numbering all grains in the thin section on a photograph and drawing a sample, using a table of random numbers, would be the best method theoretically. The influence of grain size (every grain must have the same probability of being measured – grain statistics) and clusters of grains (with almost the same spatial orientation of crystallographic and optical axes in the sample) are eliminated with the above-mentioned approach. Employing such a method is a time-consuming procedure; therefore a procedure described by Möckel (1969) has been used, which specifies that all grains within certain strips (normal to the *s*-plane) have to be measured. If however the number of mineral grains present in the thin section is on the order of the sample size, we are compelled to measure all the grains within the working area of the universal stage.

Comparison between the uniform distribution and observed distributions

Assuming that we have a population of orientations in which every orientation (all values are in principle possible) is equally likely, then we can say that the distribution is uniform. In terms of petrofabrics, this means that everywhere on a hemisphere or an equal-area projection the probability density of a continuous random vector, say the orientation of an indicatrix or crystallographic axis⁶, is constant and equals 1; this assumes that the total area of the hemisphere or the circle of equal-area projection equals unity. From this uniform distribution, we draw at random one orientation and inspect the probability that the plotted orientation falls within a given area *A* of the unit circle (i.e. the equal-area projection). It is clear that this probability equals *A* (*A* = area of the counting circle/area of the unit circle). Hence the probability that the plotted point falls outside area *A* is: $1 - A$. The distribution of \underline{x} (number of points falling within area *A* if we draw a random sample of size *N*) is binomial with parameters *N* and *A* (Kamb, 1959, Appendix). The probability of finding *n* points within area *A* is:

$$P(\underline{x} = n) = \binom{N}{n} A^n (1 - A)^{N-n} \quad (1)$$

The computation of the value of $P(\underline{x} = n)$ becomes cumbersome if *N* is large, but if *A* is small and *N* sufficiently large we may use the Poisson distribution as an approximation with parameter *NA*. Thus:

$$P(\underline{x} = n) = \exp(-NA) \frac{(NA)^n}{n!} \quad (2)$$

We could compare a random sample of orientations drawn from a uniform distribution with the observed orientations of a petrofabric diagram by applying a χ^2 test. Winchell (1937) explains the procedure for such a test, and with the aid of this test one is able to reject the null-hypothesis (uniform distribution) or not, depending on the value determined for χ^2 and the level of significance chosen.

Friedman (1964) comments that if we cannot reject H_0 , this does not always mean that the orientation pattern lacks 'significance'.

The above-mentioned test appears to be a less suitable method of analysis since the observed orientations often follow a distribution function which deviates considerably from the uniform distribution (e.g. in the case of a point-maximum). Therefore we should look for more appropriate tests, as pointed out by Watson (1965) and Bingham (1964).

Suppose now that the unit circle of the equal-area projection is divided into 100 non-overlapping areas of size *A*, hence:

$$\sum_{i=1}^{100} A_i = 1.$$

According to the null-hypothesis of a uniform distribution, each *A_i* has the same probability of having *n* points. The expectation of the total area of the projection with frequency *n* then becomes, simply:

$$E(\underline{A}_{\text{total}})_n = \sum_{i=1}^{100} A_i P(\underline{x} = n) = P(\underline{x} = n) \quad (3)$$

(cf. Möckel, 1969, p. 98).

From a table of Poisson distributions, we can immediately read off the probability of finding *n* points or more within a subarea under H_0 (uniform distribution); the value of $E(\underline{A}_{\text{total}})_n$ in equation (3) can now be determined. Areas with frequency densities of a probability less than 0.01 could be accentuated in the diagram. The statement 'statistically significant' for these areas is not strictly applicable since we do not employ a statistical test.

In petrofabric diagrams, contours are drawn between counting points to indicate areas with equal frequencies. If the equal-area projection is unity the contours indicate approximate density levels, because the content under the frequency density function is equal to unity.

The effect of counting in overlapping areas, the influence of the area of the counting circle upon the configuration of the diagrams and the introduction of a subjective element due to the choice of the

⁶ We shall use underlined letters to indicate random vectors and random variables.

counting circle have been extensively treated by Möckel (1969).

Remarks about the reproduction of the fabric diagrams. – In all the clinopyroxene and albite diagrams, contours are drawn at densities 1, 1.5, 2, 2.5, 3, etc.; however in the amphibole, scapolite and tourmaline diagrams, the contours are drawn at densities 1, 3, 5, 7, 9, etc. All the orientations have been plotted on the equal-area projection of the lower hemisphere. The measurements are rotated in the horizontal plane and N indicates geographical north.

'Significant' areas are stippled according to the following scheme:

$N=100$	$A=0.02$	
lower side of 'significant' area at frequency		$x \geq 7$
$N=150$	$A=0.02$	
lower side of 'significant' area at frequency		$x \geq 9$
$N=200$	$A=0.02$	
lower side of 'significant' area at frequency		$x \geq 10$
$N=300$	$A=0.02$	
lower side of 'significant' area at frequency		$x \geq 13$
$N=400$	$A=0.02$	
lower side of 'significant' area at frequency		$x \geq 16$
$N=100$	$A=0.04$	
lower side of 'significant' area at frequency		$x \geq 10$
$N=150$	$A=0.04$	
lower side of 'significant' area at frequency		$x \geq 13$
$N=200$	$A=0.04$	
lower side of 'significant' area at frequency		$x \geq 16$.

Thus where necessary, contours are added to define the 'significant' areas. N is the number of measured grains and A the area of the counting circle ('significant' values have been read off from a Poisson Table; $\alpha=0.01$). Density 1 is always drawn as a dashed line while density 5 is represented as a bold contour. Megascopic structural features of the hand-specimen have been incorporated in the diagram and are denoted by s_1, s_2 , etc. or l_1, l_2 , etc.

Amphibole, scapolite and tourmaline diagrams were counted using a 2% counting circle whereas for clinopyroxene and albite diagrams, a 4% counting circle was employed.

The geographical position of the samples discussed is indicated on Enclosure II.

A distribution on the sphere with antipodal symmetry

In petrofabric analyses, the problem often arises of finding an appropriate mathematical model which

bears some kind of similarity to the configurations derived from observed orientation data. Bingham (1964) presented a probability distribution on a sphere or on the projected plane which seems suitable for statistical analysis of three-dimensional orientation data. Density contours with a roughly elliptical shape around a point-maximum or great-circle configurations resemble the density contours obtained when the present distribution is applied. He proposed the probability density:

$$f(\mathbf{x}) = \frac{\exp(\zeta_1(\boldsymbol{\mu}'_1\mathbf{x})^2 + \zeta_2(\boldsymbol{\mu}'_2\mathbf{x})^2 + \zeta_3(\boldsymbol{\mu}'_3\mathbf{x})^2)}{4\pi K(\zeta_1, \zeta_2, \zeta_3)} \quad (4)$$

where $\boldsymbol{\mu}_1, \boldsymbol{\mu}_2$ and $\boldsymbol{\mu}_3$ are orthonormal vectors, \mathbf{x} a unit vector (orientation data expressed as unit vectors), and ζ_1, ζ_2 and ζ_3 real shape parameters. This distribution on a sphere with unit radius has a normalizing constant $1/4\pi K(\zeta_1, \zeta_2, \zeta_3)$; further mathematical treatment of this will not be discussed here. A special case of distribution (4) arises when two of the ζ 's are equal. Then distribution (4) is reduced to a distribution with circular symmetry about one of the axes $\boldsymbol{\mu}$ (cf. Watson, 1966).

Another particular case occurs when $\zeta_1 = \zeta_2 = \zeta_3 = 0$, then (4) has degenerated into a uniform distribution.

Maximum likelihood estimation. – If $\underline{x}_1, \underline{x}_2, \dots, \underline{x}_n$ are observations for which the distribution is known except for a number of parameters, we can estimate these parameters using the method of maximum likelihood estimation. Dependent upon the observations $\underline{x}_1, \underline{x}_2, \dots, \underline{x}_n$, we give the unknown parameters values which maximize the likelihood function (i.e. the joint density of $\underline{x}_1, \underline{x}_2, \dots, \underline{x}_n$). Applying this method to distribution (4), we can write (Bingham, 1964, *op. cit.*, p. 37) the joint density of a sample of observations of size N as follows:

$$\frac{\exp(\text{tr } ZM'XX'M)}{[4\pi K(\zeta_1, \zeta_2, \zeta_3)]^N} \quad (5)$$

where

$$Z = \begin{bmatrix} \zeta_1 & 0 & 0 \\ 0 & \zeta_2 & 0 \\ 0 & 0 & \zeta_3 \end{bmatrix}$$

Hence the log of the likelihood function is:

$$L(M, Z) = -N \log 4\pi - N \log K(\zeta_1, \zeta_2, \zeta_3) + \text{tr } ZM'XX'M \quad (6)$$

where

$$X = (\mathbf{x}_1, \mathbf{x}_2, \dots, \mathbf{x}_n)$$

which is a $3 \times N$ matrix of observations,

$$\mathbf{x}_j = \begin{bmatrix} x_j \\ y_j \\ z_j \end{bmatrix} \quad (x, y \text{ and } z \text{ are Cartesian coordinates}),$$

and $M = [\mu_1, \mu_2, \mu_3]$.

Bingham (1964) shows that the maximum likelihood estimate \hat{M} is a matrix of latent vectors of XX' and the maximum likelihood estimate \hat{Z} is given by the equation

$$y_j(\hat{Z}) = \frac{\omega_j}{N} \quad (j = 1, 2, 3) \quad (7)$$

where ω_1, ω_2 and ω_3 are the latent roots of the symmetric matrix XX' .

If we set a restriction, e.g. $\zeta_3 = 0$, the solution of (7) is unique. Tables containing values of

$$y_j(Z), \quad Z = \begin{bmatrix} \zeta_1 \\ \zeta_2 \\ 0 \end{bmatrix}$$

and values of $K(\zeta_1, \zeta_2, \zeta_3)$ are provided by Bingham (1964). The ζ_1 and ζ_2 values are graphically represented (see Fig. 39.2 and 39.3, Bingham, 1964). The relationships between the $y_j(Z)$'s are given by equations 36.10, 36.11, 36.12 and 36.13 in Bingham's dissertation. The probability density (4) has been proposed for a sphere with area 4π ; we assume the hemisphere or projected plane has an area equal to 1

(cf. Möckel, 1969, p. 102). This implies that the likelihood function (6) becomes:

$$L^* = -N \log K(\zeta_1, \zeta_2, \zeta_3) + \zeta_1 \omega_1 + \zeta_2 \omega_2 \quad (8)$$

(where $\omega_3 \geq \omega_2 \geq \omega_1$ and $\zeta_3 > \zeta_2 > \zeta_1$).

Comparison of a fabric diagram and distribution (4). -

We could represent density function (4) in a diagram by plotting density contours. The location of density contours could easily be computed for the planes normal to μ_1, μ_2 and μ_3 . The expression $\cos \varphi_1$ is substituted for $\mu_1 \cdot \mathbf{x}$ in equation (4), where φ_1 is the angle between μ_1 and \mathbf{x} (similarly, φ_2 is the angle between μ_2 and \mathbf{x} , etc.). In the plane (μ_3, μ_2) , we then have $\varphi_3 = 90^\circ - \varphi_2$; hence, we can write for (4):

$$f(\mathbf{x}) = \frac{\exp(\zeta_2 \cos \varphi_2)}{K(\zeta_1, \zeta_2, \zeta_3)} \quad (\zeta_3 = 0) \quad (9)$$

Following the same procedure for the (μ_1, μ_3) -plane, we obtain the values for the angles φ_2 in the (μ_3, μ_2) -plane, respectively φ_3 in the (μ_1, μ_3) -plane.

A fabric diagram with an elongated point-maximum was kindly provided by J. P. Engels for reproduction. Maximum likelihood estimates for M and Z were computed for 200 β -axes of clinopyroxene ($\zeta_3 = 6.30$, $\zeta_2 = 3.05$, and $\zeta_1 = 0.00$). Density contours derived from distribution (4) using the same ζ 's are compared with contours from the above-mentioned diagram in Fig. IV-2a and 2b. The result is quite satisfactory. It is

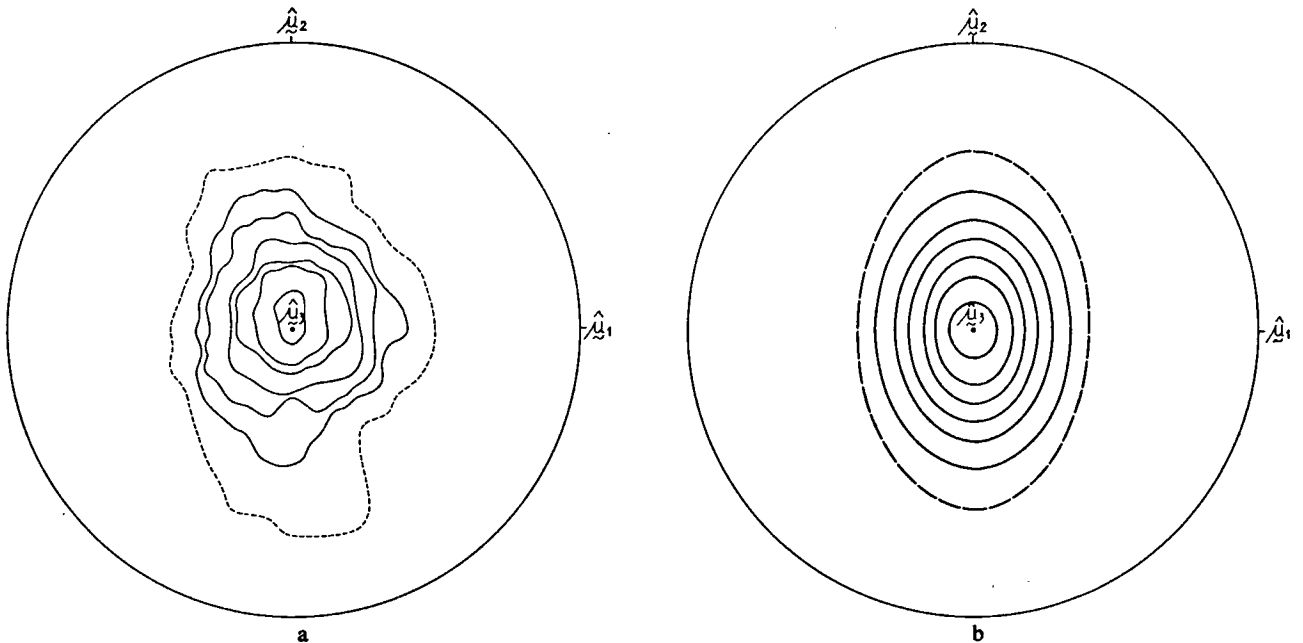


Fig. IV-2. a. Fabric diagram of 200 β -clinopyroxene from an eclogite (specimen V 1050; $A = 0.05$). b. Distribution, as proposed by Bingham (1964), with ζ -values estimated by maximum-likelihood estimation of a, assuming that the β -orientations were drawn from a population which follows this distribution. Contours are drawn at densities 1, 2, 3, ..., 7.

obvious that the application of distribution density (4) is restricted to single point-maxima or great-circle girdles in fabric diagrams. A great-circle configuration is obtained when $\zeta_3 = \zeta_2$. The distribution is then located in a circle around μ_1 . If possible and when informative, values for ζ_3 and ζ_2 are given together with the location of the appropriate latent vectors in the fabric diagrams⁷. The plane normal to μ_1 , which represents a statistically calculated great-circle girdle, is shown as a dashed line. For the sake of convenience, we use the convention $\zeta_1 = 0$ so that ζ_3 and ζ_2 are positive numbers.

AMPHIBOLE, CLINOPYROXENE, (SCAPOLITE) FABRICS IN ROCKS OF THE BASIC MASSIF

Hand-specimen 95-A4-217C: hornblende-plagiopyrigar-nite (Fig. IV-3a)

The hand-specimen was taken from an exposure at the Pena Mayor. As previously observed (cf. p. 29), the foliation of these basic rocks has a subhorizontal attitude.

Isoclinal to tight folds (F_1) are found with axes directed to the N-NNW. Probably connected with these F_1 -folds are the mineral lineations marked by amphibole and aligned parallel to the above-mentioned fold axes. The banding of the rocks is usually parallel to the axial planes except in the hinge zones of the F_1 -folds. In places, the subhorizontal attitude of the foliation has been disturbed by gentle to open N-S folding with steeply inclined axial planes. F_2 -folds have approximately the same gently inclined axial planes as the F_1 -structures, but the fold axes have an ENE-E plunge. An interesting feature is the absence of a megascopic mineral lineation which could be related to the latter deformation.

The thin section displays the hinge zone of an F_1 -fold containing greenish hornblende with a brownish-green core and pale-green diopsidic pyroxene. Garnet and scapolite occur in minor amounts.

Amphibole. – The c -axes have the tendency to spread along s_1 . A definite point-maximum is present almost parallel to the direction of the regional fold axes (NNW). The SSE-plunge of the c -axes is due to a local disturbance in the structural trend. A sub-maximum in s_1 , almost perpendicular to the point-maximum, probably does not result from additional generations of hornblende.

⁷ The symbols $\hat{\mu}_1$, $\hat{\mu}_2$ and $\hat{\mu}_3$ are indicated in the figures with a wavy line underneath.

$\pi\{100\}$ shows a partial great-circle girdle where the axis is parallel to the previously mentioned point-maximum of the c -axes. In this girdle, we can observe an elongated maximum almost normal to the s_1 -plane. The same holds for $\pi\{110\}$ although it should be noted that in the $\pi\{110\}$ -diagram, twice as many measurements have been plotted since two cleavages of the $\{110\}$ form could be constructed. The maximum concentration of $\pi\{100\}$ is nearer to πs_1 than to $\pi\{110\}$.

Hand-specimen 95-A4-217B: hornblende-plagiopyrigar-nite (Fig. IV-3b)

The thin section was taken from the same sample as the foregoing, but now a section from a fold limb was used. The rock contains some laminae with a hornblende-rich composition.

Amphibole. – As could be expected, the diagrams show the same characteristics as those from the fold hinge. The concentration of c -axes, lying in s_1 , in the NE appears to be better developed than it was in the hinge zone (cf. Fig. IV-3a). Some spread of the c -axes in a girdle around B_1 can be observed in Fig. IV-3b, diagram 1.

The preferred orientation of the maximum in the NE also has consequences for the orientations of $\pi\{100\}$ and $\pi\{110\}$: the great-circle around B_1 is less marked and the orientations also tend to spread along a great-circle around an axis normal to B_1 in s_1 .

Clinopyroxene. – The distribution of the c -axes bears a close resemblance to the orientation of the amphibole c -axes. In general, the axes are concentrated in a great-circle girdle parallel to s_1 . In this girdle the maxima in B_1 and the normal to B_1 are evident. The degree of preferred orientation cannot be compared with the related amphibole diagram since both N and A are different. The γ -pattern is irregular due to the two maxima where two small circles probably interfere, i.e. the small circles of semi-vertical angle ($c \wedge \gamma$) $\approx 42^\circ$ around these maxima. ‘Significant’ areas are lacking in this diagram.

Scapolite. – The c -axes of scapolite demonstrate a rather well-oriented maximum in s_1 , almost parallel to B_1 . In contrast to the related amphibole and clinopyroxene diagrams, the second maximum is absent. Furthermore, the c -axes are scattered along an incomplete great-circle parallel to s_1 .

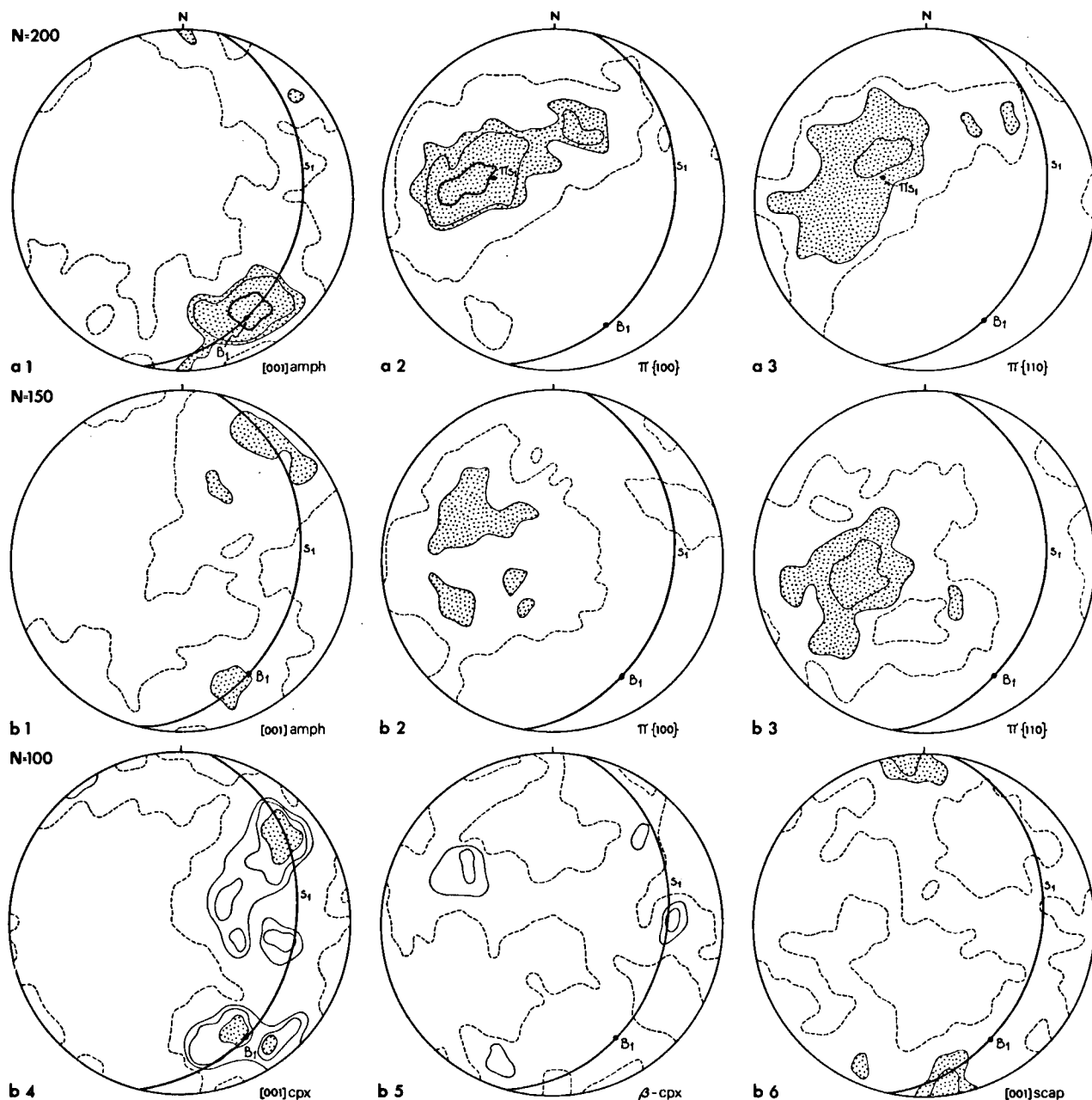


Fig. IV-3. a. Hornblende-plagiopyrigarnite 95-A4-217 C, amphibole ($A = 0.02$). b. Hornblende-plagiopyrigarnite 95-A4-217 B, amphibole ($A = 0.02$), clinopyroxene ($A = 0.04$), and scapolite ($A = 0.02$ and $N = 200$).

Hand-specimen 95-A4-221: garnet-amphibolite
(Fig. IV-4a)

To the NE of the location just described, it turns out that the predominantly E-W striking structures veer to the NE-SW. At the same time, the subhorizontal dip of the foliation changes gradually to a moderately inclined dip. The mineral lineation, formed by the parallel alignment of amphibole prisms, is often a megascopic feature.

The thin section shows a fine- to medium-grained green hornblende. The porphyroblastic garnet ($\varnothing 1-3$ mm) encloses hornblende crystals. In places, the garnet has been rotated; this could be deduced from the relationship between the internal and external structures. From different thin sections, cut perpendicular to each other, it could be established that the rotation axis extends roughly NE-SW. This postcrystalline rotation was directed toward the NW. The rotation sense does not fit into the structural picture, since broadly

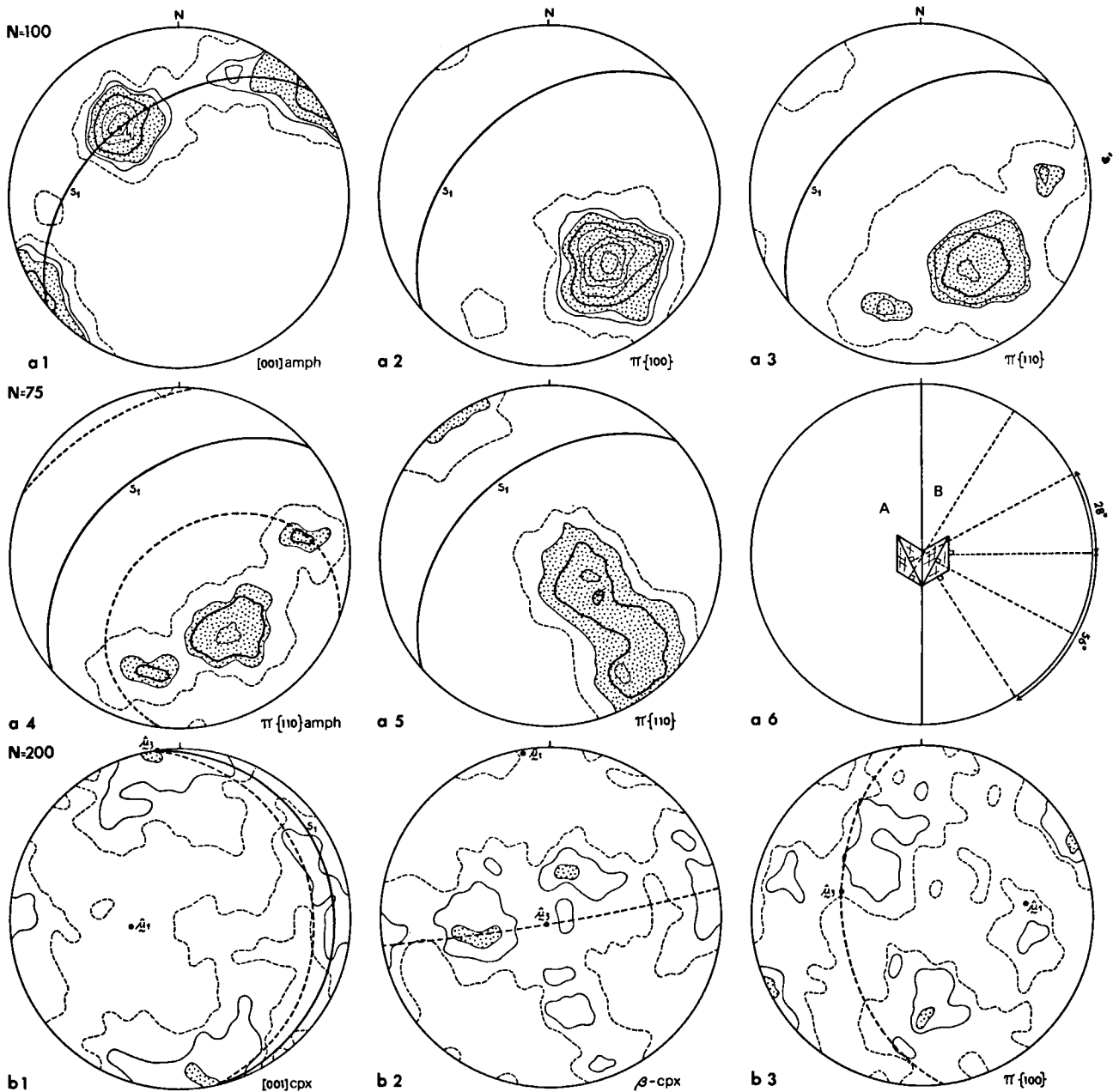


Fig. IV-4. a. Garnet-amphibolite 95-A4-221, amphibole ($A = 0.02$); diagrams 4 and 5 are partial diagrams representing $\pi\{110\}$; diagram 6 shows the possible attitudes of the $\{110\}$ - and $\{100\}$ -cleavages. b. Hornblende-plagiopyrigarnite 95-A4-218, clinopyroxene ($A = 0.04$).

speaking the direction of movement is to the SE (cf. p. 32). It is conceivable, for instance, that this sample was taken in a fold domain where an opposite rotation couple was present.

Amphibole. – The orientation of the c -axes in s_1 exhibits about the same distribution as that described for thin sections 95-A4-217C and 95-A4-217B. The axes form an incomplete girdle parallel to s_1 . The main concentration has a NNW plunge and coincides with

the lineation l_1 . A minor maximum, perpendicular to l_1 , lies in a NE-SW direction.

$\pi\{100\}$ has a strong, nearly circular, maximum normal to s_1 . The tendency to spread in a NW-SE great-circle girdle is due to the rotation of the c -axes of the submaximum. In contrast, $\pi\{110\}$ displays an intricate pattern. The diagram contains a central maximum and two subsidiary maxima which are symmetrically situated, making an angle of about 50° with the central maximum. The problem now arises: which plane was

primarily oriented along s_1 and what are the implications of the other planes? To inspect the orientation of $\{110\}$ -cleavages without the perpendicular c -axes orientations, partial diagrams of $\pi\{110\}$ are presented corresponding to one of the c -axes concentrations. Diagram 4 shows these cleavages of the corresponding c -axes in the NW-direction and diagram 5, the pattern obtained from the $\{110\}$ -cleavages of amphiboles concentrated in the NE-SW direction.

Assuming now that planes of the crystal form $\{110\}$ have been oriented parallel to s_1 , it might be expected that two sub-maxima are present about 56° from the central concentration (cf. diagram 6). Therefore a small circle with an angular radius of 56° has been constructed in diagram 4. Diagram 6 represents the possible attitudes of the $\{110\}$ - and $\{100\}$ -cleavages. Another point of departure is to assume that the $\{100\}$ -planes lie in s_1 . In that case we may anticipate two maxima of $\pi\{110\}$ 28° away from the central position. Diagram 5 probably represents this situation. Returning to diagram 6, we observe moreover that two positions (A and B) of the amphibole crystal must be considered. In diagram 4 we have already seen that a distinct preference for one of the positions is lacking.

Hand-specimen 95-A4-218: hornblende-plagiopyrigarnite (Fig. IV-4b)

This sample comes from the same locality on the Pena Mayor as hand-specimen 95-A4-217. The foliation (s_1) is subhorizontally inclined. The rock is mainly composed of greenish hornblende, plagioclase, pale-green clinopyroxene and garnet. The thin section shows a fine-grained hornblende and clinopyroxene. A large number of clinopyroxene grains are present, so that we can measure sufficient orientations of this

mineral. Garnet ($\varnothing 0.5\text{--}3$ mm) has a pitted appearance and is crowded with inclusions of hornblende, clinopyroxene and sphene.

Clinopyroxene. – The c -axes ($\zeta_3 = 0.95$; $\zeta_2 = 0.50$) show a less pronounced concentration than in the amphibole diagrams from these rocks. In the event that a mathematical model, proposed by Bingham (1964), possibly underlies the present distribution of the axes, i.e. *one* maximum eventually elongated along a great-circle girdle, the estimated values of ζ_3 , ζ_2 , and ζ_1 ($\zeta_1 = 0$) have significance. The estimated major concentration ($\hat{\mu}_3$) lies NNW, but here too we can observe a clustering of orientations along the E-W axis. The calculated great-circle nearly fits the orientation of s_1 in the hand-specimen.

The β -orientations ($\zeta_3 = 0.85$; $\zeta_2 = 0.40$) tend to cluster around a great circle. The estimated axis of this girdle ($\hat{\mu}_1$) is close to the maximum concentration of diagram 1. The development of an imperfect great-circle girdle around an E-W axis is due to the orientation of the c -axes mentioned above.

The $\pi\{100\}$ -diagram ($\zeta_3 = 0.45$; $\zeta_2 = 0.15$) shows an irregular pattern. Curiously enough the crossing girdles of the β -diagram are missing whereas we might anticipate such a configuration since $\pi\{100\}$ as well as β is perpendicular to the c -axis.

Hand-specimen 95-B4-221A: pyroxene-amphibolite (Fig. IV-5)

This sample comes from the Castelo de Vigo, where a blastomylonitic zone is exposed. The mafic rocks have been folded with fold axes that plunge gently or subhorizontally to the ENE. The foliation turns slightly in a NW-SE direction.

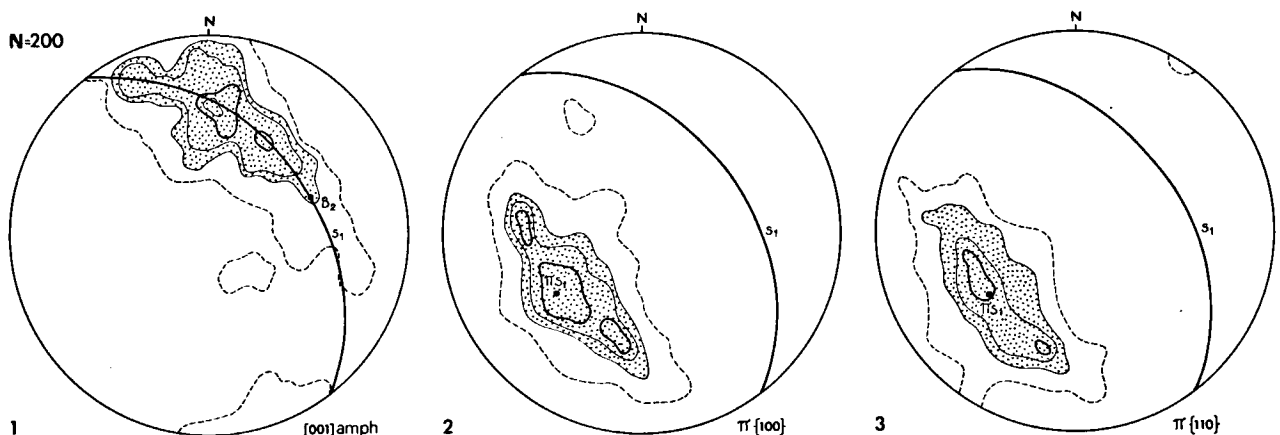


Fig. IV-5. Pyroxene-amphibolite 95-B4-221 A, amphibole ($A = 0.02$).

The thin section reveals that the laminated rock consists of recrystallized aphanitic green hornblende, clinopyroxene, quartz and fine-grained plagioclase. In laminae, however, the occurrence of a fine-grained brownish-green hornblende can be observed. These grains are deformed, especially in the hinge zone of the F_2 -folds. Therefore this generation of hornblende may be regarded as belonging to M_1 .

Amphibole. – The c -axes of the above-mentioned brownish-green hornblende have been constructed and plotted in diagram 1. The axes are scattered along a great-circle girdle, parallel to s_1 , and clustered around a point which does not coincide with B_2 .

The $\pi\{100\}$ -diagram shows an elongated maximum, elliptical in shape, around s_1 . The same trend is found in the $\pi\{110\}$ -diagram. This latter diagram contains, however, one maximum near πs_1 ; furthermore, the orientations are spread out towards the SE, forming another maximum at an angle of about 45° from the main concentration. This demonstrates perhaps that $\{110\}$ -planes are oriented parallel to s_1 and that a preference for one of the two possible positions (cf. Fig. IV-4a, diagram 6) of $\{110\}$ might exist.

Hand-specimen 95-A3-186: pyroxene-amphibolite (Fig. IV-6a)

The sample is taken from an exposure in which the structural trend is E-W. The location is situated ENE of Bando, in the north-central part of the basic massif. The foliation is moderately inclined to the NNW. A crenulation cleavage and the related folding, with axes plunging ENE (see Encl. III, diagram 13), probably belongs to F_3 .

The thin section demonstrates such a fold. Dark-green to black laminae in the rock are composed of green hornblende with a brownish core. Clinopyroxene as well as hornblende is in places converted to a bluish-green hornblende.

Amphibole. – The c -axes are well-concentrated in a point-maximum, lying in s_1 . An incomplete girdle, parallel to s_1 , contains a minor concentration along an ENE-WSW axis. The postcrystalline character of F_3 -folding eliminates the possibility that the latter maximum has any connection with this folding.

The $\pi\{100\}$ -diagram can be easily understood when we glance at diagram 3. In this $\pi\{110\}$ -diagram, we can establish beyond a doubt that the maximum concentration of the poles is perpendicular to s_1 . The

predominant position of the hornblende crystals is tentatively drawn in the centre of diagram 3. This could be derived from the presence of a sub-maximum about 50° NE of the main maximum. Consequently the $\pi\{100\}$ are situated between these $\pi\{110\}$ -maxima. For comparison a small circle with an angular radius of 56° has been drawn around the main concentration in diagram 3.

Hand-specimen 95-A3-189: garnet-amphibolite (Fig. IV-6b)

A slice of basic rocks is found in the metasediments of the Ordenes Complex near Castro Hill. The garnetiferous amphibolites have predominantly E-W striking foliations. Often this trend has been disturbed by younger open folding on N-S axes. The sample is taken from the hinge zone of a tight F_1 -fold. The fold axis plunges steeply to the N.

The thin section shows an aphanitic brownish-green hornblende, plagioclase, quartz and locally, porphyroblastic garnet.

Amphibole. – The axial plane of the F_1 -fold is indicated in the diagrams. The distribution of the c -axes displays a great-circle girdle, coinciding with the axial plane. The axes have a preferred orientation which is concentrated around B_1 . In addition we can discern a less well-developed maximum only 60° away from B_1 .

The behaviour of the $\{100\}$ - and $\{110\}$ -planes corresponds with the related diagrams for hand-specimen 95-A3-186. Although less pronounced, one can see that the $\pi\{110\}$ -maximum is located perpendicular to the axial plane. The main maximum of $\pi\{100\}$ is about 25° (SE) away from the $\pi\{110\}$ -concentration.

Hand-specimen 95-A3-190: garnet-amphibolite (Fig. IV-6c)

To study the influence of younger open folding upon the orientations of the fabric elements of amphibole, a sample was taken in which such a fold is present. The exposure is the same as the foregoing, viz. at the summit of Castro Hill. The younger open folds, probably of Hercynian age, plunge in general moderately to the north.

The thin section shows in places deformed hornblende crystals. In the hinge zone proper, one can observe chevronlike structures composed of hornblende prisms with pronounced variations in the longitudinal direction.

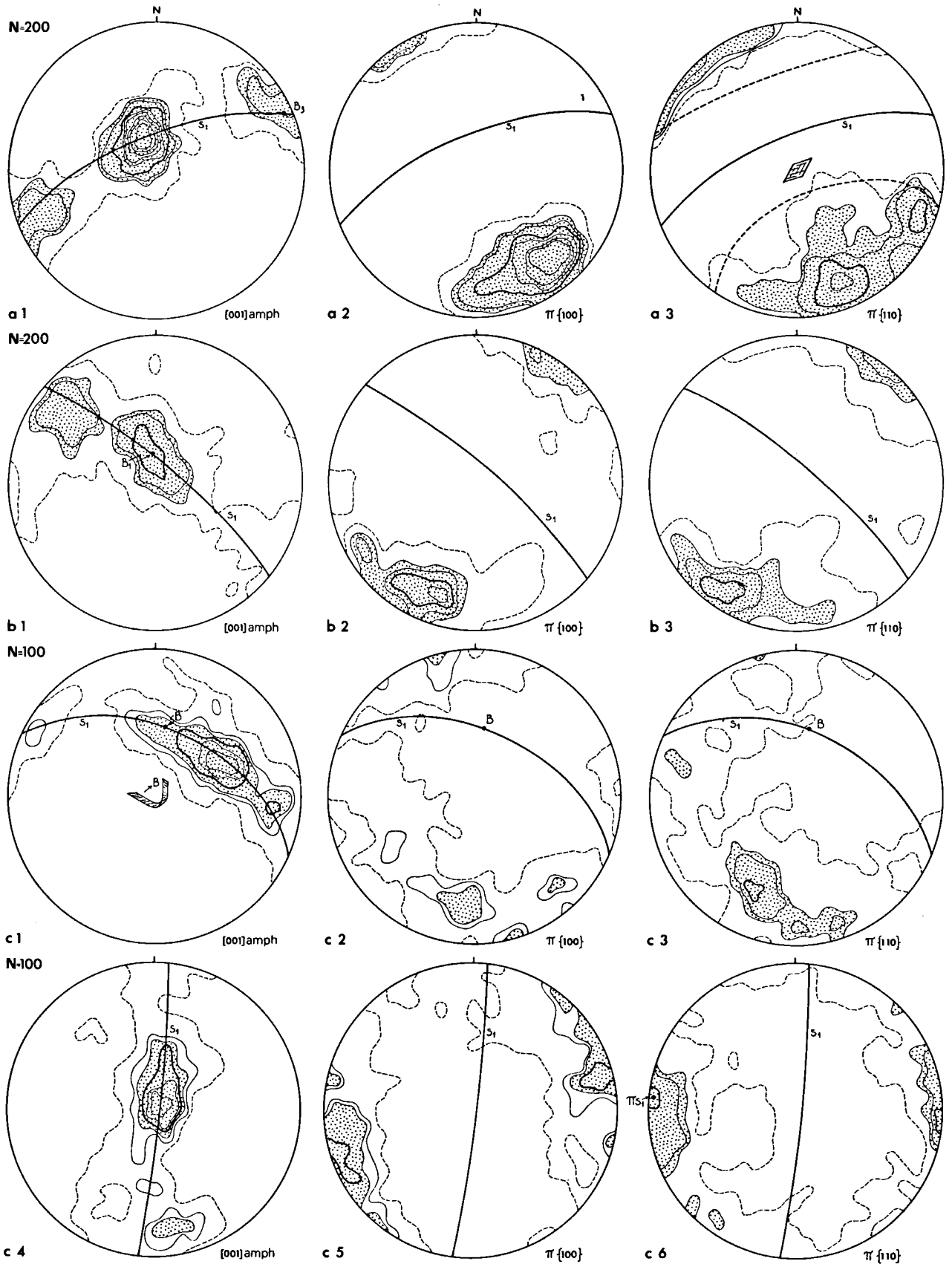


Fig. IV-6. a. Pyroxene-amphibolite 95-A3-186, amphibole ($A = 0.02$). b. Garnet-amphibolite 95-A3-189; amphibole ($A = 0.02$). c. Garnet-amphibolite 95-A3-190, amphibole ($A = 0.02$); diagrams 1-3 for one fold limb and diagrams 4-6 the opposite limb.

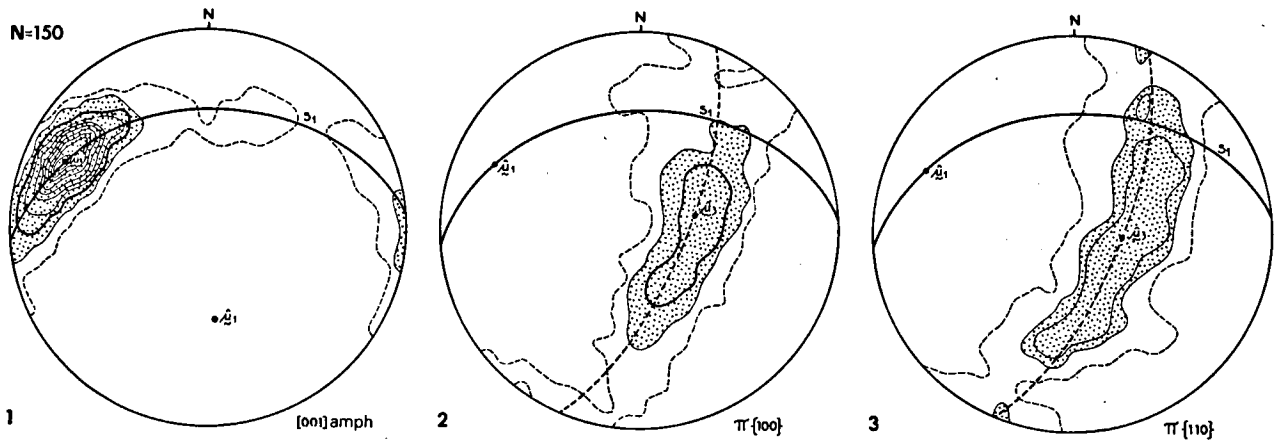


Fig. IV-7. Amphibolite 95-B3-212, amphibole ($A = 0.02$).

Amphibole. – Diagrams 1–3 relate to one fold limb; diagrams 4–6 show measurements of the opposite limb. A simplified sketch of the fold has been incorporated in diagram 1. The c -axes are distributed along an imperfect great-circle girdle with a greatly elongated maximum. Comparing this diagram with diagram 4, it is apparent that a similar distribution of the c -axes is present. Unrolling this fold, we observe that both maxima approximately coincide. The attitude of the foliation (s_1) has been drawn in all diagrams. The diagrams 2 and 3 demonstrate many similarities with the corresponding diagrams for hand-specimen 95-A3-186 (Fig. IV-6a). The same holds for diagrams 5 and 6. In particular, diagram 5 shows a gap in the maximum of $\pi \{100\}$ perpendicular to s_1 , whereas diagram 6 reveals clearly that the main concentration of $\pi \{110\}$ coincides with πs_1 .

Hand-specimen 95-B3-212: amphibolite (Fig. IV-7)

In the northeastern part of the basic massif, amphibolites occur which show a distinct mineral lineation in the foliation plane. Medium-grained hornblende prisms form this lineation, which plunges to the WNW parallel to some fold axes. These subhorizontal to gently plunging fold axes (B_2) are frequently found in blastomylonitic zones.

The thin section reveals two generations of green hornblende, i.e. an aphanitic older generation and the medium-grained porphyroblastic hornblende. The porphyroblastic growth is clearly seen on Photograph II-7 (p. 14).

Amphibole-porphyroblasts. – The c -axes ($\zeta_3 \approx 13$; $\zeta_2 \approx 10$)⁸ are extremely well-oriented around $\hat{\mu}_3$. The maxi-

⁸ The values are extrapolated from Bingham's graphs (1964), since only the values for ζ between 0–8 have been plotted.

mum has an elliptical shape and is slightly spread out along the foliation (s_1). Note the absence of a sub-maximum normal to the point-maximum in s_1 .

The $\pi \{100\}$ -diagram ($\zeta_3 = 6.8$; $\zeta_2 = 5.3$) shows a well-developed great-circle girdle around $\hat{\mu}_1$. The location of $\hat{\mu}_3$ has no direct coherence with s_1 . The $\pi \{110\}$ -diagram ($\zeta_3 = 5.8$; $\zeta_2 = 4.9$) exhibits a similar pattern. The statistically calculated orientation $\hat{\mu}_3$ is about the same as in the $\pi \{100\}$ -diagram.

Summarizing we can state that the fabric analysis of these amphiboles, probably belonging to F_2 , produces a picture completely different from the previously discussed amphiboles.

Hand-specimen 95-A3-184: metagabbro (Fig. IV-8)

The basic massif contains locally metagabbroic rocks. The occurrence of reaction rims of garnet between hornblende and plagioclase indicates that the rocks have been metamorphosed. This sample comes from the central part of the massif where the surrounding banded amphibolites have predominantly E-W structures. Locally the rock has a hornblendite composition.

The thin section shows a medium-grained green hornblende with *Schiller* inclusions. At first sight, one would suppose that the crystals are randomly oriented. The fabric analysis however shows that this does not hold.

Amphibole. – The c -axes are rather well-oriented, forming a broad incomplete E-W striking great-circle girdle. In this girdle, an elongated maximum is visible with a WNW-ESE orientation. The question arises whether the hornblende is recrystallized under metamorphic conditions or not. A connection exists between F_2 -structures and the above-mentioned fabric, therefore the intrusion of these metagabbros could have preceded F_2 .

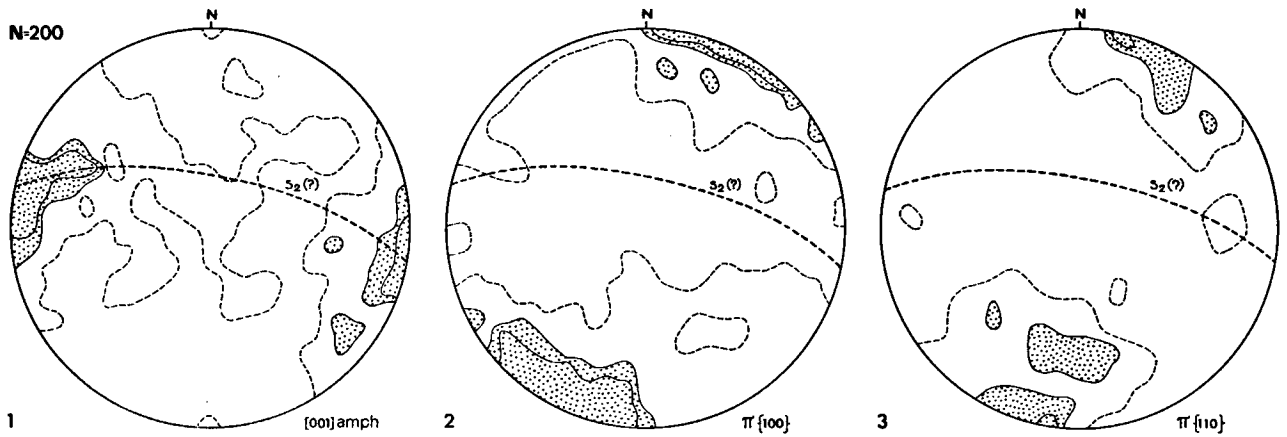


Fig. IV-8. Metagabbro 95-A3-184, amphibole ($A = 0.02$).

The $\pi\{100\}$ -diagram shows a concentration of directions almost perpendicular to the estimated girdle of the c -axes. The same holds for the $\pi\{110\}$, although there is a tendency too to form an imperfect great-circle girdle around the point-maximum of the c -axes.

Hand-specimen 95-A4-235: amphibolite (Fig. IV-9a)

We now turn our attention to the structures in the border zone of the basic massif. First we shall investigate the eastern extremity beginning with the transition zone, i.e. the zone where the E-W structures with gently inclined foliations turn to N-S structures with moderately to steeply inclined foliations. The hand-specimen was taken from an exposure where s_1 is still visible, although a younger steeply inclined N-S foliation (s_4) is developed as a tectonic banding (see Photograph III-12). The formation of s_4 is closely connected with F_4 -folding since this plane is an axial-plane foliation. The F_4 -folds plunge subhorizontally to the N.

The thin section reveals an aphanitic green hornblende, which forms the s_1 -trace, and a fine-grained recrystallized blue-green hornblende, which is concentrated in narrow bands parallel to the axial plane of the F_4 -folds (s_4).

Amphibole. – Diagrams 1–3 contain the fabrics of the older generation of hornblende. The F_4 -folding causes a change in the original orientation of s_1 but in one domain we can still study the differences between the orientations of the hornblende generations. The c -axes exhibit the familiar picture of two maxima in a great-circle parallel to s_1 . F_1 -folds plunge here subhorizontally to the N and it is plausible that the maximum near N is parallel to this fold axis.

The $\pi\{100\}$ - and $\pi\{110\}$ -diagrams are rather well

oriented. One could not however say whether the $\{100\}$ - or $\{110\}$ -planes are primarily oriented in s_1 . The $\pi\{110\}$ -diagram shows more clearly the effect of two crossing girdles due to the fact that the c -axes are concentrated into two maxima.

The c -axes of the blue-green hornblende (diagram 4) are grouped in a pronounced maximum lying in s_4 . The distribution of the c -axes deviates in places a little from s_4 since the laminae, in which these crystals occur, are not entirely straight. The development of two separate maxima is missing, in contrast to diagram 1. $\pi\{110\}$ and $\pi\{100\}$ show a weak and incomplete great-circle distribution around B_4 .

Hand-specimen 95-A4-234: amphibolite (Fig. IV-9b)

This sample was taken near the same locality as the foregoing. It forms part of an F_4 -fold of which the axial plane is moderately inclined to the ESE. The thin section shows that the rock consists essentially of fine-grained greenish hornblende and minor plagioclase. A sketch of the F_4 -fold has been drawn in the centre of diagram 1.

Amphibole. – The c -axes, measured in a fold limb, are concentrated in two maxima. The maximum perpendicular to B_4 is the more pronounced.

The $\{110\}$ -cleavages tend to lie parallel to s_4 as demonstrated by the $\pi\{110\}$ -diagram. One $\{110\}$ -position is preferred as can be derived from the occurrence of one maximum which is asymmetrically elongated. A small circle, drawn around this maximum with an angular radius of 56° , indicates clearly the asymmetric distribution of the $\pi\{110\}$ within this circle. The circular $\pi\{100\}$ -concentration lies naturally about 25° away from the $\pi\{110\}$ -maximum.

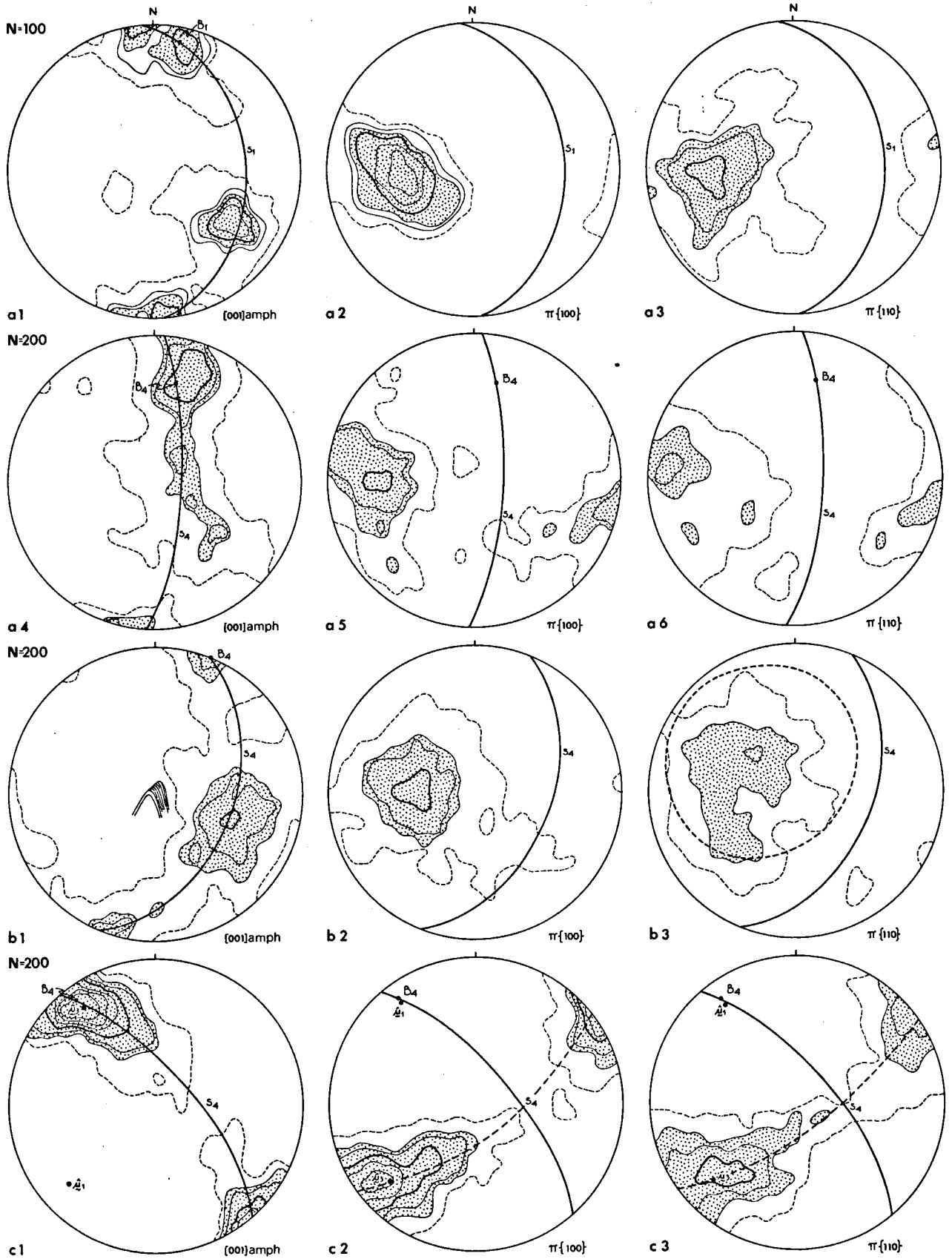


Fig. IV-9. a. Amphibolite 95-A4-235, amphibole ($A = 0.02$); diagrams 1-3 of aphanitic amphibole and diagrams 4-6 of fine-grained recrystallized amphibole. b. Amphibolite 95-A4-234, amphibole ($A = 0.02$). c. Pyroxene-amphibolite 95-A4-252, amphibole ($A = 0.02$).

Hand-specimen 95-A4-252: pyroxene-amphibolite
(Fig. IV-9c)

This sample comes from the Alboya Hill. Isoclinal to tight F_4 -folds are present; the attitudes of the axial planes deviate locally from the N-S direction, although roughly speaking they approximate this N-S orientation. The thin section reveals a pale-green porphyroclastic clinopyroxene, whereas the amphibole has recrystallized as a fine-grained blue-green hornblende. The hornblendes are concentrated along the old foliation (s_1) and do not form a new foliation which crosscuts s_1 . Still, we can state that the growth of this hornblende is connected with F_4 and that the clinopyroxene seems to be an older mineral, deformed by younger folding.

Amphibole. – The c -axes ($\zeta_3 \approx 10.3$; $\zeta_2 \approx 7.7$) are extremely well-grouped around $\hat{\mu}_3$. This elongated maximum coincides with B_4 . The axial plane s_4 has about the same orientation as the estimated great-circle around $\hat{\mu}_1$.

The π {100}-diagram ($\zeta_3 \approx 9.5$; $\zeta_2 \approx 7.2$) shows a great-circle girdle with $\hat{\mu}_1$ as axis. A point-maximum is present nearly normal to s_4 . The same pattern is exhibited by the π {110}-diagram ($\zeta_3 = 6.75$; $\zeta_2 = 5.30$). From the estimated values of ζ , one can see that the concentration of π {100} is better than that of π {110} (although the comparison is not fully justified because of the double number of orientations for the π {110}-diagram).

Hand-specimen 95-B3-86: retrograded hornblende-plagiopyrigarnite (Fig. IV-10)

At the eastern extremity of the basic massif, in general, the structures have a N-S strike. The foliations are

moderately to steeply inclined to the east. The rocks are laminated with alternating greenish and black laminae.

Microscopically a medium-grained porphyroclastic clinopyroxene is visible, occurring in stripes and at places dispersed throughout the rock. The fine-grained brownish-green hornblende is less deformed and has a blue-green rim, whereas the garnet is altered into saussurite-like aggregations. The rocks have been folded with fold axes (B_4) which plunge gently to the N. The growth of blue-green hornblende rims is probably connected with M_3 , but the original orientation of the brownish-green hornblende crystals might have been left intact. Obviously the fabric could then be linked with F_1 , and the foliation has been steepened during F_4 .

Amphibole. – The c -axes are clearly concentrated into two equally strong maxima. As remarked previously, it is not quite certain whether these amphiboles are associated with F_4 .

The π {110}-diagram tends to occupy a great-circle around B_4 .

Hand-specimen 121-B1-305: hornblende-plagiopyrigarnite (Fig. IV-11)

This rock has been found in the southern 'tail' of the basic massif. The foliation has a NE-SW strike. Especially in the neighbourhood of the Pico Sacro fault, the structural trend changes rapidly in different directions. The constituent minerals include garnet, brownish-green hornblende and pale-green clinopyroxene. The hornblende as well as the clinopyroxene has been converted into blue-green hornblende.

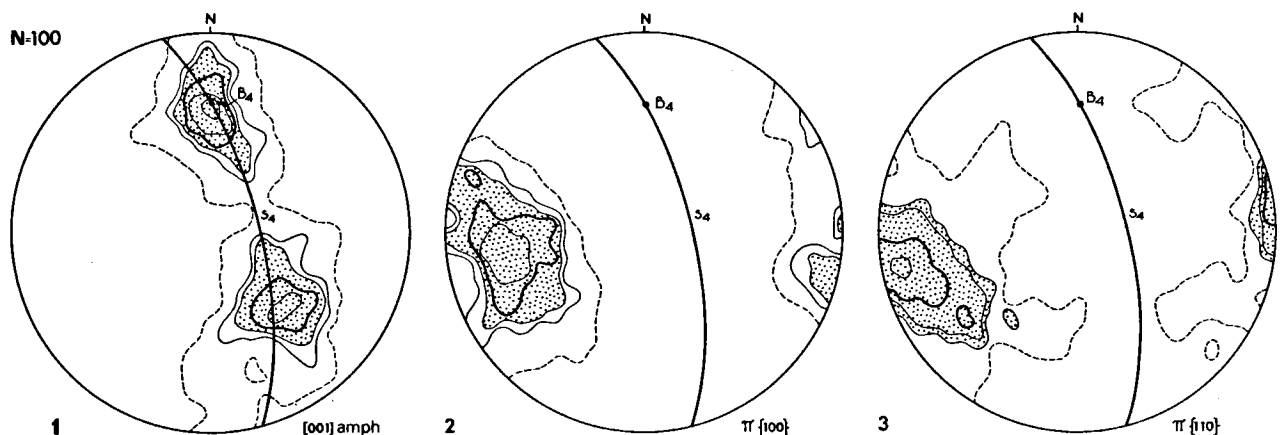


Fig. IV-10. Retrograded hornblende-plagiopyrigarnite 95-B3-86, amphibole ($A = 0.02$).

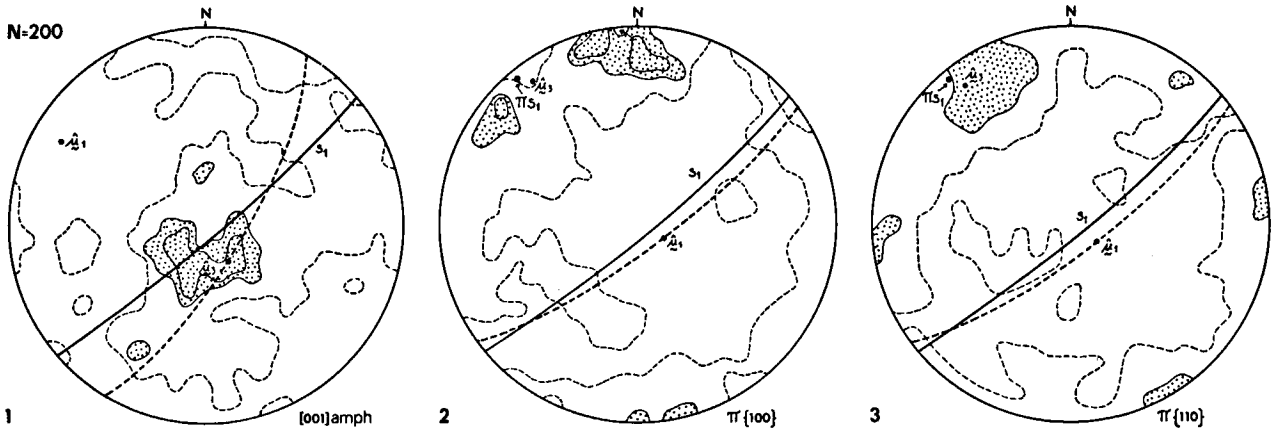


Fig. IV 11. Hornblende-plagiopyrigarnite 121-B1-305, amphibole ($A = 0.02$).

Amphibole. – The c -axes ($\zeta_3 = 1.65$; $\zeta_2 = 0.70$) have only one pronounced maximum lying in the centre of the diagram. The foliation s_1 has been drawn and the distribution of the c -axes does not completely follow this plane. The estimated great-circle however is close to s_1 .

The π {100}-pattern ($\zeta_3 = 1.80$; $\zeta_2 = 1.25$) shows a gap where πs_1 is, but π {110} ($\zeta_3 = 1.35$; $\zeta_2 = 0.95$) seems to be concentrated around πs_1 . The sub-maximum

(E-W direction), lying at an angle of about 55° from $\hat{\mu}_3$, may be inferred from the complementary orientation of the {110}-cleavages in a hornblende crystal.

Hand-specimen 95-A4-230: garnet-(pyroxene)-amphibolite (Fig. IV-12a)

Following the E-W structures in the central part to the west, we can observe that the foliations turn to a N-S

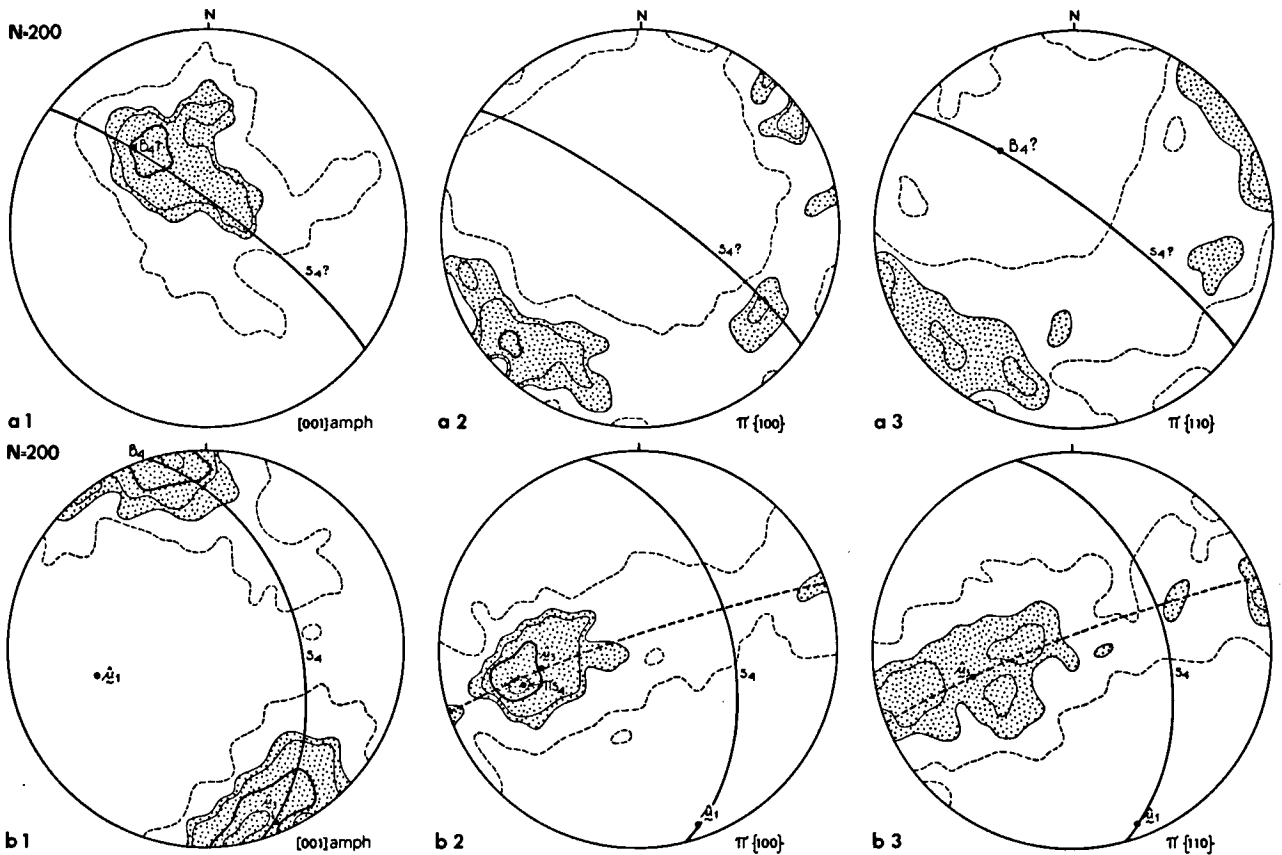


Fig. IV-12. a. Garnet- (pyroxene)-amphibolite 95-A4-230, amphibole ($A=0.02$). b. Pyroxene-amphibolite 95-A4-205, amphibole ($A=0.02$).

A sample was taken from the transition zone, containing among others blue-green hornblende, pink garnet and clinopyroxene. It is difficult to decide whether the clinopyroxene is original or a younger vein mineral. The growth of hornblende is probably connected with the isoclinal fold (B_4 ?) present in the thin section.

Amphibole. – The c -axes are neatly concentrated in an irregularly-shaped point-maximum. The fold-axis B_4 (?) coincides with this maximum.

The distribution of $\pi\{100\}$ reflects the coincidence of these planes with the axial plane (s_4). The roughly symmetric $\pi\{110\}$ -pattern supports this presumption.

Hand-specimen -95A4-205: pyroxene-amphibolite
(Fig. IV-12b)

The southern slope of the Coto de Viso is characterized by a NNW-SSE striking foliation; the attitude is steeply inclined to the E. Within the amphibolites, microfolds were observed which we assume are related to F_4 . A mineral lineation, formed by hornblende prisms, lies parallel to the fold axes and illustrates perhaps a relationship between this mineral and the deformation. Furthermore, veins, containing pale-green clinopyroxene, are concentrated in the axial planes of these microfolds. Clinopyroxene and hornblende grains show a deformation (undulatory extinction), at places to some extent granulation, of the crystals. Therefore it cannot be excluded that these minerals were mechanically rotated, adapting themselves to new orientations.

Amphibole. – The c -axes ($\zeta_3=7.00$; $\zeta_2=5.50$) are well concentrated around $\hat{\mu}_3$. An obvious feature of this fabric is the absence of a sub-maximum perpendicular to B_4 in s_4 . The axial plane s_4 completely fits the estimated great-circle around $\hat{\mu}_1$.

The $\pi\{100\}$ -diagram ($\zeta_3=5.25$; $\zeta_2=4.00$) occupies a great-circle girdle around the fold axis. The circular point-maximum is located near πs_4 . However, this maximum emphasizes the weak concentration of $\pi\{110\}$ ($\zeta_3=4.00$; $\zeta_2=3.10$) at the same place. About 30° from this gap, we observe two maxima of $\pi\{110\}$.

Hand-specimen 95-A3-175: blastomylonitic amphibolite
(Fig. IV-13a)

The rocks on the northern slope of the Coto de Viso are greatly deformed locally. A mineral lineation

(approx. NNE plunging) is clearly visible in the rocks which might have originally been metagabbros.

Under the microscope it is quite clear that the lineation (l_4) consists of rods of medium-grained porphyroclastic hornblende which are often deformed such that their longitudinal direction has about the same orientation as the rods themselves. The brownish-green hornblende shows *Schiller* inclusions and the borders are converted to blue-green hornblende. The matrix is composed of recrystallized aphanitic blue-green hornblende, plagioclase and epidote.

Porphyroclastic amphibole. – The c -axes show a strong elongated point-maximum in the NE quadrant, coinciding with l_4 . The axes tend to occupy a great-circle girdle.

In the $\pi\{100\}$ -diagram one might infer a complete girdle around l_4 . The main concentrations are separated by 45° . Between these concentrations, we notice a maximum occurring in the $\pi\{110\}$ -diagram. Probably the $\{110\}$ -cleavages occupy a moderately inclined plane (s_4 ?) and there is obviously no preference for one specific orientation of the possible attitudes of $\{110\}$.

Hand-specimen 95-E4-230: blastomylonitic pyroxene-amphibolite (Fig. IV-13b)

At the western extremity of the basic massif, the blastomylonitic rocks include clinopyroxene and hornblende. The rocks are heavily lineated (mineral lineation), but the direction of this lineation does not contribute to the structural picture here, since the rocks have been broken up in large blocks, disturbing the original orientations. Within the domain of such a block, however, we can inspect the structural properties. The Hercynian (?) cleavage (s_4) is very distinct and strikes NNE-SSW. A vague layering, formed by alternating clinopyroxene-rich bands and bands predominantly containing hornblende and plagioclase, is normal to s_4 . The matrix is recrystallized and one can see the formation of reaction rims of garnet between plagioclase and hornblende porphyroclasts.

Porphyroclastic amphibole. – The c -axes ($\zeta_3=7.35$; $\zeta_2=3.15$) exhibit an elongated point-maximum extending along the layering or foliation, which is probably s_1 ($=s_0$). The estimated great-circle coincides rather well with this layering.

The distribution of the $\pi\{100\}$ ($\zeta_3=5.50$; $\zeta_2=5.25$) and $\pi\{110\}$ ($\zeta_3=5.15$; $\zeta_2=4.90$) is circular around

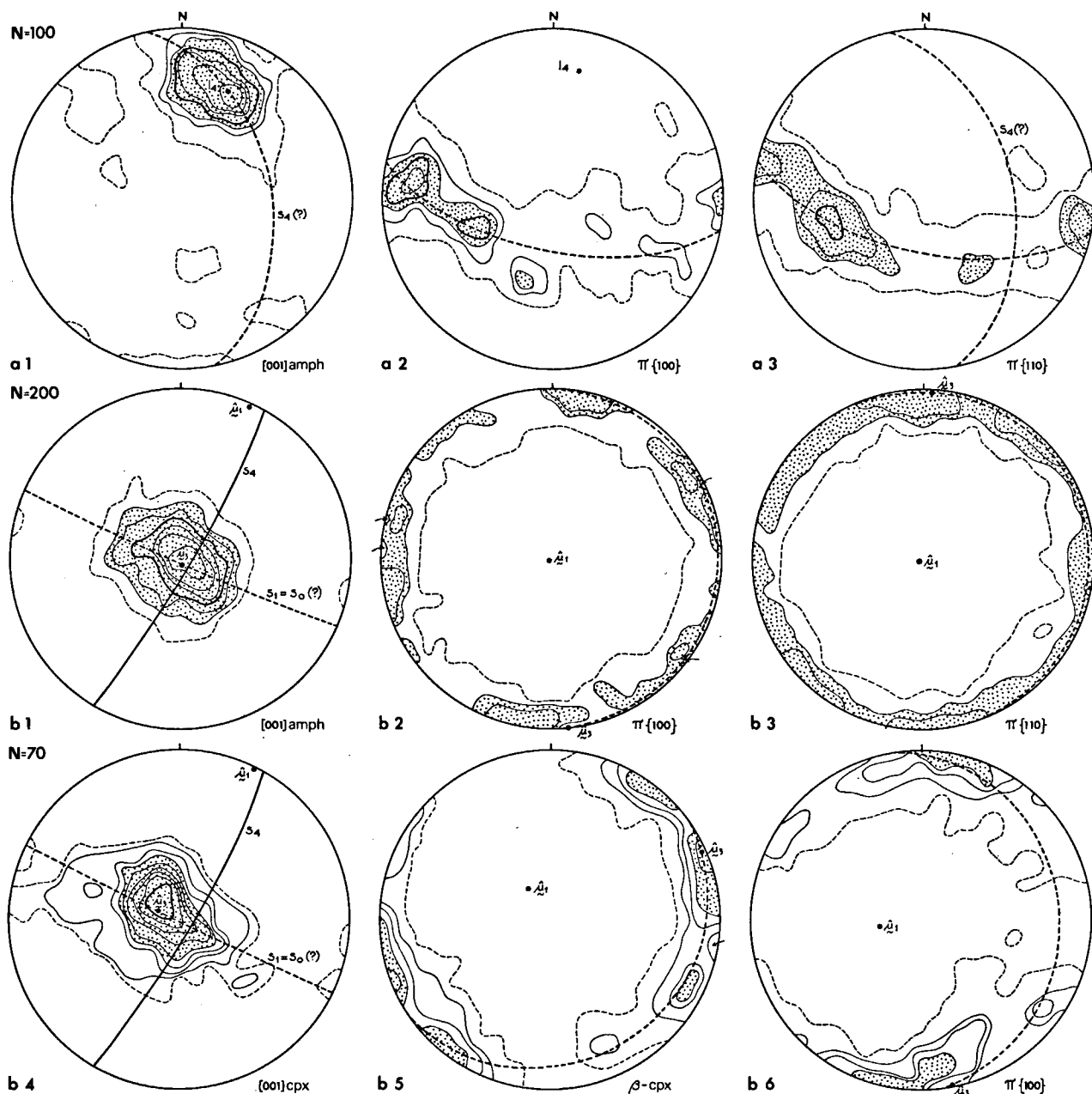


Fig. IV-13. a. Blastomylonitic amphibolite 95-A3-175, amphibole ($A = 0.02$). b. Blastomylonitic pyroxene-amphibolite 95-E4-230, amphibole ($A = 0.02$), clinopyroxene ($A = 0.04$). Significant areas are stippled for frequencies $x \geq 8$ in the clinopyroxene diagram.

the point-maximum of diagram b1. The circular shape could also be derived from the estimated shape parameters ζ (since $\zeta_3 \approx \zeta_2$).

Porphyroclastic clinopyroxene. – The c -axes pattern ($\zeta_3 = 5.95$; $\zeta_2 = 3.00$) bears a close similarity to diagram b1. The same holds for $\pi \{100\}$ ($\zeta_3 = 3.55$; $\zeta_2 = 2.25$). The β -diagram ($\zeta_3 = 3.95$; $\zeta_2 = 2.70$) displays a nearly complete great-circle girdle. A maximum concentration is found ENE-WSW.

THE RESULTS OF PETROFABRIC ANALYSES FITTED INTO THE STRUCTURAL FRAMEWORK

A structural framework was tentatively postulated in Chapter III; we shall now try to compare the microscopical fabric analyses with the results obtained from the structural geology in the field.

First of all we shall inspect the amphibole and clinopyroxene fabrics for the central part of the basic massif. Broadly speaking, we can state that the fabrics of the brownish-green hornblende are quite similar

with respect to the distribution of the *c*-axes, i.e. a main maximum usually oriented N or NNW with varying plunges and a poorly developed maximum almost normal to the main concentration lying in the foliation plane (Fig. IV-3, 4, 5 and 6). Furthermore, it appears that in general $\{110\}$ -cleavages occupy the foliation plane (Fig. IV-6), especially in the metabasites which display phenomena of postcrystalline deformation. In the case of the synkinematic growth of hornblende without a subsequent deformation, $\{100\}$ seem to be oriented along the axial plane of a fold or the foliation (Fig. IV-4, diagram a 5). Clinopyroxene *c*-axes show about the same distribution as the corresponding hornblende fabrics. It is still possible that the hornblende *c*-axes have a preferred orientation. This holds moreover for the $\pi\{100\}$ -diagrams of hornblende and clinopyroxene. The growth of this brownish-green to green hornblende and pale-green clinopyroxene during M_1 shows a correlation with the F_1 -structures discussed.

A completely different aspect is presented by the fabrics of porphyroblastic green hornblende, represented in Fig. IV-7. The *c*-axes have a nearly WNW-ESE orientation and a sub-maximum is lacking. The discrepancy is accentuated by the $\pi\{100\}$ - and $\pi\{110\}$ -diagrams, where no distinct relationship between the present foliation and the distribution of these planes can be discerned. The direction of the *c*-axes is related to the F_2 -folds, and the fabric could be characterized as a B-tectonite.

The fabrics of green to blue-green hornblende, derived from the amphibolites occurring at the border zones of the basic massif, demonstrate a scattering of *c*-axes along a moderately to steeply inclined N-S striking foliation. In this foliation, we note a preferred orientation, usually plunging slightly to the N (Fig. IV-9). The fabrics often contain a sub-maximum, perpendicular to B_4 , but several fabrics do not show such a maximum. Thin section (95-B3-85), prepared from a F_4 -fold, reveals a preferred orientation of *c*-axes normal to B_4 . From the foregoing, it is obvious that the fabrics dealt with do not always exhibit the same pattern. Figs. IV-9a and 9c are good examples of fabrics from F_4 -structures.

Evidently several fabrics could not be incorporated in the framework, in which three stages of hornblende growth have been proposed. Consequently, they are only tentatively placed in this system.

The fabrics of a metagabbro (Fig. IV-8) have points

in common with the F_2 -structures. The same applies for the fabrics of porphyroclastic amphibole and clinopyroxene in blastomylonitic amphibolites (Fig. IV-13a and b). The latter fabrics have been greatly influenced by younger folding. The recrystallization of the matrix of these rocks is perhaps associated with M_3 .

LITERATURE

The results of other investigations into hornblende fabrics will be compared with our results.

Schmidt (1928) found that the *c*-axes were aligned parallel to the tectonic *b*-axis in an amphibole-zoisite-schist from Rennfeld. He shows an additional diagram from a hornblende-gneiss from Drei Pfarrer with the same pattern, but there is also a tendency to form a concentration of *c*-axes parallel to the tectonic *a*-axis. He mentions a concentration of $\pi\{010\}$ in both diagrams near the tectonic *a*-direction.

Wenk (1937) studied the banded gneisses of Ornö Huvud in Sweden. The fabrics exhibit the same features as above, i.e. a preferred orientation of hornblende *c*-axes parallel to the tectonic *b*-axis and the location of $\{100\}$ -planes in the present *s*-plane.

The same holds for diagrams of amphibolite samples from Gröller Joch (S. Tirol), reported by Ladurner (1951). The *c*-axes of hornblende coincide with the tectonic *b*-axis; some orientations are grouped normal to this axis in the *s*-plane. $\pi\{110\}$ are occasionally located near πs , but usually $\pi\{100\}$ occupy the pole of the *s*-plane.

Garnetiferous amphibolites from the Lewisian (Mc Lachlan, 1953) show a preferred orientation of their *c*-axes parallel to the lineation in the rock. The poles of $\{110\}$ -cleavages form a maximum, split up into two parts, near the normal to *s*.

Kojima & Hide (1957) published diagrams of aegirine augite-amphibole-quartz-schists from the Sambagawa belt (Japan). According to them, $\{100\}$ -planes are always parallel to the *ab*-planes. They found two mutually perpendicular maxima for the *c*-axes, viz. parallel to the tectonic *a*- and *b*-directions.

Schwerdtner (1964) recorded the usual pattern of *c*-axes, concentrated along the tectonic *b*-axis, as well as $\{110\}$ -cleavages which seem to be oriented along the layering.

Labhart (1965) investigated amphibolite-migmatites from the Aar massif (Switzerland). He concluded that $\{110\}$ -cleavages are parallel to the *ab*-plane. Consequently, he found in his diagrams submaxima 50 – 60° from the main concentration of $\pi\{110\}$.

Samples from the Penser-Weisshorn amphibolite (S. Tirol) have been described by Briegleb (1966). He subdivided the hornblende fabrics into three types of which the most important are:

1. *s*-tectonites characterized by the concentration of *c*-axes along a great-circle girdle with a pronounced maximum in B. The $\pi \{110\}$ tend to spread along a great-circle girdle with B as axis. In this girdle is a significant maximum perpendicular to *s*;
2. B-tectonites with a main concentration in B of the *c*-axes. $\pi \{100\}$ as well as $\pi \{110\}$ extend along a great circle with B as axis.

Summarizing, one can say that a pronounced preferred orientation of hornblende *c*-axes parallel to the fold axis or lineation is a common feature. The occurrence of a sub-maximum, perpendicular to the fold axis in *s*, has often been observed. On the other hand, the reverse situation, i.e. a pronounced maximum in A and a poorly developed one in B, is a comparative rarity. Nevertheless, Fig. IV-9b shows such a tendency and as already remarked this situation seems to exist in sample 95-B3-85 (cf. p. 62). With regard to the orientations of $\{110\}$ and $\{100\}$, we might say that on this point there is a difference of opinion.

REMARKS ABOUT THE CAUSE OF THE OBSERVED PREFERRED ORIENTATIONS

The question arises what mechanism caused the observed fabrics, especially for hornblende crystals. Microscopical investigation reveals mostly undeformed hornblende, even when the associated fold is visible (see Fig. III-1). From these observations we could state that syntectonic recrystallization of hornblende has taken place. Perhaps the growth of the crystals postdated the deformation. The theory of Kamb (1959), based on crystallization under uniaxial stress for certain minerals, also appears to be an attractive approach for monoclinic minerals. I do not wish to enter into the thermodynamic calculations of this theory, but the occurrence of two mutually perpendicular maxima of the *c*-axes in the plane probably normal to the direction of greatest compression does suggest that the uniaxial stress system must be extended to a triaxial stress model. Especially at deep-seated levels in an orogene, it is possible that different stresses (tensile or compressive) act in three directions.

The process of plastic deformation perhaps offers an

explanation for the fabrics of porphyroclastic amphibole and clinopyroxene (cf. Fig. IV-13). Griggs *et al.* (1960) found as a glide system for deformed clinopyroxene the following results: $\{100\}$ is a translation glide plane (T) containing $[001]$ as translation glide direction (t). Data for deformed hornblende crystals are lacking but in analogy with clinopyroxene we might expect a similar system. If the B-axis should be an axis of maximum elongation, then a preferred orientation of the *c*-axes in B is plausible (Fig. IV-13a).

ALBITE AND TOURMALINE FABRICS OF LOW-GRADE SCHISTS

Albite-blasts occur in the low-grade schists of the Complex of Santiago de Compostela. Microscopical fabric analyses were carried out for albite and to a lesser extent for tourmaline. Under the microscope, the albite-blasts seldom show twinning planes or cleavages so that crystallographic directions could not be determined for this mineral. Fortunately, the indicatrix axes of albite approximately coincide with the crystallographic axes. The anorthite content of the blasts varies between 0–5%, suggesting that $c \wedge \beta \approx 18-16^\circ$, $b \wedge \gamma \approx 13-10^\circ$ and $a \wedge \alpha \approx 22-18^\circ$. Thus it follows that the pole of $\{010\}$ is close to the projection of γ in the diagram; by measuring only indicatrix axes, we may be able to derive some crystallographic information.

Hand-specimen 121-A1-206: porphyroblastic albite-schist (Fig. IV-14a)

This sample comes from a locality in the south. The schists, directly adjacent to the basic massif, have a schistosity which strikes NW-SE. The thin section displays albite-blasts ($\varnothing 2-0.3$ mm) with inclusions of quartz and muscovite. Apart from the schistosity (s_5), we could observe a crenulation cleavage (s_6). A pronounced striation (l_6) on the s_5 -plane, due to micro-folding of this plane, plunges subhorizontally or gently to the NW.

A point-maximum of α ($\zeta_3 = 1.85$; $\zeta_2 = 0.95$) lies near the intersection of s_5 and s_6 . The γ -pattern ($\zeta_3 = 0.95$; $\zeta_2 = 0.70$) shows a great-circle around l_6 . Presumably the $\{010\}$ -planes were concentrated along s_5 and during F_6 were rotated around l_6 . A subsidiary concentration of γ -directions is still visible near πs_5 . The β -diagram ($\zeta_3 = 1.05$; $\zeta_2 = 0.50$) has a concentration in s_5 as is to be expected from the distribution of the α - and γ -

directions. The diagrams reflect not only a preferred orientation of {010} but also a tendency for one crystallographic axis (c or a) to concentrate in a specific direction (a parallel to l_6 and c approximately perpendicular to l_6).

Hand-specimen 94-E4-149: porphyroblastic albite-schist (Fig. IV-14b)

The sample was taken from an exposure SE of Santiago de Compostela. The schistosity (s_5) turns to a NNW-SSE strike as does l_6 . The thin section shows albite-blasts (\varnothing 0.4–0.1 mm) and predominantly muscovite and aphanitic undulose quartz. In pressure-shadows, the growth of chlorite can be observed. The pressure-shadows are elongated nearly parallel to l_6 (see Fig. III-12).

Inspection of the γ -diagram ($\xi_3 = 2.60$; $\xi_2 = 2.05$) reveals that there is a close resemblance to the corresponding diagram for the foregoing sample. Here too we may infer that the γ 's form a great-circle around l_6 . The pole of the estimated great-circle is near l_6 . It appears that {010}-planes are concentrated along s_5 as well as s_6 . The distribution of the α -directions ($\xi_3 = 2.20$; $\xi_2 = 0.25$) is in accordance with the α -pattern of sample 121-A1-206. The α 's show however a definite small-circle distribution. A small-circle has been drawn around $\hat{\mu}_3$ with an angular radius of 20° , which is approximately the value of $a \wedge \alpha$. This suggests that the crystallographic a -axis is oriented parallel to l_6 . The principle β -point-maximum ($\xi_3 = 0.80$; $\xi_2 = 0.30$) lies between s_5 and s_6 .

Hand-specimen 94-E4-150: porphyroblastic albite-schist (Fig. IV-14c)

The rock is mainly composed of muscovite, quartz and chlorite. Undulose quartz grains are elongated parallel to s_6 . This sample contains albite-blasts that were rotated after their growth. The blasts show inclusions of rutile and opaque minerals aligned parallel; from the s_i/s_e relation, it can be inferred that the rotation axis is parallel to l_6 and that the rotation sense is counter-clockwise looking N.

The α -diagram ($\xi_3 = 2.25$; $\xi_2 = 0.35$) displays a point-maximum near l_6 . The estimated great-circle girdle is close to s_6 . The orientations of γ ($\xi_3 = 1.65$; $\xi_2 = 1.30$) are clustered in a great-circle almost perpendicular to l_6 . Sub-maxima near πs_6 and πs_5 are lacking, probably the result of intensive post-crystalline rotation. The β -diagram ($\xi_3 = 1.15$; $\xi_2 = 0.70$) has approximately the

same configuration, i.e. an irregular great-circle girdle perpendicular to l_6 .

Thin section 94-E4-150(2) was taken from the same sample but now parallel to the horizontal plane in which S-shaped inclusions in the albite-blasts are visible. The diagrams bear a close similarity to those described above. A single remark about the γ -diagrams should be added. Except for the great-circle around l_6 , we can discern in both diagrams a spread of the γ 's around a subvertical axis. This is probably due to a paracrystalline rotation of the blasts during F_5 . Thus the {010}-planes were oriented along s_5 and during their growth were rotated around a subvertical axis (B_5).

Hand-specimen 94-E4-140A: porphyroblastic albite-schist (Fig. IV-15a)

The sample was taken 2 km south of Santiago de Compostela, where the regional schistosity strikes N-S. The thin section (94-E4-140 A1) reveals that the rock is composed of muscovite, chlorite, quartz, albite and microcrystalline garnet. The predominant schistosity (s_5) has been crenulated during F_6 causing a fine lineation on this plane. This lineation (l_6) plunges very gently N or S. A postcrystalline rotation of the albite-blasts can be seen in Fig. III-12.

The γ -diagram ($\xi_3 = 0.90$; $\xi_2 = 0.50$) shows a broad great-circle girdle perpendicular to l_6 . The estimated great-circle fits the present distribution of γ quite well. The α -directions ($\xi_3 = 1.15$; $\xi_2 = 0.15$) are clustered near l_6 , probably forming a small-circle around $\hat{\mu}_3$ with an angular radius of 20° ($a \wedge \alpha$). Consequently, the orientations of β are mainly concentrated along a great-circle approximately located around $\hat{\mu}_1$.

Another section (94-E4-140 A2) was taken from the same sample. The diagrams are roughly similar to those discussed above.

The distribution of γ however shows a sub-maximum perpendicular to s_5 . A tendency of γ to spread along a great-circle girdle around an axis, presumably steeply plunging in s_5 , is visible. This may be an indication of synkinematic growth of the albite-crystals. This supposition is strengthened by the presence of sigmoidally arranged inclusions in the blasts. The α -directions are scattered along a great-circle, approximately coinciding with s_5 . Moreover, the α 's tend to spread along a small-circle with $\hat{\mu}_3$ as axis (angular radius 20°).

Hand-specimen 94-E2-152C: porphyroblastic albite-schist (Fig. IV-15b)

The orientations of α ($\xi_3 = 1.05$; $\xi_2 = 0.55$) show an

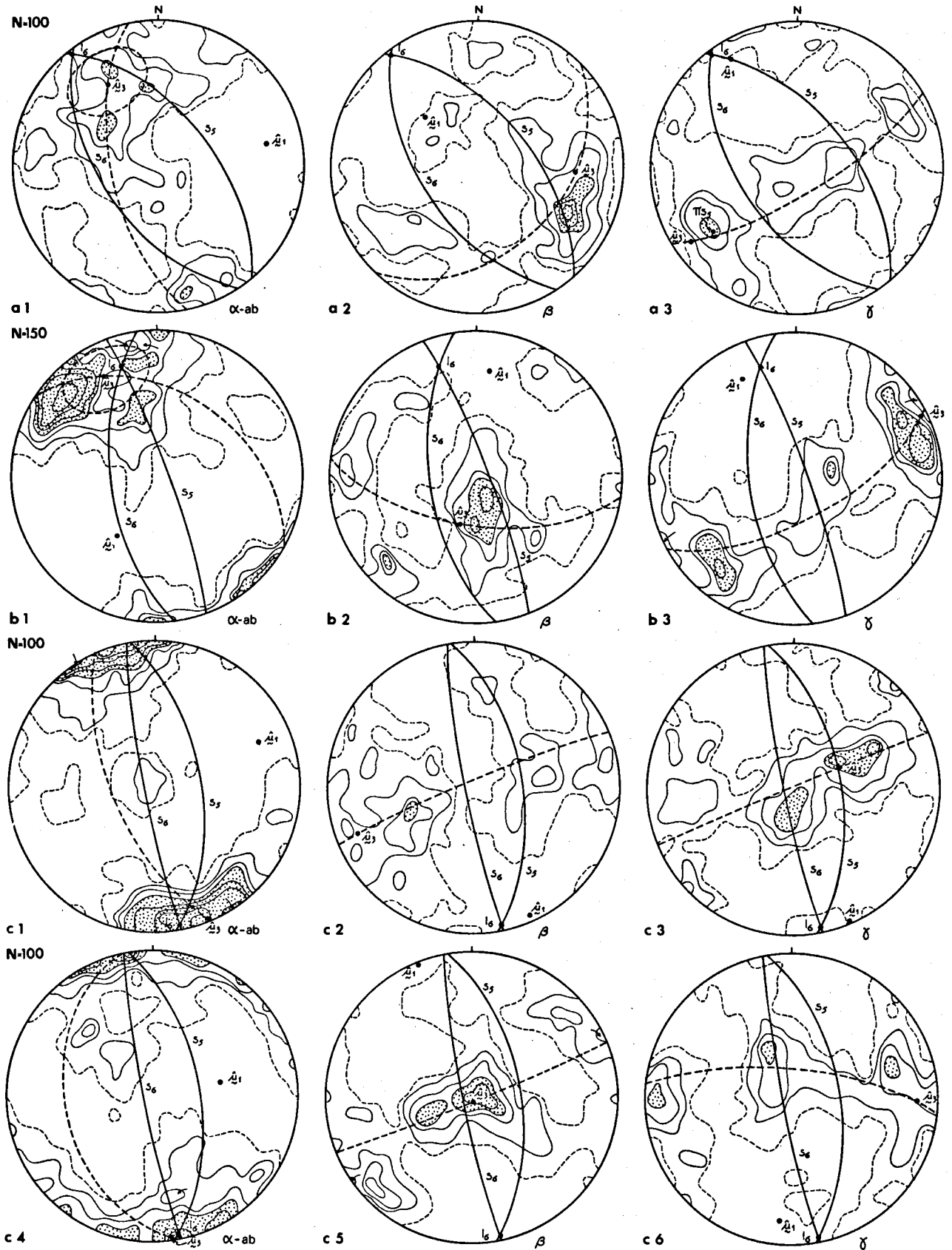


Fig. IV-14. a. Porphyroblastic albite-schist 121-A1-206, albite ($A = 0.04$). b. Porphyroblastic albite-schist 94-E4-149, albite ($A = 0.04$). c. Porphyroblastic albite-schist 94-E4-150, albite ($A = 0.04$).

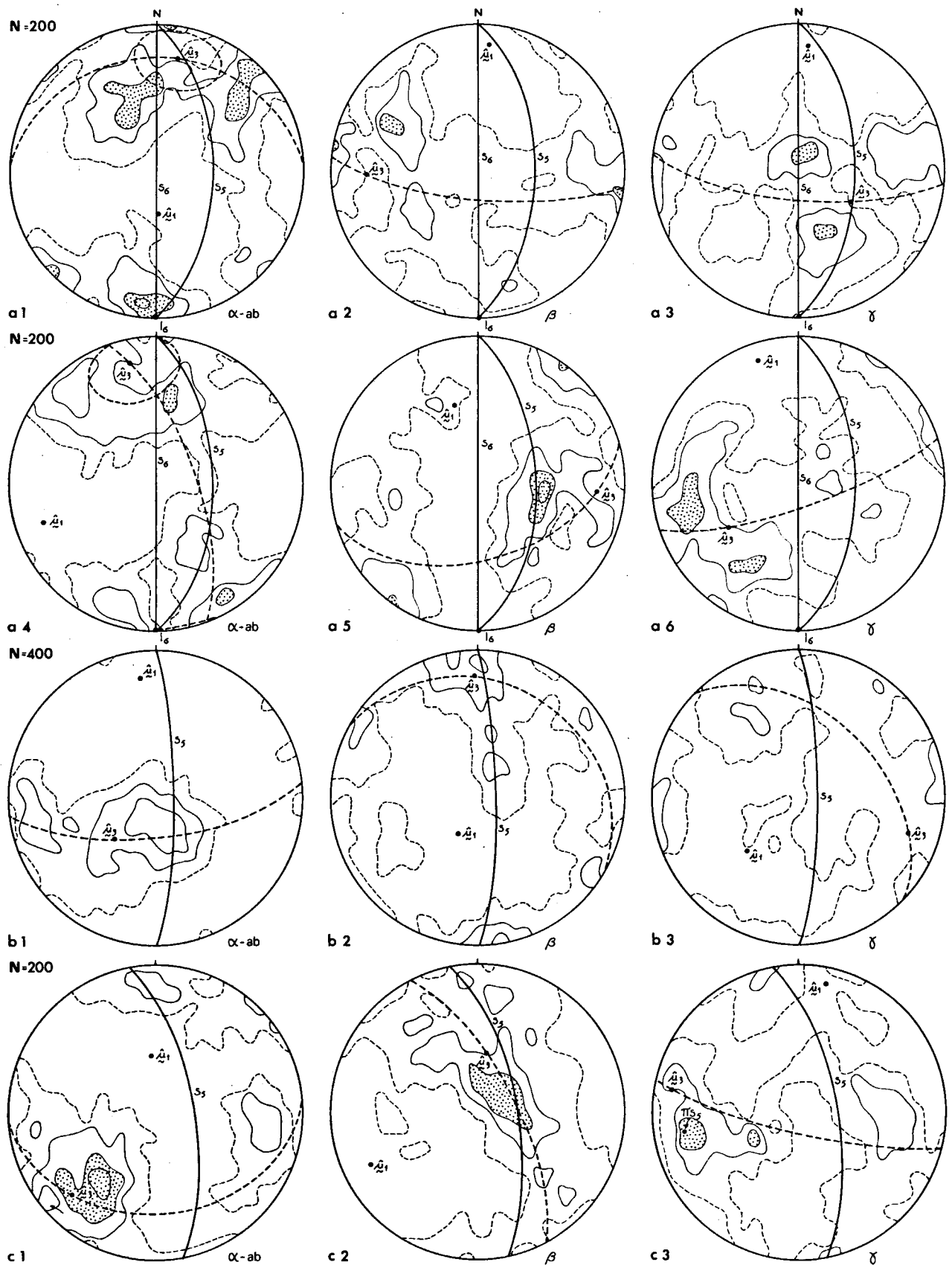


Fig. IV-15. a. Porphyroblastic albite-schist 94-E4-140 A, albite ($A = 0.04$). b. Porphyroblastic albite-schist 94-E2-152 C, albite ($A = 0.04$). c. Porphyroblastic albite-schist 94-E2-152 B, albite ($A = 0.04$). The stippled significant areas in Fig IV-15b are omitted because the Poisson Table does not extend to these frequencies.

evident tendency to spread along a great-circle girdle perpendicular to s_5 . The location of the estimated point-maximum is close to s_5 . The β -directions are approximately distributed along s_5 , although the estimated great-circle does not reflect this situation. It is possible however that the presence of sub-maxima influences the position of the estimated great-circle. The γ -diagram displays an irregular pattern. A sub-maximum is still visible perpendicular to s_5 . The spreading of the axes could be attributed to the influence of slip planes which are connected with late-Hercynian phyllonitization.

Hand-specimen 94-E2-152B: porphyroblastic albite-schist (Fig. IV-15c)

This sample comes from a location north of Santiago de Compostela, situated in a band of schists between two-mica granites and orthogneisses. The zone of the porphyroblastic albite-schists, beginning in the southern part of the mapped area, extends to the north, always adjacent to the strip of orthogneisses. The presence of abundant albite and quartz gives the rock a gneissose aspect. The blasts (\varnothing 0.3–0.05 mm) enclose dusty strings of opaque minerals, showing an s_1 -pattern without evident relationship to s_2 . In pressure-shadows, the tails of which are subhorizontally elongated, the occurrence of recrystallized biotite can be observed. This probably means that this biotite growth is due to the intrusion of the two-mica granites, giving rise to the formation of new minerals.

The α -pattern ($\zeta_3 = 1.05$; $\zeta_2 = 0.50$) shows a concentration in the southwestern quadrant. The estimated great-circle girdle is perpendicular to s_5 . In contrast to this configuration is the distribution of β ($\zeta_3 = 1.35$; $\zeta_2 = 0.90$). The β 's form an almost complete great-circle girdle parallel to s_5 . The point-maximum lies in the centre of the diagram, whereas the position of $\hat{\mu}_3$ is outside the proper maximum. The γ -directions ($\zeta_3 = 0.35$; $\zeta_2 = 0.20$) occupy a broad great-circle nearly perpendicular to s_5 . The estimated point-maximum $\hat{\mu}_3$ is close to πs_5 from which the preferred orientation of {010} along s_5 may be concluded.

Hand-specimen 94-E2-105: tourmaline-bearing muscovite-chlorite-garnet-schist (Fig. IV-16)

In the schists adjacent to the two-mica granites, rocks occur which are partly tourmalinized. Locally one can observe that the c -axes of tourmaline are aligned

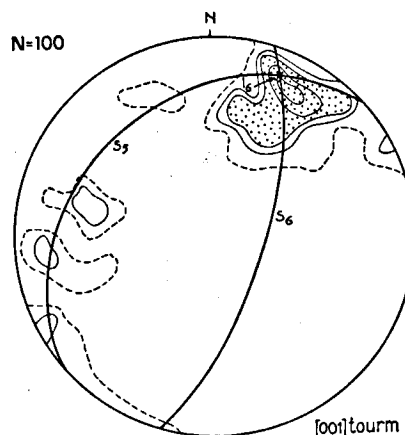


Fig. IV-16. Tourmaline-bearing muscovite-chlorite-garnet-schist 94-E2-105, tourmaline ($A = 0.02$).

parallel to l_6 . The fabric diagram accentuates this observation, showing a prominent point-maximum near l_6 .

GENERAL REMARKS ABOUT THE ALBITE FABRICS

The microscopical fabric study of the albite-porphyroblasts indicates that this mineral reacted to stress as shown by the preferred orientation of several fabric elements. It has been suggested that the albite-porphyroblasts crystallized after the main phase of the Hercynian orogeny. As previously mentioned (cf. p. 63), the indicatrix axes of albite do not coincide exactly with the crystallographic axes. Summarizing the fabric diagrams, we can state that especially the γ -directions show in each sample a great-circle distribution with a concentration of orientations nearly perpendicular to an s -plane. This may indicate that the {010}-planes controlled these fabrics (because $\gamma \approx$ crystallographic b). Furthermore, it appears that the diagrams, presented in Figs. IV-14 and IV-15a, exhibit a constantly recurring orientation pattern for α , i.e. a concentration of axes near l_6 . An important feature of the α -diagrams is the presence of a small-circle distribution around $\hat{\mu}_3$ with an angular radius of about 20° ($\alpha \wedge a$). The location of l_6 , measured directly from the lineation present in the hand-specimen, is close to $\hat{\mu}_3$. This indicates that these diagrams probably reflect a preferred orientation of the crystallographic a -axis parallel to l_6 .

In thin sections, which are cut perpendicular to s and parallel to l_6 , the albite-blasts display an elliptical shape. This means that the blasts are frequently

elongated parallel to α or, more likely, parallel to the crystallographic a -axis. This elongation was perhaps present after crystallization but it could also have originated from flattening during younger phyllonitization; the latter might also have accentuated the elongation.

The fabric diagrams of Figs. IV-15b and IV-15c do not correspond with the other fabrics. The β -directions are concentrated along the present s -plane whereas α 's occupy a great-circle girdle perpendicular to this plane.

LITERATURE

The following is a short review of the results of several investigations dealing with feldspar fabrics.

Seng (1934) described the orthoclase fabrics of a granulitic rock from the Bohemian massif. The $\{010\}$ -planes show a preferred orientation in s , since the γ -fabric is dominated by a point-maximum perpendicular to s . The β -orientations were concentrated in s , showing a strong maximum there.

Wenk (1937) studied the plagioclase fabrics of samples from the banded gneisses of Ornö Huvud (Sweden). He reported a strong maximum of $[100]$ in tectonic b while $\{001\}$ -planes tend to be oriented along the ab -plane.

Crampton (1957) reported fabrics of albite-blasts from rocks occurring in the Moine schists of the

Scottish Highlands. The β -directions are aligned parallel to a pronounced lineation. The α -diagram shows a point-maximum perpendicular to the β -concentration in the ab -plane. From this it follows that γ (\approx crystallographic b) has a preferred orientation normal to the s -plane, which implies that $\{010\}$ -planes preferentially occupy this plane.

Barbu (1960) analysed the fabrics of feldspar in the magmatic rocks of Rumania. The fabric diagrams, showing $\pi \{001\}$ and $\pi \{010\}$ together in one diagram, are dominated by a pronounced great-circle girdle around tectonic b ; moreover, a sub-maximum near b is present.

Okamura (1960) described fabric diagrams of albite from the Ryôke gneiss and granodiorite complex in southwest Japan. The poles of $\{010\}$, constructed directly from measured twin planes, show a point-maximum which coincides with the tectonic c -axis. The poles are also distributed along a great-circle girdle around tectonic b .

Trommsdorff (1964) observed albite fabrics of an albite-gneiss from the western extremity of the *Hohe Tauern*, at the border between Austria and Italy. The $\{010\}$ -planes of albite probably occupy the s -plane although this conclusion was drawn from a γ - and a β -diagram. The β -orientations show a tendency to spread along s . Translation gliding parallel to $\{010\}$ may explain the observed orientations of plagioclase. Such a translation along $\{010\}$ has been reported by Sen (1959) for deformed plagioclase from a banded norite.

SAMENVATTING

Het gebied rondom Santiago de Compostela maakt deel uit van het Hesperische massief in noordwest Spanje; een overwegend Hercynisch metamorf gebied, waarin echter gesteenten voorkomen waarvan vermoed wordt dat zij polymetamorf zijn. Op structurele en petrografische gronden kan het gebied verdeeld worden in twee complexen, nl. het Ordenes Complex en het Complex van Santiago de Compostela. Het Ordenes Complex bestaat uit mesozonaal gemetamorfoseerde paragneizen en schisten en uit retrograde hoornblende-plagiopyrigarnieten, amfibolieten, metagabbro's en ultramafische gesteenten. Het Complex van Santiago de Compostela wordt gevormd door epizonaal gemetamorfoseerde schisten waarin soms albitporfiroblasten voorkomen. De intrusieve gesteenten, indien als zodanig nog herkenbaar, zijn in een aparte groep geplaatst.

De mineraalparagenese klinopyroxeen-granaat-hoornblende in de mafische gesteenten van het Ordenes Complex wijst op granuliet-facies metamorfose tijdens een pré-Hercynische (?) orogenese. De geassocieerde structuren (F_1) hebben subhorizontale assenvlakken en horizontale tot zwak naar het noorden duikende plooiasen. In de metasedimenten vormde zich lokaal de mineraal-associatie distheen-granaat-(\pm stauroliet). Tijdens F_2 werden vooral in overschuivingszones isoclineaal geplooid blastomylonieten (amfiboliet facies) gevormd. Deze naar het zuiden gerichte overschuivingen resulteerden in een 'imbricatiestructuur'. F_3 is een postkristallijne deformatie waarbij microplooiing optrad met overwegend steile assenvlakken en ongeveer E-W, horizontaal gerichte plooiasen. Een intrusie van gabbro's (de latere metagabbro's) vond misschien plaats voor F_2 .

Na de pré-Hercynische orogenese intrudeerden granieten tijdens de overgang van het Cambrium naar het Ordovicium. Deze tijdsbepaling is gebaseerd op dateringen van soortgelijke gesteenten in het gebied rond Vigo (Zuid-Galië), waarvan de vormingsouderdom op rond 500 miljoen jaar werd gesteld. Enkele intrusieven met een dioritische samenstelling hebben vermoedelijk dezelfde ouderdom.

De Cambro-Orodovicische granieten en diorieten werden tijdens de Hercynische orogenese veranderd in orthogneizen respectievelijk metadiorieten. De metamorfe sedimenten en metabasieten van het Ordenes Complex ondergingen retrograde metamorfose terwijl de sedimenten van het Complex van Santiago de Compostela onder groenschist-facies omstandigheden werden gemetamorfoseerd tot chloriet-muscoviet-spessartierijke granaat-schisten. Tijdens deze metamorfe fase (M_3) werden de gesteenten geplooid (F_4) waarbij steile N-S strekkende assenvlakken werden gevormd. De plooiasen duiken zwak naar het noorden. Albietblastese vond plaats gelijktijdig met fase F_5 (steil duikende plooiasen) maar hield vermoedelijk langer aan dan deze deformatie. De metamorfose ging door en culmineerde lokaal in partiële opsmelting van de metasedimenten. Het intruderen van tweeglimmer granieten volgde na de periode van migmatitisatie. De vorming van de mineralen sillimaniet, andalusiet, chloritoid, cordiëriet (?) en biotiet staat in relatie met deze granietintrusies. F_6 is een fase van microplooiing, waarbij naar het noorden duikende plooiaslineaties (I_6) werden gevormd op schistositeitvlakken. Deze fase vond plaats na de albietblastese.

Laat-Hercynische phyllonitisatie en breukbewegingen gingen lokaal gepaard met retrograde metamorfose van de gesteenten. De intrusies van dolerietgangen in het gebied worden beschouwd als jonge evenementen in de Hercynische cyclus.

De resultaten van maakselanalyse van metamorfe basische gesteenten ondersteunen de structurele veldwaarnemingen. Met behulp van deze methode was het mogelijk drie fasen van hoornblende kristallisatie aan te tonen; elke fase gevormd onder verschillende structurele en metamorfe voorwaarden. De oriëntaties van de c -assen van amfibool en klinopyroxeen liggen bij voorkeur evenwijdig aan plooiasen in het gesteente. Speciale aandacht werd geschonken aan de oriëntaties van de $\{110\}$ - en $\{100\}$ -vlakken van amfibool. In gesteenten die postkristallijn gedeformeerd zijn, werd vaak een voorkeursoriëntatie van $\{110\}$ -vlakken van amfibool in het s -vlak waargenomen. De maaksels van albiet in de albietporfiroblastenschisten vertonen een voorkeursoriëntatie van $\{010\}$ -vlakken in het s -vlak. De kristallografische a -richting van albiet (ongeveer evenwijdig met α) is vermoedelijk parallel georiënteerd aan de plooiaslineatie (I_6). Deze plooiaslineatie valt samen met de lengterichting van de ellipsoïdvormige albietporfiroblasten.

Statistische parameters kunnen geschat worden indien de waargenomen verdelingen min of meer overeenkomen met een mathematische modelverdeling. De geschatte parameters in dit onderzoek gelden voor verdelingen met een ellipsvormig maximum, eventueel liggend in een grootcirkel gordel.

REFERENCES

- Anthoiz, P. M., 1966. Géologie sommaire de la région de Moira (Tras-os-Montes, Portugal). *Leidse Geol. Med.*, 36, pp. 299-302.
- Atherton, M. P., 1968. The variation in garnet, biotite and chlorite composition in medium grade pelitic rocks from the Dalradian, Scotland, with particular reference to the zonation in garnet. *Contr. Min. Petr.*, 18, pp. 347-372.
- Atherton, M. P. & Edmunds, W. M., 1966. An electron microprobe study of some zoned garnets from metamorphic rocks. *Earth Planet. Sci. Lett.*, 1, pp. 185-193.
- Avé Lallemand, H. G., 1965. Petrology, petrofabrics and structural geology of the Sierra de Outes-Muros region (La Coruña, Spain). *Leidse Geol. Med.*, 33, pp. 147-175.
- Bailey, E. B., 1923. The metamorphism of the SW. Highlands. *Geol. Mag.*, 60, pp. 317-331.
- Barbu, A., 1960. Studiul structural petrologic al feldspatilor din roci magmatice. *Stud. cercetări de Geol.*, 4, pp. 711-738.
- Bingham, C., 1964. Distributions on the sphere and on the projective plane. Ph. D. Dissertation, Yale Univ.
- Bowes, D. R. & Park, R. G., 1966. Metamorphic segregation banding in the Loch Kerry basite sheet from the Lewisian of Gairlock, Ross-shire, Scotland. *Jour. Petr.*, 7, pp. 306-330.
- Briegleb, D., 1966. Beitrag zur Typisierung geregelter Hornblendetektone. *N. Jb. Min. Mh.*, pp. 309-319.
- Capdevila, R., 1967. Extension du métamorphisme régional hercynien dans le Nord-Ouest de l'Espagne (Galice orientale, Asturies, Leon). *C. R. Somm. Sé. Soc. Geol. France*, 7, pp. 277-279.
- , 1968. Zones de métamorphisme régional progressif dans le segment hercynien de Galice nord-orientale (Espagne). *C. R. Acad. Sci. Paris*, 266, pp. 309-312.
- Carlé, W., 1945. Ergebnisse geologischer Untersuchungen im Grundgebirge von Galicien, NW. Spanien. *Geotekt. Forsch.*, 6, pp. 13-36.
- Cogné, J., 1960. Schistes cristallins et granites en Bretagne méridionale.

- dionale: Le domaine de l'anticlinal de Cornouaille. Mém. expl. Carte Géol. France, pp. 1-382.
- , 1966. Une 'nappe' cadomienne de style pennique: la série cristallophyllienne de Champtoceaux en bordure méridionale du synclinal d'Ancenis (Bretagne-Anjou). Bull. Serv. Carte Géol. Als. Lorr., 19, pp. 107-137.
- Crampton, C. B., 1957. Regional study of epidote, mica, and albite fabrics of the Moines. Geol. Mag., 94, pp. 89-104.
- Cunningham-Craig, E. H., 1904. Metamorphism in the Loch-Lomond district. Quart. Jour. Geol. Soc. London, 60, pp. 10-30.
- Dimroth, E., 1966. Deformation in the Grenville province between Gatineau and Petite Nation rivers, Quebec. N. Jb. Min. Abh., 105, pp. 93-109.
- Engel, A. E. J. & Engel, C. G., 1962. Hornblendes formed during progressive metamorphism of amphibolites, Northwest Adirondack Mountains, New York. Bull. Geol. Soc. Am., 73, pp. 1499-1514.
- Engel, A. E. J., Engel, C. G. & Havens, R. G., 1961. Variations in properties of hornblendes formed during progressive metamorphism of amphibolites, northwest Adirondack Mts. New York. Prof. Paper U. S. Geol. Surv., 424-C, pp. 313-316.
- Escher, A., 1967. Tectonic levels in the precambrian of South-Greenland. Grøn. Geol. Unders., Miscellaneous Papers, 55.
- Evans, B. W. & Leake, B. E., 1960. The composition and origin of the striped amphibolites of Connemara, Ireland. Jour. Petr., 1, pp. 337-363.
- Felius, R. O., 1967. Petrografie en mineralogische beschrijving van een gebied op de zuidelijke grens van de Ordenes-schisten en het basisch complex in Galicië (NW. Spanje). M. Sc. thesis, Leiden University, unpublished.
- Fleuty, M. J., 1964. The description of folds. Proc. Geol. Ass., 75, pp. 461-493.
- Flinn, D., 1962. On folding during three-dimensional progressive deformation. Quart. Jour. Geol. Soc. London, 118, pp. 385-434.
- Floor, P., 1966. Petrology of an aegirine-riebeckite gneiss-bearing part of the Hesperian massif: the Galifeiro and surrounding areas, Vigo, Spain. Leidse Geol. Med., 36, pp. 1-203.
- Friedman, M., 1964. Petrofabric techniques for the determination of principal stress directions in rocks. State of stress in the earth's crust, W. R. Judd, ed., Proc. Internat. Conf. Santa Monica, California, 13-14 June 1963, pp. 450-552.
- Frietsch, R., 1957. Determination of the composition of garnets without chemical analysis. Geol. Fören. Förh., 79, pp. 43-51.
- Goldschmidt, V. M., 1921. Geologisch-petrografische Studien im Hochgebirge des südlichen Norwegens: V Die Injektionsmetamorphose im Stavanger-Gebiete. Vidensk. Skr., I. Mat. Naturv. Klasse, 10.
- Griggs, D. T., Turner, F. J. & Heard, H. C., 1960. Deformation of rocks at 500° to 800°C. Geol. Soc. Am., Mem. 79, pp. 39-104.
- Hapuarachchi, D. J. A. C., 1967. Hornblende-granulite subfacies mineral assemblages from areas in Ceylon. Geol. Mag., 104, pp. 29-35.
- Hoschek, G., 1967. Untersuchungen zum Stabilitätsbereich von Chloritoid und Staurolith. Contr. Min. Petr., 14, pp. 123-162.
- Hounslow, A. W. & Moore Jr., J. M., 1967. Chemical petrology of Grenville schists near Fernleigh, Ontario. Jour. Petr., 8, pp. 1-28.
- Howard, A. K., 1968. Flow direction in triclinic folded rocks. Am. Jour. Sci., 266, pp. 758-765.
- Hsu, L. C., 1968. Selected phase relationships in the system Al-Mn-Fe-Si-O-H: a model for garnet equilibria. Journ. Petr., 9, pp. 40-84.
- Kamb, W. B., 1959a. Ice petrofabric observations from Blue Glacier, Washington, in relation to theory and experiment. Jour. Geophys. Res., 64, pp. 1891-1909.
- , 1959b. Theory of preferred crystal orientation developed by crystallization under stress. Jour. Geol., 67, pp. 153-171.
- Knill, J. L., 1960. A classification of cleavages, with special references to the Craignish district of the Scottish Highlands. Intern. Geol. Congr., 21st. session, 18, pp. 317-325.
- Knorring, O. v. & Kennedy, W. Q., 1958. The mineral paragenesis and metamorphic status of garnet-hornblende-pyroxene-scapolite gneiss from Ghana (Gold Coast). Min. Mag., 31, pp. 846-859.
- Köhler, A., 1942. Drehtischmessungen an Plagioklaszwillingen von Tief- und Hochtemperaturoptik, Tsch. Min. Petr. Mitt. N. F., 53, pp. 159-179.
- Kojima, G. & Hide, K., 1957. On new occurrence of aegirine augite-amphibole-quartz schists in the Sambagawa crystalline schists of the Besshi-Shirataki district, with special reference to the preferred orientation of aegirine-augite and amphibole. Jour. Sci. Hiroshima Univ., Series C, 2, pp. 1-21.
- Koning, H., 1966. Les types des roches basiques et ultrabasiqes qu'on rencontre dans la partie occidentale de la Galice (Espagne). Leidse Geol. Med., 36, pp. 253-242.
- Labhart, T. P., 1965. Petrotektonische Untersuchungen am Südrand des Aarmassivs. Beitr. Geol. Karte d. Schweiz, N. F., 124, 81 pp.
- Ladurner, J., 1951. Deformation, Wachstum und Regelung der Epidote als Gefügekorn und Einkristall. N. Jb. Min. Abh., 82, pp. 317-412.
- Langheinrich, G., 1964. Vergleichende Untersuchungen über das Verhältnis der Schieferung zur Faltung unter Berücksichtigung des Stockwerk-problem. N. Jb. Geol. Pal. Abh., 120, pp. 41-80.
- Lovering, J. F. & White, A. J. R., 1964. The significance of primary scapolite in granulitic inclusions from deep-seated pipes. Jour. Petr., 5, pp. 195-218.
- Lotze, F., 1945. Zur Gliederung der Varisziden der Iberischen Meseta. Geotekt. Forsch., 6, pp. 78-92.
- Matte, Ph., 1968. La structure de la virgation hercynienne de Galice (N.W. de l'Espagne). Thèse, Montpellier, Faculté des Sciences, 128 pp.
- McLachlan, G. R., 1953. The bearing of rolled garnets on the concept of b lineation in Moine rocks. Geol. Mag., 90, pp. 172-177.
- Mehnert, K. R., 1957. Petrographie und Abfolge der Granitisation im Schwarzwald, II: N. Jb. Min. Abh., 90, pp. 33-90.
- Miyashiro, A., 1961. Evolution of metamorphic belts. Journ. Petr., 2, pp. 277-411.
- Möckel, J. R., 1969. Structural petrology of the garnet-peridotite of Alpe Arami (Ticino, Switzerland). Leidse Geol. Med., 42, pp. 61-130.
- Oele, J. A., 1966. The structural history of the Vall Ferrera area, the transition zone between the Aston massif and the Salat-Pallaresa anticlinorium (Central Pyrenees, France, Spain). Leidse Geol. Med., 38, pp. 129-164.
- Okamura, Y., 1960. Structural and petrological studies on the Ryôke gneiss and granodiorite complex of the Yanai district, southwest Japan. Jour. Sci. Hiroshima Univ., Series C, 3, pp. 143-215.
- Parga-Pondal, I., 1963. Mapa petrográfico estructural de Galicia. Inst. Geol. y Minero de España, Madrid.
- , 1966. La investigación geológica en Galicia. Leidse Geol. Med., 36, pp. 207-210.
- Portugal, V. Ferreira, M. R., 1965. Geologia e petrologia da região de Rebordelo-Vinhais. Rev. Fac. Cienc. Univ. Coimbra, 36, 287 pp.
- , 1968. The metamorphism and the structures of the Precambrian belt of northeast Portugal. Intern. Geol. Congr., 23st session, Abstracts, p. 106.

- Powell, D. E. & Treagus, J. E., 1967. On the geometry of S-shaped inclusion trails in garnet porphyroblasts. *Min Mag.*, 36, pp. 453-456.
- Ramsay, J. G., 1958. Superimposed folding at Loch Monar, Inverness-shire and Ross-shire. *Quart. Jour. Geol. Soc. London*, 113, pp. 271-308.
- , 1960. The deformation of early linear structures in areas of repeated folding. *Jour. Geol.*, 68, pp. 75-94.
- , 1962. Interference patterns produced by the superposition of folds of similar type. *Jour. Geol.*, 70, pp. 466-481.
- , 1967. Folding and fracturing of rocks. New York, McGraw-Hill, 568 pp.
- Rijks, E. J. H., 1968. Petrografie en mineralogie van het gebied rondom Buño (Galicië, NW Spanje). M. Sc. thesis, Leiden University, unpublished.
- Roever, W. P. de, & Nijhuis, H. J., 1964. Plurifacial alpine metamorphism in the eastern Betic Cordilleras (SE Spain), with special reference to the genesis of the glaucophane. *Geol. Rdsch.*, 53, pp. 324-336.
- Sander, B., 1948. Einführung in die Gefügekunde der geologischen Körper. 1, Wien, Springer-Verlag, 215 pp.
- Scheumann, K. H., 1961. 'Granulit' eine petrographische Definition. *N. Jb. Min. Mh.*, pp. 75-80.
- Schmidt, W., 1928. Zur Regelung zweiachsiger Mineralien. *N. Jb. Min. Geol. Pal.*, 57, pp. 203-223.
- Schwerdtner, W. M., 1964. Preferred orientation of hornblende in a banded hornblende gneiss. *Am. Jour. Sci.*, 262, pp. 1212-1229.
- Sen, S., 1959. Translation gliding in deformed plagioclase from a banded norite near Willow Lake, Oregon. *Congr. Geol. Intern.* 20st session, sección 11-A, pp. 263-275.
- Seng, H., 1934. Beiträge zur petrographisch-tektonischen Analyse des sächsischen Granulitgebirges. *Min. Petr. Mitt.*, 45, pp. 373-424.
- Sitter, L. U. de, & Zwart, H. J., 1960. Tectonic development in supra- and infra-structures of a mountainchain. *Intern. Geol. Congr.*, 21st session, 18, pp. 248-256.
- Sobhen Ray, 1967. Albite schists from Mosabani-Surda Tract, Singhbhum district, Bihar. *Quart. Jour. Geol. Min. Metall. Soc. India*, 39, pp. 49-53.
- Tex, E. den, 1965. Metamorphic lineages of orogenic plutonism. *Geol. Mijnb.*, 44, pp. 105-132.
- , 1966. Aperçu pétrologique et structural de la Galice cristalline. *Leidse Geol. Med.*, 36, pp. 211-223.
- Tobi, A. C., 1959. Petrographical and geological investigations in the Merdaret-Lac Crop region (Belledonne massif, France). *Leidse Geol. Med.*, 24, pp. 181-218.
- Trommsdorff, V., 1964. Untersuchungen an Interngefügen III. Beispiele aus der unteren Schieferhülle des Tauern-Westendes. *Sitz. ber. österr. Ak. Wiss., Math.-naturw. Kl. I*, 173, 39 pp.
- Tröger, W. E., 1967. Optische Bestimmung der gesteinsbildende Minerale. Teil II, Stuttgart, Schweizerbart'sche Verlagsbuchhandlung, 822 pp.
- Turner, F. J. & Hutton, C. O., 1941. Some porphyroblastic albite schists from Waikouaiti river, Otago. *Trans. Roy. Soc. N. Z.*, 71, pp. 223-240.
- , & Weiss, L. E., 1963. Structural analysis of metamorphic tectonites. New York, McGraw-Hill, 545 pp.
- Vogel, D. E., 1967. Petrology of an eclogite- and pyrigarnite-bearing polymetamorphic rock complex at Cabo Ortegal, NW Spain. *Leidse Geol. Med.*, 40, pp. 121-213.
- Waard, D. de, 1965. A proposed subdivision of the granulite facies. *Am. Jour. Sci.*, 263, pp. 455-461.
- Warnaars, F. W., 1967. Petrography of a peridotite-, amphibolite- and gabbro-bearing polyorogenic terrain NW of Santiago de Compostela (Spain). Ph. D. thesis, University of Leiden, 208 pp.
- Watson, G. S., 1965. Equatorial distributions on a sphere. *Biometrika*, 52, pp. 193-201.
- , 1966. The statistics of orientation data. *Jour. Geol.*, 74, pp. 786-797.
- Wenk, E., 1937. Zur Genese der Bändergneise von Ornö Huvud. *Bull. Geol. Inst. Upsala*, 26, pp. 53-91.
- Winchell, H., 1937. A new method of interpretation of petrofabric diagrams. *Am. Min.*, 22, pp. 15-36.
- Winkler, H. G. F., 1967. Die Genese der metamorphen Gesteine. Berlin, Springer-Verlag, 2nd ed., 237 pp.
- Woensdregt, C. F., 1966. Informe preliminar sobre los estudios de la petrografia del extremo occidental de Galicia. *Leidse Geol. Med.*, 36, pp. 261-278.
- Yakolev, B. G., 1966. Garnets from rocks of the crystalline basement of the Tatar, USSR. *Doklady Acad. Sci. U.S.S.R. Earth Sci.*, 171, pp. 192-196.
- Zwart, H. J. & Oele, J. A., 1966. Rotated magnetite crystals from the Rocroi massif (Ardennes). *Geol. Mijnb.*, 45, pp. 70-75.
- , *et al.*, 1967. A scheme of metamorphic facies for the cartographic representation of regional metamorphic belts. *IUGS Geol. Newsletter*, Vol. 1967, No 2, pp. 57-72.
- , 1967. The duality of orogenic belts. *Geol. Mijnb.*, 46, pp. 283-310.